New insights into adenosine's chronoselective atrial depressant effect

The interplay of adenosine A_1 receptor with ion channels and signaling enzymes

Bruno Bragança
Mestrado em Bioquímica
Departamento de Química e Bioquímica
2012

Orientador
Doutora Ana Patrícia Fontes de Sousa, Professora Auxiliar, ICBAS/UP
Coorientador
Doutor Paulo Correia de Sá , Professor Catedrático, ICBAS/UP

U.PORTO

FACULDADE DE CIÊNCIAS
UNIVERSIDADE DO PORTO

INSTITUTO DE CIÊNCIAS BIOMÉDICAS ABEL SALAZAR
UNIVERSIDADE DO PORTO

Todas as correções determinadas pelo júri, e só essas, foram efetuadas.

O Presidente do Júri,

Porto, _____/_____/_____

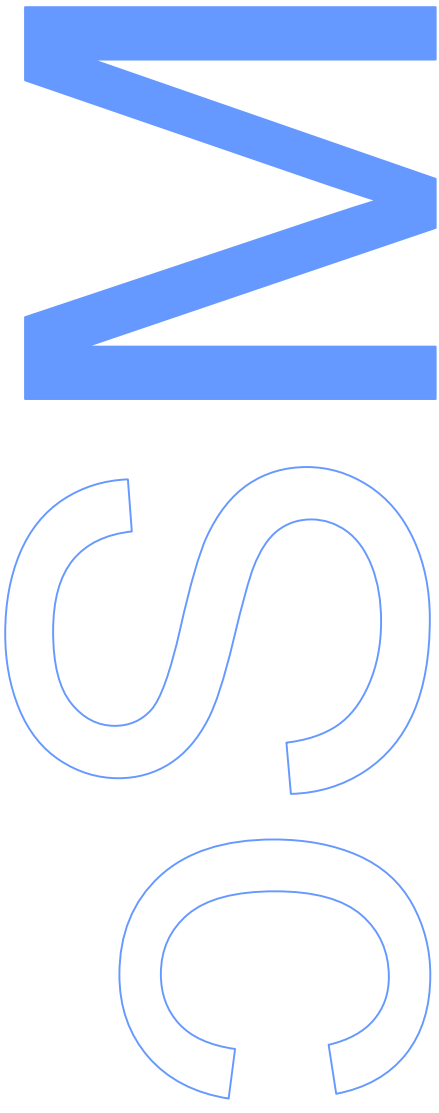

The work presented here has contributed to the following publications:

1. Publications in Peer-Reviewed Journals

1.1. Manuscripts under review:

2012 – Oliveira-Monteiro N, Bragança B, Ferreirinha F, Faria M, Fontes-Sousa AP, Correia-de-Sá P. **Rationale for understanding chronoselectivity of adenosine A_1 receptor in the rat spontaneously beating atria: enrolment of $K_{Ca}2$ (SK) and Ca_v1 (L-type) ion channels.** *American Journal of Physiology-Heart and Circulation.*

1.2. Abstracts published in international journals:

2012 – Oliveira-Monteiro N, Fontes-Sousa AP, Bragança B, Marques S, Faria M, Correia-de-Sá P. **Ca_v1 (L) channel blockade uncovers adenosine negative inotropism leading to a loss of A_1 "chronoselectivity" in the spontaneously beating rat atria.** *Purinergic Signalling*; 8: 171.

2012 **–** Bragança B, Oliveira-Monteiro N, Nogueira-Marques S, Ferreirinha F, Faria M, Fontes-Sousa AP, Correia-de-Sá P. **Inhibition of $K_{Ca}2$/SK leading to calcium influx via Ca_v1 (L) channels affords a rationale for adenosine A_1 receptor "chronoselectivity" in the rat spontaneously beating atria**. *European Heart Journal*; 33(Abstract Suppl 1) 2012: 1045.

2. Conference Presentations

2.1. Oral communications:

2011 – Oliveira-Monteiro N, Fontes-Sousa AP, Bragança B, Marques S, Faria M, Correia-de-Sá P. **Rationale for chronoselectivity of adenosine A_1 receptor in the rat spontaneously beating atria: on the role of Ca_v1 (L) and $K_{Ca}2$ (SK) ion channels.** XLI Reunião Anual da Sociedade Portuguesa de Farmacologia, XXIX Reunião de Farmacologia Clínica and X Reunião de Toxicologia 2011, Coimbra – Portugal, 2-4th February.

2012 – Bragança B, Oliveira-Monteiro N, Nogueira-Marques S, Carvalho P, Fontes-Sousa AP, Correia-de-Sá P. **Chronoselectivity of adenosine A_1 receptor in the spontaneously beating rat atria: interplay with adenosine A_{2a} and β-adrenoceptors.** XLII Reunião Anual da Sociedade Portuguesa de Farmacologia, XXX Reunião de Farmacologia Clínica and XI Reunião de Toxicologia 2012, Lisboa – Portugal, 1-3th February.

2012 – Bragança B**,** Oliveira-Monteiro N, Ferreirinha F, Fontes-Sousa AP, Correia-de-Sá P. **Differential expression of A_1 receptors between sinoatrial node and cardiomyocytes does not account for adenosine chronoselectivity in the spontaneously beating rat atria.** IJUP'^{12}- Investigação Jovem na Universidade do Porto, Porto – Portugal, 22-24th February.

2012 – Bragança B, Oliveira-Monteiro N, Nogueira-Marques S, Ferreirinha F, Faria M, Fontes-Sousa AP, Correia-de-Sá P. **Rescuing positive inotropic $K_{Ca}2$/SK and Ca_v1 (L) currents may account for adenosine A_1 receptors chronoselectivity in the spontaneously beating rat atria.** 20th *International Symposium of Scientific Initiation* of University of São Paulo – Brazil, 22-26th October.

2.2. Poster presentations:

2010 – Oliveira-Monteiro N, Bragança B, Faria M, Fontes-Sousa AP, Correia-de-Sá P. **Atrial "chrono-selectivity" of adenosine via A_1 receptors is compromised by blocking cardiac Ca_v1 (L-type) channels.** IJUP´10- Third Meeting of Young Researchers of U.Porto – Porto – Portugal, 17-19th February.

2011 – Oliveira-Monteiro N, Silva I, Ferreirinha F, Nogueira-Marques S, Bragança B, Duarte-Araújo M, Fontes-Sousa AP, Correia-de-Sá P. **Neonatal depletion of peptidergic nerve fibres reduces muscarinic receptor-mediated effects in the ileum, but not in atria of adult *Wistar* rats.** IJUP´11- Fourth Meeting of Young Researchers of U.Porto – Porto – Portugal, 17-18th February.

2011 – Oliveira-Monteiro N, Fontes-Sousa AP, Bragança B, Marques S, Faria M, Correia-de-Sá P. **The Ca_v1 inhibitor, verapamil, predisposes atria to the negative inotropic action of adenosine by uncoupling A_1 receptor-mediated $K_{Ca}2$/SK channel closure from its effector.** 2nd Iberic Meeting on Medicinal Chemistry (IMMC), Porto – Portugal, 12-15th June.

2011 – Oliveira-Monteiro N, Fontes-Sousa AP, Bragança B, Marques S, Faria M, Correia-de-Sá P. **Ca_v1 (L) channel blockade uncovers adenosine negative inotropism leading to a loss of A_1 "chronoselectivity" in the spontaneously beating rat atria.** International Conference on Purinergic Drugs and Targets-4th Joint German-Italian Purine Club Meeting, Bona – Germany, 22-25th July.

2012 – Bragança B, Oliveira-Monteiro N, Nogueira-Marques S, Ferreirinha F, Faria M, Fontes-Sousa AP, Correia-de-Sá P. **Inhibition of $K_{Ca}2$/SK leading to calcium influx via Ca_v1 (L) channels affords a rationale for adenosine A_1 receptor "chronoselectivity" in the rat spontaneously beating atria.** European Society of Cardiology Congress, Munich – Germany, 25-29th August.

Acknowledgments

This work was partially funded by the Foundation for Science and Technology of Portugal (FCT) within the framework of the project PEst-OE/SAU/UI0215/2011.

It has been a long time since I entered the Laboratory of Pharmacology and Neurobiology of ICBAS/UP. There, I have learned so many things that go beyond the work that I am presenting in this thesis.

It is a pleasure to thank those who made this thesis possible. Without their continued efforts and support, I would have not been able to bring my work to successful completion.

First of all, I would like to thank Professor Paulo Correia de Sá for the opportunity to work with him and his wonderful research team as an MSc student. He has been a true supervisor and mentor! Thank you for sharing your wealth of knowledge and experience with me.

I am heartily thankful to my supervisor, Professor Ana Patrícia Fontes de Sousa, whose encouragement, guidance and support was fundamental to finish my master's thesis. Since I arrived at this lab you have treated me like I was your son and, coincidence or not, soon I will get two little sisters (I hope!). Despite being really happy with your pregnancy glow, now I'm feeling like I was a full year mother's training program. I'm just kidding, as always! God bless and protect you and your little angels.

I thank Mrs. Fernanda Malhão Pereira and Mrs. Célia Carreiras Lopes (Laboratory of Histology and Embryology, Department of Microscopy, ICBAS/UP), for their precious help with the Masson's trichrome staining.

I extend my appreciation to Fátima Ferreirinha, PhD, for her endless expertise and time spent on confocal microscopy imaging and analysis, the results of which are an important part of my thesis. Her contribution to this work was a major benefit.

I am also thankful to all the other professors, research team members and administrative staff for their timely help: Professor Graça Lobo, Professor Laura Oliveira, Professor Margarida Araújo, Alexandrina Timóteo, BSc, Miguel Cordeiro, PhD,.and Milaydis Napolskij, BA.

Apart from constant immersion in an environment of knowledge, this year was full of funny moments. I will never ever forget the friends that I made in this lab: Marina Mendes,

Patrícia Marques, Diogo Paramos, Bernardo Matos, Catarina Baldaia, Catarina Pereira and Nádia Monteiro.

I would also like to thank Isabel Silva, Belmira Silva, Cátia Vieira, Aurora and all the remaining colleagues for their support throughout the year.

I wish to express my deepest appreciation to the number one love of my life, Patrícia Araújo, for her constant care and support.

Lastly, I offer my regards and blessing to my parents who always supported me during the completion of the project.

Abbreviations

AC - adenylyl cyclase
ADO - adenosine
ADP - adenosine 5'-diphosphate
AMP - adenosine 5'-monophosphate
AngII - angiotensin II
AT_1 - angiotensin II receptor type 1
4-AP- 4-aminopyridine
AP - action potential
ATP - adenosine 5′-triphosphate
A_xR - adenosine receptors (A_1R, $A_{2A}R$, $A_{2B}R$ and A_3R)
β-AR - β-adrenoceptor
Ca^{2+} - calcium ion
$[Ca^{2+}]_i$ - cytosolic calcium concentration
CaM - calmodulin
CaMKII - calmodulin kinase II
cAMP - cyclic adenosine 3′,5′-monophosphate
Ca_V1 (L-type) channels - L-type calcium channel
CICR - calcium-induced calcium release
Cx43 - connexin 43
DAG - diacylglycerol
DPCPX - 1,3-dipropyl-8-cyclopentylxanthine
E-C coupling - excitation-contraction coupling
GIRK ($K_{IR}3.1/K_{IR}3.4$) - G protein-coupled inwardly-rectifying potassium channel
GPCR(s) - G-protein coupled receptor(s)
$I_{Ca,L}$ - L-type Ca^{2+} current
I_f - Hyperpolarization-activated cyclic nucleotide-gated (HCN) current (or "funny" current)
I_K - potassium current
$I_{KAdo,Ach}$ - ADO- and ACh-activated outward potassium current
$I_{K,ATP}$ - ATP-dependent outward potassium current
I_{Na} - sodium current
IP_3 - inositol 1,4,5-trisphosphate
K^+ - potassium ion
LCRs - local Ca^{2+} releases
M_2R - M_2 muscarinic ACh receptor
Na^+ - sodium ion
NCX - sodium/calcium exchanger
NE - norepinephrine
NF160 - neurofilament 160
PIP_2 - phosphatidylinositol-4,5-bisphosphat
PLC - phospholipase C
PMA - phorbol 12-myristate 13-acetate
PKA - protein kinase A
PKC - protein kinase C
RyR - ryanodine channel
SA node - sinoatrial node
SK/$K_{Ca}2$ - small conductance calcium-activated potassium channel
SR - sarcoplasmic reticulum
Troponin C - TnC
Troponin I - TnI
UTP - uridine 5'-triphosphate

Abstract

In supraventricular tissues adenosine decreases spontaneous pacemaker activity (negative chronotropy), atrioventricular nodal conduction (negative dromotropy) and myocardium contraction force (negative inotropy) through the activation of adenosine A_1 receptor (A_1R) (Headrick *et al*., 2011). A_1R is a Gαi/o-protein coupled receptor. Once activated, A_1R may inhibits catecholamine-stimulated adenylyl cyclase (anti-β-adrenergic effect), increases hyperpolarizing K^+ currents carried through GIRK/$K_{IR}3$ channels (Belardinelli *et al*., 1995) and stimulates phospholipase Cβ activity and PKC translocation (Parsons *et al*., 2000; Yang *et al*., 2009b). Preliminary data from our lab showed that adenosine is a "chronoselective" atrial depressant via the activation of A_1R, yet this property is not shared by other cardiodepressant agents, like acetylcholine acting through muscarinic M_2 receptor (M_2R) activation (Oliveira-Monteiro *et al*., unpublished observations). The mechanism(s) underlying adenosine "chronoselectivity" remains to be identified. Given their involvement in atrial physiology, we sought it would be interesting to investigate the expression and function of subtype-selective K^+ and Ca^{2+} channels in the spontaneously beating rat atria. The putative enrolment of PLC/PKC signaling pathway on A_1R chronoselectivity was also investigated.

Both the A_1R agonist, R-PIA (0.001–1 μM), and the muscarinic M_2 receptor agonist, oxotremorine (0.01–3 μM), decreased in a concentration-dependent manner the rate (negative chronotropic effect) and the strength of contractions (negative inotropic effect) in the spontaneously beating rat atria. Unlike muscarinic M_2 receptor activation with oxotremorine, the A_1 receptor-mediated negative chronotropic effect of R-PIA was evidenced at much lower concentrations than its negative inotropic action (chronoselective effect). The effects of oxotremorine and of R-PIA were prevented upon blocking M_2Rs with AF-DX 116 (10 μM) and A_1Rs with DPCPX (100 nM), respectively. Blockade of GIRK/$K_{IR}3$ channels with tertiapin Q (300 nM) prevented negative chronotropism and inotropism of both A_1 and M_2 receptor agonists, respectively R-PIA and oxotremorine. Inhibition of K_v and $K_{ATP}/K_{IR}6$ currents, respectively with 4-aminopyridine and glibenclamide, were devoid of effect. Blockade of $K_{Ca}2$/SK channels with apamin and Ca_V1 (L-type) channels with verapamil, sensitized atria to the negative inotropic action of R-PIA, without affecting the nucleoside chronotropic effect and the oxotremorine effect. The same occurred when rat atria were pre-treated with PLC and PKC inhibitors, such as U73122 (3 μM) and chelerythrine (3 μM), respectively. Immunolocalization studies showed that differences in the distribution of A_1 receptors between the sinoatrial node and surrounding cardiomyocytes might not afford a rationale for adenosine chronoselectivity.

Immunolabeling of $K_{IR}3.1$, $K_{Ca}2.2$, $K_{Ca}2.3$ and Ca_v1 was also observed throughout the right atria.

Functional data support Gβγ/PLC/PKC signaling axis as an important pathway to counteract the negative inotropic effects of GIRK/$K_{IR}3$ opening following A_1R stimulation. After GIRK/$K_{IR}3$ activation, Gβγ subunits released from the vicinity of A_1R may negatively regulate these channels through PIP_2 hydrolysis. Decrease of K^+ current carried by GIRK/$K_{IR}3$ channel along with lower $K_{Ca}2$/SK channel conductance embrace a compensatory mechanism for A_1R, which is not present with M_2R activation. As Ca_V1 (L-type) channel blockade sensitized atria to contractile depression promoted via Ca^{2+} influx, these channels connect inhibition of hyperpolarizing K^+ currents to greater time available for Ca^{2+} influx. This study strengthens the differences between A_1R and M_2R signaling in the heart, particularly with respect to PLC/PKC modulation, providing new insights into adenosine's chronoselectivity.

Resumo

Em tecidos supraventriculares a adenosina diminui a atividade marcapasso das células do nó sinusal (cronotropismo negativo), a condução auriculoventricular (dromotropismo negativo) e também a força contrátil do miocárdio (inotropismo negativo), sendo estes efeitos mediados pela ativação do recetor da adenosina do subtipo A_1 (Headrick *et al*., 2011). O recetor A_1 é um recetor acoplado a proteínas $G\alpha_i/o$ cuja estimulação despoleta a ativação de várias vias de sinalização, incluindo: inibição da ciclase do adenilato estimulada por catecolaminas (efeito anti-β-adrenérgico); hiperpolarização da membrana dos cardiomiócitos, em consequência da abertura de canais GIRK/$K_{IR}3$ (Belardinelli *et al*., 1995); estimulação da fosfolipase Cβ e, consequente, translocação da PKC (Parsons *et al*., 2000; Yang *et al*., 2009b). Em estudos anteriores realizados no nosso laboratório verificou-se que a adenosina, atuando em recetores A_1, apresenta-se como agente depressor auricular com propriedades "crono-seletivas" singulares, não compartilhadas por outros agentes cardiodepressores, tal como a estimulação de recetores muscarínicos sensíveis à ACh do subtipo M_2 (Oliveira-Monteiro *et al*., observações não publicadas). Até ao momento os mecanismos responsáveis pelas propriedades crono-seletivas deste nucleósido não são perfeitamente conhecidos. Dada a importância da função auricular na fisiologia cardíaca, propusemo-nos estudar a função e a expressão de determinados subtipos de canais de K^+ e Ca^{2+} em aurículas isoladas de ratazana a contrair espontaneamente, sendo também avaliado o hipotético envolvimento da via da PLC/PKC na crono-seletividade mediada pela ativação dos recetores A_1.

Tanto a R-PIA (0.001-1 μM), um agonista seletivo A_1, como a oxotremorina (0.01-3 μM), um agonista do recetores muscarínico M_2, diminuíram de uma forma dependente da concentração a frequência (efeito cronotrópico negativo) e força de contração (efeito inotrópico negativo) em aurículas de ratazana a contrair espontaneamente. Contrariamente ao observado na ativação de recetores M_2 sensíveis à oxotremorina, os efeitos cronotrópicos negativos resultantes da ativação A_1 foram observados a concentrações de agonista muito inferiores às necessárias para produzir uma redução significativa da força contrátil (efeito "crono-seletivo"). Os efeitos da oxotremorina e da R-PIA foram prevenidos após o bloqueio dos recetores M_2 (AF-DX 116; 10 μM) e A_1 (DPCPX; 100 nM), respetivamente. O bloqueio dos canais GIRK/$K_{IR}3$ com tertiapina Q (300 nM) preveniu os efeitos cronotrópico e inotrópico negativos mediados pelos agonistas dos recetores A_1 (R-PIA) e M_2 (oxotremorina). A inibição dos canais K_v e $K_{ATP}/K_{IR}6$ com 4-AP e glibenclamida, respetivamente, não produziu qualquer efeito nas respostas resultantes da estimulação A_1 e M_2. Por outro lado, o bloqueio dos canais

$K_{Ca}2$/SK com apamina, assim como o bloqueio dos canais Ca_V1 do tipo L com verapamil, sensibilizaram o tecido auricular para as respostas inotrópicas negativas da R-PIA, não afetando a resposta cronotrópica produzida por este agonista, nem as respostas produzidas pela oxotremorina. Resposta similar foi observada após a inibição da PLC (U73122; 3 μM) e da PKC (cheleritrina; 3 μM). Estudos de imunolocalização por microscopia confocal demonstraram uma distribuição homogénea dos recetores A_1 da adenosina entre o nó sinusal e o músculo auricular circundante e, como tal, a crono-seletividade observada não ter como base a expressão diferencial deste recetor no tecido supraventricular. Observou-se ainda que os canais $K_{IR}3.1$, $K_{Ca}2.2$, $K_{Ca}2.3$ e Ca_v1 se encontravam presentes em todo o tecido auricular.

Em suma, os dados funcionais deste trabalho demonstram que o eixo formado pelas subunidades Gβγ, PLC e PKC representam uma importante via de sinalização dos recetores A1, que contrapõe os efeitos inotrópicos negativos decorrentes da abertura de canais GIRK/$K_{IR}3$. Após a abertura de canais GIRK/$K_{IR}3$, as subunidades Gβγ libertadas após a ativação A_1 poderão também regular negativamente a condutância deste mesmo canal, através da promoção da hidrólise de PIP_2 por via da estimulação da PLC. A diminuição das correntes hiperpolarizantes GIRK/$K_{IR}3$, conjuntamente com uma menor condutância iónica por parte dos canais $K_{Ca}2$/SK, poderão representar um mecanismo compensatório intrínseco dos recetores A_1 que, aparentemente, não se encontra presente na sinalização dos recetores M_2. Como o bloqueio de canais de Ca_V1 (tipo-L) sensibilizou as aurículas para a depressão contrátil, é possível que a inibição das correntes hiperpolarizantes de K^+ possa aumentar o tempo disponível para o influxo de Ca^{2+}. Este estudo reforça ainda as diferenças funcionais existentes entre os recetores A_1 e M_2, particularmente no que diz respeito à modulação da PLC/PKC, fornecendo novas pistas para a crono-seletividade da adenosina.

Table of contents

List of figures

I. Introduction

Every day the heart muscle rhythmically contracts and relaxes thousand times in order to ensure the correct perfusion of all body organs and tissues.The cardiac cycle produces pressure changes within the cardiovascular system allowing blood movement from higher pressure regions to lower ones. Low pressure blood flowing through vena cava (systemic circulation) and pulmonary veins (pulmonary circulation) firstly fills atrial chambers (right and left, respectively) and then the corresponding ventricles. Inside right and left ventricles blood is pressurized by heart muscle contraction (systole) providing enough energy to overcome the vascular resistance to blood flow through arterial blood vessels of pulmonary and systemic circulation, respectively. Following contraction, the heart muscle undergoes a relaxation period (diastole) that ends cardiac cycle. Cardiac cycle is a sequence of mechanical events timely ordered by heart's first pacemaker – the sinoatrial node (SA node). Here, spontaneous and rhythmical impulses are generated and conducted over the whole heart through its electrical wiring system (SA node, atrioventricular node, *His* bundle). The myogenic nature of cardiac action potentials (APs) explains why a denervated heart still maintains spontaneous contractions (Kurachi *et al*., 2000).

The heart is endowed with a "little brain" that integrates signals and coordinates cardiovascular responses, reacting to instantaneous body needs by means of cardiac output and arterial pressure adjustment. Heart function is under the control of the autonomic nervous system that innervates several key structures of the heart, such as the SA node and the myocardium. The "flight-or-fight response" activates sympathetic efferent fibers and stimulates norepinephrine (NE) release from sympathetic varicosities that mostly binds to β_1-adrenoceptors (β_1-AR) thus increasing heart rate (positive chronotropy), contractility (positive inotropy) and impulse conduction speed (positive dromotropy). On the other side, acetylcholine (ACh) released from parasympathetic (vagal) efferents binds to M_2 muscarinic ACh receptors (M_2R) and refrains catecholamine-stimulated cardiac output (negative chronotropy, inotropy and dromotropy). ACh effects are almost exclusively orchestrated through inhibitory M_2R, which is by far the most expressed muscarinic receptor in the mammalian heart (Krejci and Tucek, 2002). The other non-M_2 muscarinic receptors are expressed at low abundance, despite no conclusive data about the relative expression of each receptor in atria and ventricles (Krejci and Tucek, 2002; Myslivecek *et al*., 2008).

M_2R and β_1-AR comprise two important families of G-protein coupled receptors (GPCRs) in what heart regulation concerns. GPCRs are single polypeptide chains that

span the cellular membrane seven times and bind to GTP binding proteins (also known as G-protein). G-proteins are guanine-nucleotide regulatory heterotrimeric protein complexes of G_α, G_β, and G_γ subunits with a remarkable variety of physiological actions on numerous effectors, such as protein kinases, phosphodiesterases, phospholipases, transcription factors, intracellular receptors and ion channels (Milligan and Kostenis, 2006). Although chaotic at first glance, GPCRs signaling partners are organized and compartmentalized in membrane microdomains providing fidelity, speed and graded responses to GPCR agonists (Patel *et al*., 2008).

In resting conditions, the heart is predominantly under the tonic influence of the parasympathetic system. Autonomic nerves and other neurohormonal mechanisms control the cardiac output by changing either the stroke volume or the heart rate. Heart rate is set by SA node activity whereas ventricular stroke volume is regulated by multiple mechanisms, including preload, afterload and muscle inotropy. Even though stroke volume is much more dependent on the mechanical properties of ventricular myocardium, atria have also an important role on stroke volume regulation, particularly during cardiac sympathetic drive (e.g. physical activity) or myocardial dysfunction (Kurachi *et al*., 2000). Supporting the functional relevance of atria, some supraventricular arrhythmias (e.g. supraventricular tachycardia, atrial fibrillation) withdraw the contribution of atrial contraction to ventricular filling. This compromise of ventricular filling together with the rapid ventricular rate associated to these arrhythmias could lead to hemodynamic perturbations (Samet, 1973). Abnormalities in impulse initiation and conduction are the main arrhythmogenic mechanisms. Fortunately, there are some clinical approaches available to reverse these cardiac rhythm abnormalities, such as carotid sinus massage, catheter ablation and anti-arrhythmic drug therapy (e.g. adenosine [ADO]) (Blomstrom-Lundqvist *et al*., 2003). Heart function impairment compromises the correct perfusion of all tissues and organs; consequently, the fundamental physiological processes that ensure the correct body homeostasis are compromised.

1. The heart's first pacemaker – the sinoatrial node

Heart contraction is primarily triggered at the SA node. This outstanding structure remained unknown for many years, until the seminal work of Arthur Keith and Martin Flack (Keith and Flack, 1907). The SA node has a complex and heterogeneous structure of non-contractile cardiac myocytes located within the right atria boundary with the superior vena cava (intercaval region) and extending to the inferior vena cava in most mammals (Boyett *et al*., 2000) (Figure 1). Within this interface, the SA node is surrounded by epicardic and

endocardic layers, and it is just a thin layer that nearly occupies the entire atrial wall thickness (Anderson and Ho, 1998; Boyett *et al*., 2000; Monfredi *et al*., 2010). While in some mammals the SA node is too small to be seen without at least magnifying lens, as it happens with small mammals (e.g. rat, guinea pig), the human's SA node can be seen with the naked eye. Therefore, the precise location of the SA node of experimental animal models (e.g. rat) often requires identification of either anatomical or molecular markers. Histological sections allow us to identify some of the anatomical markers of the SA node. The Masson's trichrome staining is usually used for the histological identification of the SA node because SA nodal cells are inserted in a collagen matrix, rich in elastic fibers randomly orientated, and surrounded by atrial muscle, exhibiting bluish and reddish tones, respectively. The abundance of connective tissue serves as an important insulating matrix from the neighborhood hyperpolarizing currents of surrounding atrial muscle (Boyett *et al*., 2000; Monfredi *et al*., 2010).

The adult human's SA node is located under the epicardic surface of the *crista terminalis* where a subepicardic large artery - the sinus node artery – is usually visible (Anderson and Ho, 1998). The architecture of the SA node and its surrounding area is species dependent (Boyett *et al*., 2000). In some animals it is possible to identify particular areas of the right atrial appendage such as: SA node center, paranodal area and *crista terminalis*. The terminal crest is a thick atrial muscle that comprises high density of large cardiomyocytes disposed in a longitudinal rearrangement (Dobrzynski *et al*., 2005). Cardiomyocytes from *crista terminalis* (atrial muscle) are densely packed, whereas SA node center is a meshwork of SA nodal cells, randomly distributed throughout an extracellular matrix of connective tissue. The paradonal area lies between the atrial muscle and SA node and it has a poor organized mixture of nodal and atrial-like cells, located near the SA node (Chandler *et al*., 2009; Monfredi *et al*., 2010). As we move towards the periphery of the SA node, the structural and electrophysiological properties of the atrial tissue modify itself (Figure 1). For example, cells from the SA node center have roughly a smaller diameter than cells from its periphery, and even smaller compared with atrial muscle cells (Dobrzynski *et al*., 2005; Allah *et al*., 2011).

In some mammals, SA nodal cells can be classified as "pale" cells, according to its morphological characteristics. "Pale" cells are round-shaped cells with an evident nucleus and long cytoplasmatic extensions along with poorly developed sarcomeres and sarcoplasmic reticulum (SRs) that give them an empty look (James *et al*., 1966). They are generally found in clusters with few intercellular junctions, whose function is primarily to generate APs and, therefore, they are considered the true pacemaker cells (James *et al*., 1966; Monfredi *et al*., 2010). Notwithstanding, the morphological identification of SA node cells is not so straightforward, since it has been found within the SA node cells with

various sizes, morphologies (e.g. elongated spindle, spindle and spider cells) and electrical properties (Boyett *et al*., 2000) (Figure 1). Toward the periphery are found "transitional cells" that are elongated and exhibit a transition phenotype, or a mixture of different cells, or even both, between the "pale" cells and the myocytes from working myocardium (James *et al*., 1966; Boyett *et al*., 2000; Balbi *et al*., 2011). In fact, as we get closer to the atrial muscle, the density, organization and size of myocyte-like cells raise up and the atrial tissue becomes more specialized for contraction and electric impulse conduction than for spontaneous impulse generation (Boyett *et al*., 2000; Dobrzynski *et al*., 2005; Allah *et al*., 2011) (Figure 1). Other cells have also been described in the SA node, such as adipocytes, present in the periphery of the SA node from adult mammals (Melo *et al*., 2001), and "fibroblast-like cells" that are immersed in the loose collagen matrix of the SA node (Dobrzynski *et al*., 2005; Balbi *et al*., 2011).

Apart from anatomical markers, this specialized heart structure can be identified by several molecular markers. The discovery of molecular markers of the SA node is highly related to its unique cellular features. Molecular markers are based on the differential expression pattern of some ion channels throughout the atria, which include calcium (Ca^{2+}), potassium (K^+), sodium (Na^+) channels and other proteins (Chandler *et al*., 2009). However, it should be noted that, in some experimental models, the molecular markers of the SA node could not be the same between animals from different species and they could even change during animal's development (Boyett *et al*., 2000; Allah *et al*., 2011).

The SA node exhibits low abundance of atrial natriuretic peptide and gap junction connexin 43 (Cx43), while the opposite is true for the atrial muscle (Chandler *et al*., 2009). The paranodal area exhibits a mixed phenotype, with cells expressing either proteins or none of them (Chandler *et al*., 2009; Monfredi *et al*., 2010). Low Cx43 expression among other connexins reinforce the poor electrical coupling provided by higher amounts of connective tissue within the SA node (Dobrzynski *et al*., 2005). The middle (160/165-kDa) neurofilament (NF160) is a positive marker of the SA nodal area that is nearly absent in the atrial muscle (Dobrzynski *et al*., 2005). Since SA node possesses pacemaker cells, the expression of ion channels responsible for the pacemaker or "funny" current (I_f) (see above) may also be used as marker of the SA nodal area (Chandler *et al*., 2009). L-type calcium channel (Ca_V1) subtypes expression can also be regarded as molecular markers of atrial areas. The number of putative markers for each atrial area is huge and these are listed in numerous articles (Tellez *et al*., 2006; Chandler *et al*., 2009; Allah *et al*., 2011; Yanni *et al*., 2011), strengthening the concept of an incredible heterogeneous and complex tri-dimensional structure of the right atrium (Boyett *et al*., 2000; Dobrzynski *et al*., 2005).

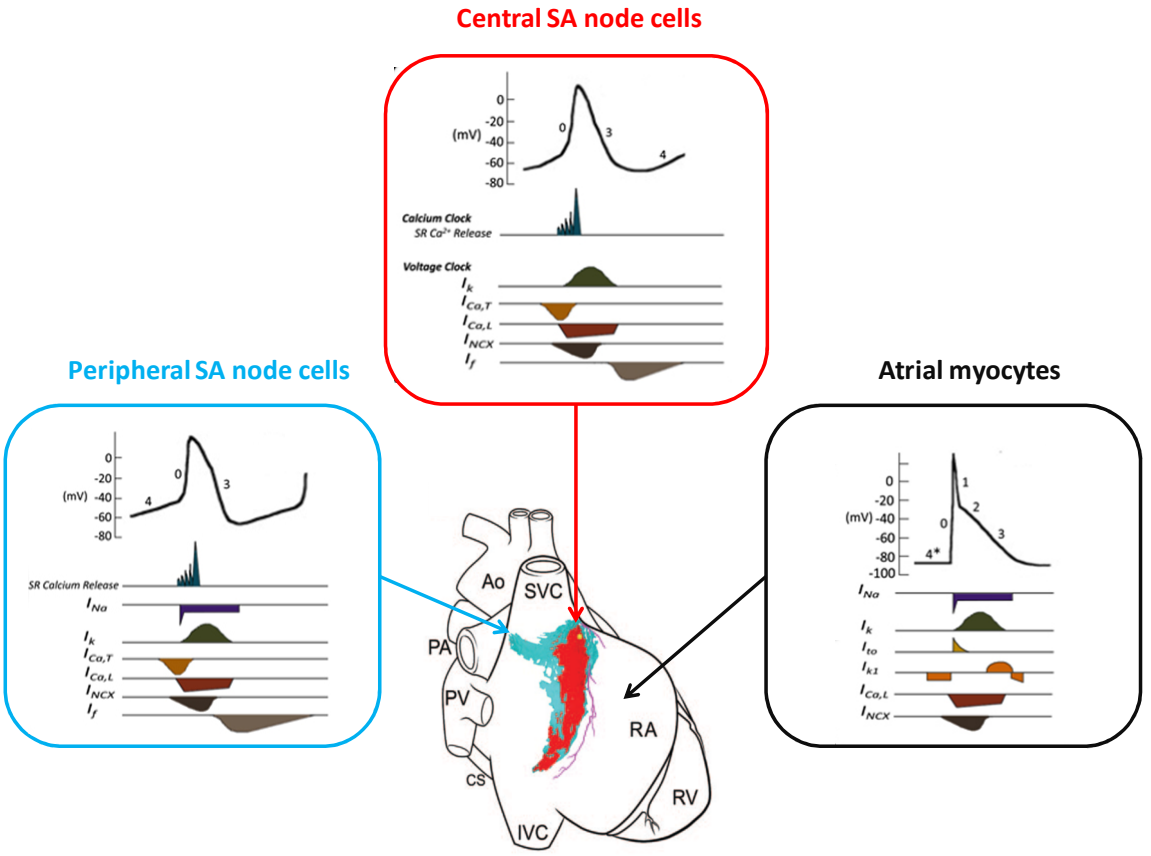

Figure 1. The mammalian heart and the electrophysiologic heterogeneity of the right atrium. In the center of figure is a schematic representation of mammalian heart (aorta (Ao); pulmonary artery and vein (PA and PV, respectively); coronary sinus (CS); superior and inferior vena cava (SVC and IVC, respectively); right atrium (RA) and right ventricle (RV)). The central (leading pacemaker site) and peripheral area of the SA node are red and blue labeled, respectively. Inside the three boxes are depicted the most important outward and inward currents that shape action potentials from central (red box) and peripheral (blue box) SA node cells, and from atrial myocytes (black box). Resting (4*); diastolic depolarization (4); upstroke (0); early repolarization (1); plateau (2) and final repolarization (3) are the phases of the action potentials. The ionic currents depicted show the time course and direction (e.g. inward if below the line) of the ionic currents. Currents: sodium current (I_{Na}); slow and fast delayed rectifier (I_K); T-type calcium current ($I_{Ca,T}$); L-type calcium current ($I_{Ca,L}$); slow inward rectifier current (I_{K1}); funny current (I_f); Na^+/Ca^{2+} exchanger; transient outward current (I_{to}). Adapted from (Dobrzynski *et al*., 2005) and (Park and Fishman, 2011).

The generated pacemaker AP has enough power to excite neighboring cells around the SA node center, driving the electrical impulse through the heart conduction system. The SA node center is not entirely electrically-insulated and, from the SA node center toward periphery, bundles of heterogeneous cellular population (a mixture of atrial and SA node cells) arise and break *crista terminalis* toward the remaining atrial muscle. These cellular bundles ensure a physical connection between SA node center and its periphery, while it also shields the SA node from the interfering currents generated peripherally (Oosthoek *et al*., 1993; Dobrzynski *et al*., 2005). Thus, atrial muscle driving is achieved by a highly specialized conduction pathway that stem from the tiny SA node

center (Boyett *et al*., 2000). *Crista terminalis* is devoid of large amounts of connective tissue and it is particularly enriched in connexins, like the high-conductance Cx43, in clear contrast with the SA node center (van Kempen *et al*., 1991), which make it suitable for a high-speed electrical impulse conduction.

2. Spontaneous generation of pacemaker action potentials

Since Keith and Flack's discovery lot of efforts have been taken to figure out what is behind the spontaneous electrophysiological activity of the heart's primary pacemaker. The ionic currents behind the typically pacemaker AP (Figure 1) have been resolved with the aid of advanced methodological approaches, such as the patch-clamp technique. SA nodal cells have an unstable resting potential, lower maximum diastolic potentials and the highest depolarization rates (phase 4) among other cardiac cell types (Figure 1), so they set the pace for heart beat (Amin *et al*., 2010). The remarkable electrophysiological properties of these cells accounts for the singular expression profile of ionic channels. For example, these cells lack fast sodium currents which results in lower upstroke velocity (phase 0) and slower impulse conduction (Boyett *et al*., 2000) (Figure 1). However, different AP profiles have been recorded from cells within the SA node area (figure 1), which goes in line with the proposed heterogeneous cellular population for this area (Boyett *et al*., 2000). The distinctive ion channel expression pattern underlies this electrophysiological diversity. The cells around the SA node center have a phase 0 with higher slope and amplitude as compared to the centrally located cells, which have a fast sodium current (I_{Na}) (Amin *et al*., 2010) (Figure 1). Such current supports the higher impulse conduction velocity at the SA node periphery (Boyett *et al*., 2000).

The periodical and synchronous APs' generation is the electrical hallmark of the SA node and it looks like it has its own clock. The mammalian heart has, forsooth, two coupled-clocks that drive heart spontaneous activity. The cutting edge coupled-clock system concept holds a "membrane voltage clock" and the "Ca^{2+} clock" (Figure 2). The time-keeping elements in the "membrane voltage clock" are a wide variety of ionic current from channels and transporters that span the sarcolemma, such as: voltage-dependent Ca^{2+} currents (L- and T-type Ca^{2+} currents); voltage-dependent K^+ current (transient outward current (I_{to}) and delayed rectifier K^+ current that includes ultra-rapid ($I_{K,ur}$), rapid ($I_{K,r}$) and slow ($I_{K,s}$); "funny" or pacemaker current (I_f); sustained inward current (I_{st}), background sodium-sensitive current ($I_{b,Na}$); voltage-independent K^+ currents (e.g. ACh- and ADO-activated K^+ current, $I_{K,ACh,ADO}$; ATP-sensitive K^+ current ($I_{K,ATP}$)); Na^+/Ca^{2+} exchanger (I_{NCX}) and Na^+/K^+ATPase (I_{NaK}) currents (Boyett *et al*., 2000; Lakatta *et al*.,

2010). This large ensemble of ionic currents shapes the membrane potential of each AP on a beat-to-beat basis. The "Ca^{2+} clock" is based on intracellular Ca^{2+} dynamics across the internal (e.g. SR, mitochondria) and external compartments. These two clocks represent a broad array of synchronized events and, as a result, it is not possible to detach the membrane clock from the Ca^{2+} clock, since both interact and mutually influence each other's activity (Lakatta *et al*., 2010).

The lack of a stable resting membrane potential (phase 4) is the holy grail of spontaneous activity of SA node cells (Figure 1). During the mid-diastolic depolarization (phase 4), Ca^{2+} from the SR is continuously leaking out through ryanodine-sensitive channels (RyR2), i.e. local Ca^{2+} releases (LCRs), increasing cytosolic Ca^{2+} concentration ($[Ca^{2+}]_i$) that, in turns, drives the depolarizing Na^+/Ca^{2+} (NCX) current (three sodium ions are exchanged for each Ca^{2+}). The rate of LCRs generation gradually increases during the late diastolic depolarization that precedes the next AP upstroke (Huser *et al*., 2000). The Ca^{2+} cycling beneath the spontaneously generation of LCRs is closely linked to spontaneous cycle length and it is regulated by mechanisms that affect both sarcoplasmic and cytosolic Ca^{2+} concentrations (Figure 2) (Vinogradova *et al*., 2004; Sanders *et al*., 2006). Regarding the Ca^{2+} cycling regulation concept, in a recent report, the modulation of mitochondrial Ca^{2+} buffer capacity, with blockers of Ca^{2+} pumps and release channels highlighted the mitochondria as an organelle with an incredible impact on the coupled SR Ca^{2+} loading and pacemaker activity of SA node cells (Figure 2) (Yaniv *et al*., 2012).

Meanwhile, as the membrane potential becomes less negative due to LCR, the conductance of T-type calcium channels (Ca_V3) increases in such way that promotes a further elevation of ($[Ca^{2+}]_i$) (Catterall, 2011) and, consequently, inward conductance of I_{NCX} increases (Huser *et al*., 2000; Bogdanov *et al*., 2001; Sanders *et al*., 2006). Toward the end of the phase 4 (late diastolic depolarization), high I_{NCX} conductance brings the membrane potential to the Ca_V1 (L-type) channels threshold activation (about -40 mV). As Ca^{2+} enters mainly through activated Ca_V1 (L-type) channels, and a little bit through reverse-mode of NCX current at very positive membrane potentials ($E_m>E_{NCX}$) or high $[Na^+]_i$ (Sipido *et al*., 1997), the Ca^{2+} conductance through RyR suddenly increases and a sharply elevation of ($[Ca^{2+}]_i$) occurs, i.e. Ca^{2+}-induced Ca^{2+} release (CICR) (Fabiato, 1983; Bogdanov *et al*., 2001; Bers, 2002). Following this massive SR Ca^{2+} release, the membrane potential quickly reverses from negative to positive, and a depolarization occurs. Rather than being a simple electric impulse yielded from the coupled-clock system, the AP is itself a synchronizing event of the two "clocks". The occurrence of an AP empties SR Ca^{2+} stores and timely inactivates the RyRs, resetting the SR function. If the AP does not readily take place, the Ca^{2+} cycling homeostasis is compromised, and the

spontaneous SR Ca^{2+} release begins to vanish until it disappears. Therefore, the AP sets up the timing and magnitude of the diastolic Ca^{2+} release (Vinogradova *et al*., 2004).

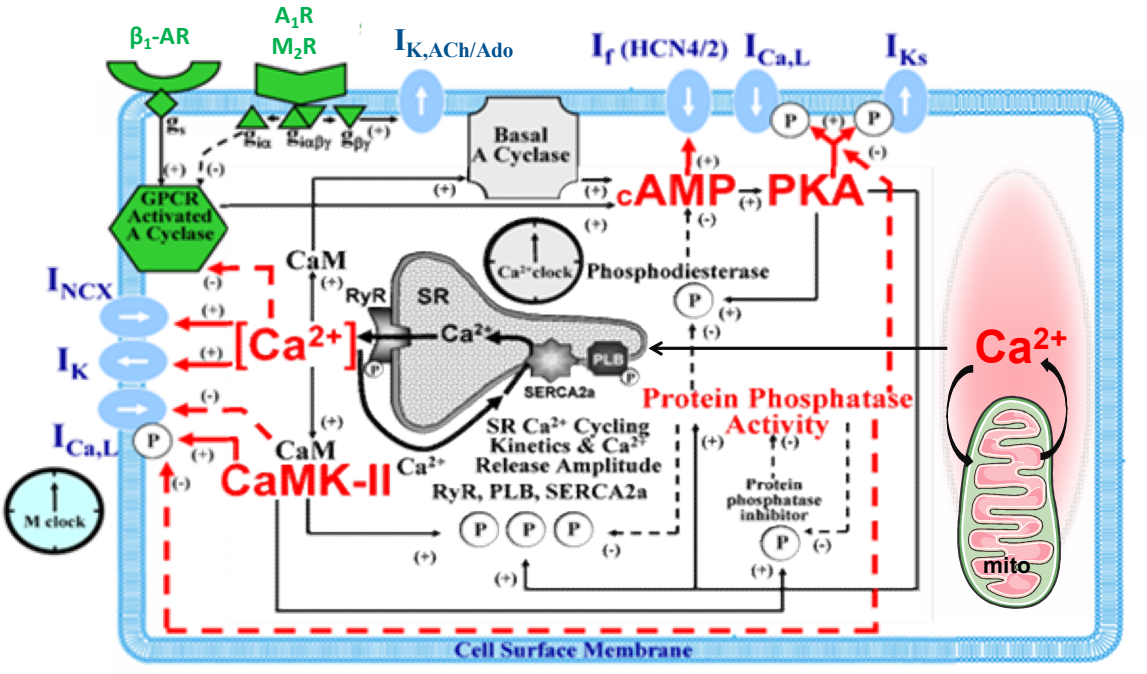

Figure 2. The coupled-clock pacemaker system. Cells within the SA node generate spontaneous actions potentials. The spontaneous activity derives from the dynamical interaction of subcellular (Ca^{2+} clock) and sarcolemmal (M-clock) proteins. The net Inward current during early diastolic depolarization phase (I_f and I_K decay) raise the membrane potential. As the membrane potential become less negative, other electrogenic currents increase their own conductance ($I_{Ca,T}$ and I_{NCX}) and spontaneous SR Ca^{2+} leakage (local Ca2+ release) gradually increases, which causes the membrane potential to go even less negative. Suddenly, an inward Ca^{2+} current carried by L-type voltage-gated calcium channel triggers a massive SR Ca^{2+} release through ryanodine receptors (RyR) that generates the action potential upstroke (phase 0) and membrane potential reaches a maximum. Meanwhile, outward K^+ current increase (hyperpolarizing) and after few milliseconds the maximum diastolic depolarization potential is reached again. The "clock ticking" is under autonomic control, it speeds up when β_1-adrenoceptors are stimulated by catecholamines and slows down when Gαi protein-coupled receptors (e.g. A_1R and M_2R) are activated. Adenylyl cyclase (AC) integrates autonomic signals by changing cAMP formation rate and, subsequently, PKA activity. This modified representation of the coupled-clock pacemaker system from (Lakatta *et al*., 2010) include the recent advances in this research field, where mitochondrial calcium buffering capacity modulates cardiac pacemaker cell automaticity (Yaniv *et al*., 2012).

After reaching the maximum depolarization potential, $[Ca^{2+}]_i$ decreases as the K^+ outward currents increase (I_K) and the membrane potential fades out to negative potentials (phase 3). The $[Ca^{2+}]_i$ transient decay is partially attributable to the calmodulin (CaM) that serves as an important feedback mechanism for restoring $[Ca^{2+}]_i$ to basal levels (Lakatta *et al*., 2010; Catterall, 2011). The binding of Ca^{2+} to CaM deactivates the $I_{Ca,L}$ (Pitt *et al*., 2001). Even though the negative modulation of $I_{Ca,L}$ by CaM leads to $[Ca^{2+}]_i$ reduction, SR pumping by SERCA2, which refuels the Ca^{2+} clock, and Ca^{2+} extrusion via I_{NCX}, accounts for the large reduction of $[Ca^{2+}]_i$ at the end of AP (Vinogradova *et al*., 2004; Lakatta *et al*., 2010). Additionally, higher K^+ conductance during the third phase (Figure 1)

of the AP strengthens these Ca^{2+} release recovery mechanisms by enchaining the forward mode of NCX and by reducing the Ca^{2+} channel voltage-dependent activation. As soon as the membrane potential gets closer to –40 mV, the slow, mixed Na^{+}-K^{+}, inward current pacemaker current (I_f) gradually increases (DiFrancesco and Tortora, 1991), along with a time-dependent decay of potassium conductance that push the membrane potential out of the maximum diastolic potential and a new cycle begins (Figure 1) (Lakatta *et al*., 2010).

3. Regulation of chronotropy

Despite pacemaker cells have been regarded as a clock, the spontaneous AP firing at the SA node is not a monotonous process and can speed up or slow down its ticking. The SA node is an integrated structure that reacts against the instantaneous body needs. Sympathetic drive increases heart rate while the parasympathetic system does the opposite. Autonomic control of heart rate is mostly achieved through ACh- and NE-sensitive receptors placed on the surface of SA nodal cells. In the heart, including the SA node, the main subtype of receptors sensitive to ACh is the M_2R whereas β_1-AR is the most expressed NE-sensitive receptor. While β_1-AR is a $G\alpha_s$-coupled receptor (vide infra) and stimulates adenylyl cyclase (AC), the $G\alpha_{i/o}$-coupled M_2 muscarinic receptor (M_2R) inhibits AC decreasing cAMP levels (Figure 2) (Vinogradova *et al*., 2006; Lyashkov *et al*., 2009). Therefore, one can afford a key role for intracellular cAMP levels on chronotropy regulation. The positive effect of cAMP is attributable to its stimulating effect on protein kinase A (PKA) activity, an important kinase that winds both M and Ca^{2+} clocks (Figure 2) (Lakatta *et al*., 2010). In fact, the role of the cAMP/PKA pathway for cardiac pacemaking is more important than anyone could have ever imagined until Vinogradova's experiments, which demonstrated that SA nodal cells have surprisingly higher PKA activity and cAMP levels as compared to other cardiac cell type. Pharmacological modulation of cAMP/PKA pathway showed that higher PKA activity, rather than cAMP itself, is obligatory for the basal spontaneous and rhythmic occurrence of LCRs in these cells (Vinogradova *et al*., 2006). The steady-state of cAMP levels yields from the balance between the production and metabolization rates of cAMP by AC and phosphodiesterases, respectively. Besides manipulation of cAMP from its steady-state, the phosphatase activity of some proteins, like protein phosphotases, also affects phosphorylated proteins by PKA and Ca^{2+}/CaM-dependent protein kinaseII (CaMKII), which may bring forth changes in pacemaker AP firing (Figure 2) (Lyashkov *et al*., 2009; Lakatta *et al*., 2010).

In the early diastolic depolarization phase, perturbation of cAMP equilibrium may also affect gating properties of HCN (hyperpolarization-activated cyclic nucleotide-gated) channels and increase their carried current (I_f) during stimulation of AC or inhibition of

phosphodiesterases (DiFrancesco and Tortora, 1991). However, in some experiments, direct pharmacological suppression of I_f did not produce extensive changes in the automaticity of SA nodal cells (Sanders *et al*., 2006; Lyashkov *et al*., 2009).

Besides AC inhibition, vagal stimulation also decreases spontaneous firing by increasing K^+ conductance ($I_{K,ACh}$) through G protein-coupled inwardly-rectifying potassium channels (GIRK/K_{IR}3) accompanied by a detectable hyperpolarization of the maximum diastolic potential (Han and Bolter, 2011). Activation of GIRK/K_{IR}3 channels were the first effectors to be described for Gβγ dimer (Logothetis *et al.*, 1987). GIRK/K_{IR}3 channel belongs to the inward rectifier channels family and it is a heterotetrameric complex of K_{IR}3.4 and K_{IR}3.1 subunits (Krapivinsky *et al.*, 1995). This ionic current is shared by other $G\alpha_{i/o}$-coupled receptors such as the A_1R that also reduces heart beating (Kurachi *et al*., 1986; Belardinelli *et al*., 1988).

Ca^{2+} ion is more than a simple power source of pacemaker APs; it also acts as a gear in the “clocking machine”. It accelerates its own dynamics by a feedforward mechanism based on Ca^{2+} stimulation of several enzymes, including some AC isozymes, PKA and CaMKII, and, in its absence (i.e. in the presence of Ca^{2+} chelators) spontaneous AP firing are no longer observable (Sanders *et al*., 2006). These kinases phosphorylate sarcolemma (e.g. Ca_V1 (L-type) channels) and SR (e.g. phospholamban and RyR) proteins, increasing the cell Ca^{2+} load and Ca^{2+} cycling that mirror higher spontaneous AP firing (Lakatta *et al*., 2010). The relation between overall Ca^{2+} dynamics and spontaneous firing come together to define the LCR period, i.e. the time-course that separates the spontaneous emergence of two LCR events. The LCR period is inversely related to pacemaker AP length and decreases when some of the AP phases are shortened. The diastolic depolarization phase (phase 4) underlies the spontaneous SR Ca^{2+} release, or LCR, and it is increased by phosphorylation. The frequency and size of LCRs are enhanced by ryanodine channel (RyR) phosphorylation. When RyR is phosphorylated, the RyR channel is more sensitive to $[Ca^{2+}]_i$ thereby increasing fractional SR Ca^{2+} release for a given I_{Ca} trigger (Bers, 2002; Vinogradova *et al*., 2006). RyR channel is not the only protein phosphorylated from the SR PKA and other kinases also modify the function of other protein of the SR Ca^{2+} refueling machinery, namely SERCA2a. SERCA2a is a Ca^{2+} ATPase responsible for pumping cytosolic Ca^{2+} into SR and it is naturally inhibited by -phospholamban. Phosphorylation of phospholamban relieves SERCA2a inhibition, increasing SR Ca^{2+} load (Vinogradova *et al*., 2006). Noteworthy, in absence of this compensatory mechanism, higher SR Ca^{2+} release or low SR Ca^{2+} uptake would gradually deplete the SR Ca^{2+} stores and, concomitantly, slow down, or even stop, the spontaneously firing in SA nodal cells (Bogdanov *et al*., 2001; Sanders *et al*., 2006; Yaniv *et al*., 2012).

Given the Ca^{2+}-dependence of spontaneous AP firing, it might be expected an interplay of the well-recognized inositol triphosphate (IP_3)-mediated Ca^{2+} store release (Berridge, 1993). In fact, a recent study conducted in mouse SA nodal cells addressed this relevant assumption by studying the expression levels and location of all IP_3R subtypes. More than any other IP_3R subtype, IP_3R subtype II (IP_3R2) was found to be highly expressed in SA nodal cells as well as in cells from atrioventricular node and atrial tissue. Furthermore, IP_3R2s lie beneath the sarcolemma in close proximity with SR proteins, and after application of either membrane-permeable IP_3, the spontaneous Ca^{2+} release and pacemaker firing rate increased in the SA nodal cells (Ju *et al*., 2011). This study agrees with previous ones about IP_3R expression in cardiomyocytes (Lipp *et al*., 2000) (see below) and supports chronotropy modulation by receptors coupled to IP_3 production.

To sum up, higher $[Ca^{2+}]_i$ increases spontaneous AP firing rate in SA node cells directly related to higher SR Ca^{2+} cycling (higher load and release) and shorter LCR periods (Yaniv *et al*., 2012). As a consequence, the late phase of diastolic depolarization slope increases and $I_{Ca,L}$ threshold is easily overcome. Inward Ca_V1 (L-type) current is also a phosphorylation target of PKA and other kinases that increase $I_{Ca,L}$ amplitude and bring it to earlier phase of diastolic depolarization due to shifting of channel gating to more negative potentials (Vinogradova *et al*., 2006; Catterall, 2011).

4. Excitation-contraction coupling

The spontaneous AP firing at the SA node has the heart muscle contraction as the final goal. The heart muscle has, in turn, to generate enough mechanical energy to impel the blood through vessels and tiny capillaries. But when a heart impulse is no longer able to induce an efficient contraction (e.g. during arrhythmic phenomena), the heart works in an unsustainable way in a medium to long term. Therefore, every AP generated at the SA node must produce a contraction, which means a coupling between the electrical excitation and the heart muscle contraction: the excitation-contraction coupling (E-C coupling) (Figure 3) (Bers, 2002). The E-C coupling underlies a complex cascade of events that happen in a well-ordered way in just a few milliseconds. The E-C coupling arises from the overlapping mechanisms behind contraction and electrical activity of the heart. The sarcolemma is the place where these two phenomena meet. Here, some of the mechanisms for pacemaker potential generation are as well involved on the E-C coupling mechanism to generate a contraction. Fundamentally, heart muscle contractions arise from the synchronous contraction of a large number of cells, and feeling the pulse just gives us an idea about how powerful and stronger they can be. The heart muscle is

nothing more than a well-organized and repetitive tridimensional structure composed by millions of rod-shaped cells running parallel to heart's surface. These cells are gifted in terms of contractile machinery and they are usually called myocytes. The sarcomere is the functional contractile unit of myocytes, and the assembly of repeating sarcomeres, packed side-by-side, defines a myofibril. Bundles of myofibrils enclosed by the sarcolemma membrane draw the myocyte. Myofibrils are a large ensemble of thick (myosin filaments) and thin filaments (actin, tropomyosin and troponin) longitudinally disposed in a symmetric and parallel way. Running transversely or even longitudinally to myocytes, intercalated discs have desmosomes that firmly tight adjacent myocytes making them twitch simultaneously, i.e. a syncytium. Intercalated discs are filled with connexins (gap junctions) that provide low-resistance pathways for electrical and chemical transmission between myocytes.

Contrary to pacemaker cells, the atrial and ventricular myocytes have stable resting potentials (around -85 mV) (phase 4) generated by an outward K^+ flux (I_{K1}) through $K_{ir}2$ channels (Figure 1) (Boyett *et al*., 2000; Chandler *et al*., 2009; Amin *et al*., 2010). Spreading of depolarizing waves generated from the leading pacemaker through gap junctions excite adjacent myocytes by dramatically increasing their Na^+ conductance through voltage-dependent Na^+ channels (phase 0). Inward sodium current produces a sharp upstroke in the membrane potential and then produces a long-lasting increase of Ca^{2+} ion conductance through voltage-dependent Ca_V1 (L-type) channels (Figure 1). Ca_V1 (L-type) channels change their own Ca^{2+} conductance in response to membrane potential and, therefore, they are called voltage-gated channels (Catterall, 2011). Once membrane potential reaches the maximum depolarization potential, I_{Na} deactivation and increase of transient outward K^+ current (I_{to}) take place to produce an early repolarization (phase 1). The $I_{Ca,L}$ and the gradually K^+ conductance increase of voltage-dependent K+ channels (delayed outward rectifying currents: I_{Kur}, I_{Kr} and I_{Ks}) contribute to the plateau phase of the AP (phase 2). The successive activation of outward rectifying currents (I_{Kr}, I_{Ks} and I_{K1}) deactivates Ca_V1 (L-type) channels leading to a net outward ionic current that drives membrane potential toward K^+ equilibrium (phase 3 and 4) (Figure 1) (Amin *et al*., 2010). Along with the electrophysiological changes produced by an AP from a neighborhood myocyte, Ca^{2+} ions passing through Ca_V1 (L-type) channels increase subsarcolemmal Ca^{2+} concentration from 100 nM to 10 μM (Ca^{2+} spike). Ca_V1 (L-type) channels are remarkably located in the well-known transverse tubules of a sarcomere's Z-disk. The acclivitous surface of cardiomyocytes is replenished of these specialized structures, where the Ca_V1 (L-type) channels are closely connected with clusters of RyR2 from the SR, forming the cytosolic cleft (or dyadic junction), which is the functional unity of the cardiac E-C coupling – the couplon (also known as Ca^{2+} release units) (Figure 3) (Sun *et*

al., 1995; Catterall, 2011). In general, the fundamental processes beneath EC-coupling of ventricular myoctes are very similar to those present in atrial myocyte contraction (Bers, 2002). However, there are some differences between atrial and ventricular myocytes that lastly influence the contraction properties of these two cell types. While in ventricular myocytes t-tubules are deeper invaginations of sarcolemma that occupy a large surface of these cells (around 50%), atrial myocytes have few and less-developed t-tubules. Offsetting the lack of t-tubules, atrial myocytes have an extensive tubular network formed from internal SR membranes, also known as Z-tubules at the Z-line level. The distinctive rearrangement of this tubular system within atrial myocytes mirrors a differential location pattern of several key pieces involved in EC-coupling driving such as RyR and Ca_V1 (L-type) channels. Two populations of RyR channels are usually found in atrial myocytes, namely junctional and non-junctional RyR populations. Junctional RyR population are clusters of RyRs just localized beneath the sarcolemma, whereas non-junctional RyR channels represent the bulk population of RyR channels placed deeply inside of atrial myocytes (Bootman *et al*., 2011). Ca_V1 (L-type) channels from ventricular myocytes are mostly located in the t-tubules whereas functional Ca_V1 (L-type) channels of atrial myocytes are mainly restricted to their periphery (Mackenzie *et al*., 2004).

When an AP arrives at the sarcolemma of a certain myocyte, almost instantaneously (<1 ms), Ca^{2+} ions passing through Ca_V1 (L-type) channels "pull the trigger" and large amounts of SR Ca^{2+} are then released through RyRs, i.e. the CICR ("Ca^{2+}-induced Ca^{2+} release"). The close proximity of RyR to Ca_V1 (L-type) channels from sarcolemma means that junctional RyRs are much more sensitive to Ca^{2+} concentration changes within the dyadic junction and therefore much important for CICR than RyRs not junctionally located (Bootman *et al*., 2011). CICR creates a Ca^{2+} wave that sweeps over the entire myoplasm (Fabiato, 1983; Sipido *et al*., 1997; Bers, 2002; Cheng and Lederer, 2008). The recent laser scanning confocal microscopy techniques, together with the new generation of Ca^{2+} sensitive fluorescent probes is currently helping to get a deep insight into CICR phenomenon and how it is regulated. Rather than an isolated event, this massive $[Ca^{2+}]_i$ transient is a spatio-temporal summation of many Ca^{2+} sparks produced by numerous CICR events across the entire t-tubular system (Cheng and Lederer, 2008). Notwithstanding, under basal conditions, spontaneous Ca^{2+} sparks occur just by fluctuations of sarcoplasmic and cytosolic free Ca^{2+} concentrations and appear to be identical to $I_{Ca,L}$-evoked ones in terms of amplitude, kinetics, and spatial properties. However, AP-evoked Ca^{2+} sparks have higher frequencies (≈ 100 fold) when compared to spontaneous ones and, consequently, the latter have an overall Ca^{2+} transient usually too small to induce an E-C coupling (Cheng and Lederer, 2008). Thus, rather than a simple

local Ca^{2+} diffusion, CICR implies a precise engagement of numerous RyR/Ca_V1 (L-type) channels complexes.

Elicited Ca^{2+} sparks from ventricular myocytes are globally homogenous than those elicited in atrial myocytes, probably due to the above described ultrastructural differences between these two cell types. Atrial Ca^{2+} sparks are generated at the cellular periphery where junctional RyRs are located; they spread laterally till eventually they reach the centre of these cells (Mackenzie *et al*., 2004). As demonstrated by Mackenzie *et al*., under basal conditions Ca^{2+} movement toward internal Ca^{2+} stores (SR) is hindered by Ca^{2+} buffering properties of mitochondria and SERCA pumps. Therefore, atrial myocytes have a contractile reserve formed by internal SR Ca^{2+} store gated by non-juctional RyRs that are promptly recruited to enhance myocytes contractility during positive inotropic stimuli (e.g. adrenergic stimulus) (Mackenzie *et al*., 2004).

Other channels and transporters may also induce CICR [e.g. Ca_V3 (T-type) calcium channels, reverse-mode NCX] even though their role is not as important as the Ca_V1 (L-type) channels for E-C coupling (Sipido *et al*., 1997; Bers, 2002). During CICR, Ca_V1 (L-type) channels are mainly deactivated by a Ca^{2+}-dependent mechanism mediated by CaM (Pitt *et al*., 2001; Catterall, 2011; Best and Kamp, 2012) while RyR channel undergoes an inactivation period and only becomes ready to fire when SR Ca^{2+} backs to diastolic levels (Bers, 2002).

Although CICR is an all-or-nothing phenomenon, E-C coupling paradoxically exhibits a graded response that is dependent on amplitude and duration of $I_{Ca,L}$ (Bers, 2002). Several theories have emerged to explain this mysterious response but none, so far, has been completely conclusive (Cheng and Lederer, 2008). Essentially, E-C coupling is a function of amplitude and duration of global $[Ca^{2+}]_i$ transients that accounts for the number and properties of discrete Ca^{2+} releasing units timely recruited by an AP (Bers, 2002; Cheng and Lederer, 2008). The number of evoked $[Ca^{2+}]_i$ transients is voltage dependent whereas the single properties of each “couplon” is voltage-independent (Cheng and Lederer, 2008). For example, RyR channel gating properties, a key point for “couplons” regulation, is modulated by different ways (vide infra) such as: SR Ca^{2+} levels; post-transdutional modifications (e.g. (de)phosphorylation) and other protein-protein interactions (Bers, 2002).

The amount of Ca^{2+} released to cytosol during CICR largely exceeds the bulk intracellular Ca^{2+} concentration (from ≈ 100 nM to ≈ 1 μM) needed for contraction. In the resting state, or diastole, thin and thick filaments are partially superimposed, troponin I (TnI) is connected to actin hiding myosin binding sites on the actin molecule, and myosin “heads” have bound ATP molecules. This remains stable until the increase of cytosolic Ca^{2+} during an AP. As the Ca^{2+} signal penetrates deeper into the cell, large amounts of

Ca^{2+} bind to low affinity troponin C (TnC) sites inducing a structural change in the troponin complex that switches-on the contractile machinery. By pulling TnI off, Ca^{2+} binding to TnC exposes myosin-binding sites throughout actin filament (de Tombe, 2003). As soon as the myosin heads bind to actin filaments, the force-generating actin–myosin reaction hydrolyses ATP for the elastic bending and active tilting of myosin heads. The movement of myosin heads push the actin filaments and induce a decrease in sarcomere length, i.e. contraction (systole) (de Tombe, 2003). During sarcomere shortening, the Ca^{2+}-affinity of TnC gradually increases thereby more cross-bridges react with thin filaments, which explains cooperative activation of cardiac myofilaments (Bers, 2002; Solaro, 2008).

At the end of systole, the cytosolic Ca^{2+} concentration goes down, and then the contractile process is resumed getting it ready to fire to a new AP. When $[Ca^{2+}]_i$ drops to diastolic levels, the labile connection between Ca^{2+} and TnC is broken switching off the contractile machinery, and relaxation occurs. The relaxation process also needs synthesis of new ATP molecules to displace the ADP bound to myosin heads. Noteworthy, if cytosolic Ca^{2+} is not quickly removed the thin and thick filaments will continue to slide past each other decreasing even more the sarcomere length. Thus, the cardiac cycle depends on the kinetics and amount of cytosolic Ca^{2+} released in early systole and its withdrawal during diastole. The mechanism underlying this $[Ca^{2+}]_i$ drop is highly effective and similar to what happens in SA nodal cell SERCA and NCX (driven by Na^+-K^+ pump) removes the cytosolic Ca^{2+} into SR and to extracellular milieu, respectively. The plasma membrane Ca^{2+} ATPase (PMCA) and mitochondrial Ca^{2+} uniport also have an important role, although less important than the other ones, in driving Ca^{2+} out of the cytosol (Bers, 2002). These cytosolic Ca^{2+} removal mechanisms, aided by Ca^{2+} buffering molecules, are critical not only for relaxation but also to prevent the deleterious cellular effects produced by high cytosolic Ca^{2+} concentrations. However, the relative impact of each Ca^{2+} extrusion mechanism to decrease $[Ca^{2+}]$i may change between species as well as in pathological conditions (Bers,2002). In non-pathological conditions, the active Ca^{2+} concentration that induces a contraction is short-lived due to the highly efficient Ca^{2+} extrusion mechanisms present in myocytes. Reasonably, any perturbation on Ca^{2+} extrusion mechanisms yields an alteration of intracellular Ca^{2+} dynamics.

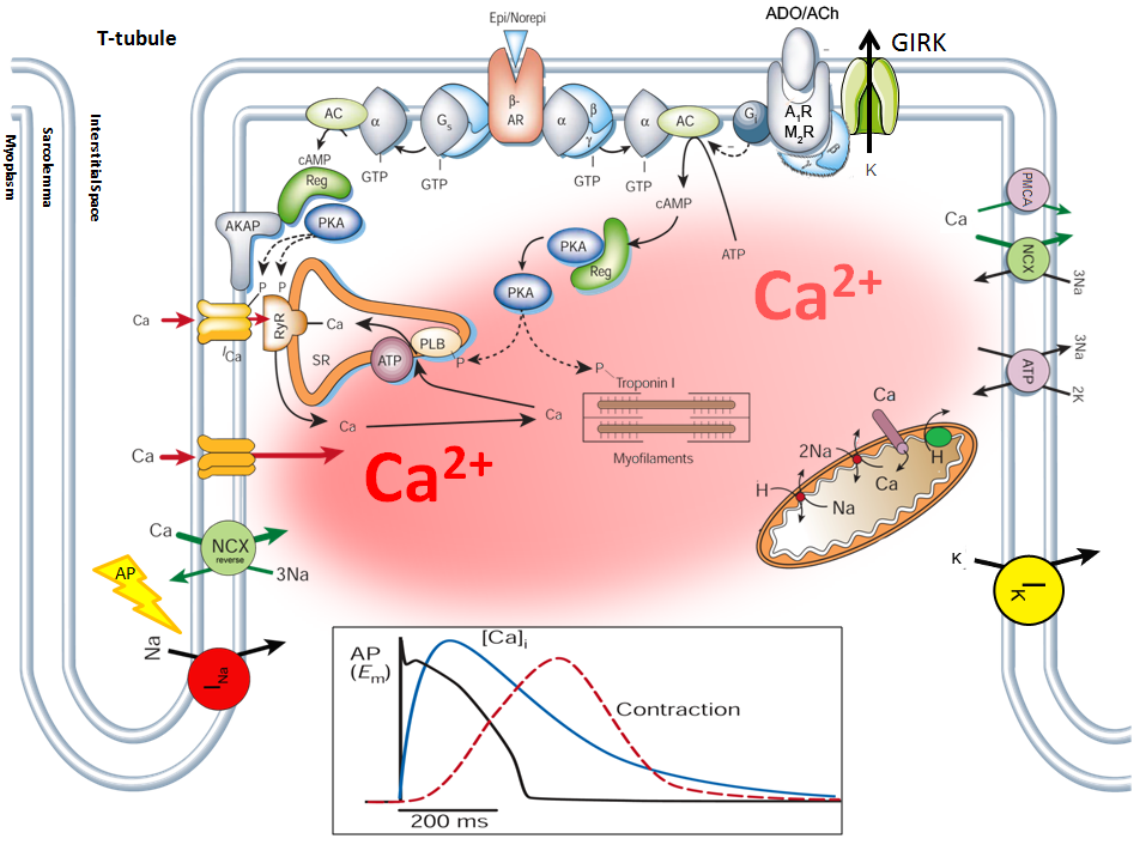

Figure 3. The excitation-contraction (E-C) coupling. Once an action potential (AP) reaches the t-tubular system of cardiomyocytes, Ca^{2+} entry through L-type voltage-gated calcium channels (I_{Ca}) ignites Ca^{2+}-induced SR Ca^{2+} release via ryanodine receptors (RyR), thus raising cytosolic Ca^{2+} concentration $[Ca^{2+}]_i$. Then, higher $[Ca^{2+}]_i$ switches on the contractile machinery that allows myocyte contraction. Just before reaching maximum active tension, the $[Ca^{2+}]_i$ drops to diastolic levels and muscle undergoes relaxation. Ion pumps (SERCA2a, PMCA and Na^+/K^+-ATPase pump), exchanger (Na^+/Ca^{2+} exchanger) and mitochondrial Ca^{2+} uniport drive Ca^{2+} removal from cytosol. Catecholamine (NE) binds to β-adrenoceptors (β-AR) and enhances adenylyl cyclase activity that further enhances the activity of cAMP-dependent protein kinase (PKA), whereas the opposite is true for Gαi/o-coupled receptor (e.g. M_2R and A_1R). PKA phosphorylates several key proteins related to E-C coupling (e.g. phospholamban, L-type Ca^{2+} channels (Ca_V1 (L-type) channels), RyR, inhibitory troponin (TnI)). During repolarization phase, outward potassium currents (I_K) bring sarcolemmal potential to diastolic potentials. GIRK/$K_{IR}3$ channel opening following A_1R and M_2R activation also accelerates the repolarization phase of APs. At the bottom of the figure, a typical action potentials, $[Ca_{2+}]_i$ transient and active tension generated during myocyte contraction are plotted as function of time (Adapted from (Bers, 2002)).

5. Regulation of Inotropy

The contraction strength of atrial and ventricular myocardium, also called as inotropy, has a large impact on stroke volume. Regulation of inotropy can be broadly achieved by interfering with either intracellular Ca^{2+} handling, myofilament Ca^{2+} sensitivity or cross-bridge kinetics (Bers, 2002; Solaro, 2008). Once again protein kinases and their downstream targets (often other kinases) have a central role on receptor-transmitted signal integration for inotropy regulation (Figure 3). Their activities control dynamics and intensity of cytoplasmic Ca^{2+}-transients triggered by APs that lastly control the

chemomechanical coupling between Ca^{2+} and myofilaments. Ca^{2+}-handling comprise uptake and extrusion mechanism of cytosolic Ca^{2+} ions, which are quite similar with those implicated in chronotropy regulation (Figure 2). As mentioned above, E-C coupling shows a graded response dependent of Ca^{2+} transients characteristics during a CICR (Bers, 2002; Cheng and Lederer, 2008), which in turns directly modulates the cross-bridge cycling rate, the number and the force of productive actin-myosin interactions (de Tombe, 2003). The amount of Ca^{2+} released from each CICR event is strictly related to SR Ca^{2+} concentration and it is tunable by $[Ca^{2+}]_i$. Essentially, when $[Ca^{2+}]_i$ increases, the SR Ca^{2+} content increases too (increase SR Ca^{2+} load) and, as a result, the likelihood of RyR opening is higher. When SR Ca^{2+} load and RyR activity are both elevated, the magnitude and frequency of spontaneous local Ca^{2+} release (Ca^{2+} sparks) is greater, even though Ca^{2+} sparks length remains unchanged (Lukyanenko *et al*., 1996). Thus, CICR phenomenon is enhanced by increasing Ca^{2+} influx, decreasing Ca^{2+} efflux, or enhancing Ca^{2+} uptake into SR (e.g. catecholamines or an increase in stimulation frequency, AP duration, I_{Ca} or $[Na^{+}]_i$) (Bers, 2002). Some of these effects are shared by adrenoceptors (e.g. β_1-AR) and other $G\alpha_s$-coupled receptors. For example, PKA (and CaMKII) relieves the tonic SERCA2a inhibition by phospholamban phosphorylation, which increases SR Ca^{2+} load and muscle relaxation, phoshorylates RyR channels increasing their Ca^{2+}-sensitivity and SR Ca^{2+}-leakage, and phosphorylates Ca_V1 (L-type) channels augmenting their own Ca^{2+}-conductance (Figure 3) (Kamp and Hell, 2000; Bers, 2002; Vinogradova *et al*., 2006; Catterall, 2011).

In addition, $G\alpha_q$-coupled receptors have been allocated to CICR mechanism. $G\alpha_q$-protein stimulates inositol phospholipids hydrolysis that, in turn, enhances IP_3R-induced Ca^{2+} store release (Berridge, 1993) and activates protein kinase C (PKC) (Nishizuka, 1992). PKC family is a group of serine/threonine kinases isoforms generally divided into 3 groups based on their structure and co-factors required for activation, namely: conventional PKCs (cPKCs: α, βI, βII and γ) require Ca^{2+}, phospholipids, DAG (or phorbol ester) for activation; novel PKCs (nPKCs: δ, ε, θ and η) are quite related to the conventional family but they are Ca^{2+}-independent; atypical PKCs (aPKCs: ζ and λ) are totally different from other family because they are not activated by DAG or phorbol esters neither by Ca^{2+} ions (Puceat and Vassort, 1996). PKC δ and ε were the major isozymes found in cardiomyocytes, at least in rats (Yang *et al.*, 2009b). PKC activation implies a translocation by receptor for activated protein kinase C (RACKs) and anchoring to specific cellular structures (Fenton *et al.*, 2009). Regarding the IP_3 role on inotropy, IP_3R2 is by far the highest IP_3 receptor subtype expressed in cardiomyocytes, with a 6-fold relative abundance in atrial myocytes when compared to ventricular ones. Moreover, IP_3R activation increases the rate and magnitude of spontaneous Ca^{2+} sparks (Lipp *et al*.,

2000). Interestingly, Lippin and colleagues found that this IP_3 receptor subtype is strategically placed near the Ca^{2+}-release units at the subsarcolemmal region and, curiously, located in the vicinity of IP_3 generation sites where enzymes (e.g. PLCβ) and $G\alpha_q$ protein-coupled receptors are placed. Interestingly, IP_3 seems to recruit a contractile reserve embraced from non-junctional regions of atrial myocytes (Mackenzie *et al*., 2004). Rather than truly effectors of CICR, it is thought that IP_3Rs act as positive modulators of E-C coupling (Lipp *et al*., 2000; Bers, 2002).

Besides length and amplitude of intracellular Ca^{2+} transients, the contraction force development depends on the myofilament Ca^{2+} sensitivity. Myofilament Ca^{2+} sensitivity can be changed by several factors such as: post- translational modifications (e.g. phosphorylation), stretch, pH, Pi and Mg^{2+} levels (Bers, 2002).

PKA and PKC are by far the most studied kinases related to phosphorylative regulation of myofilament mechanics. Other kinases, such as protein kinase G and CaMKII as well as myosin-light chain kinase also have an active role in myofilament regulation (Solaro, 2008). In general, myofilament phosphorylation decreases the sarcomere sensitivity for Ca^{2+}, which means that higher $[Ca^{2+}]_i$ is needed for a given contractile response as compared with lower levels of phosphorylated contractile proteins(de Tombe, 2003). Numerous GPCRs are targeted for myofilament modulation by phosphorylation, such as the well-know β_1-AR. Sympathetic activation increases force of contraction, chronotropy and lusitropy. In this situation, as the maximum rates of both tension development and relaxation increase, the time-course of each contraction decreases. Myofilament proteins are also phosphorylation targets by other kinases (e.g. PKC) showing sometimes similar and overlapping responses (Puceat and Vassort, 1996; Solaro, 2008). In general, TnI phosphorylation by PKA or PKC, induces conformational changes in troponin complex decreasing TnC-affinity for Ca^{2+} along with an increase in kinetics of actin-cross bridge reaction (Solaro, 2008). Thus, phosphorylation of thin filament proteins increases the turnover of myosin-actin cross-bridges, explaining the positive inotropy and lusitropy during adrenergic stimulation. Noteworthy, phosphorylative regulation is not so obvious and site-specific phosphorylation of myofilament proteins through isoform-specific kinases must not be overlooked. In fact, TnI (and other sarcomeric proteins) have multiple phosphorylation sites that exhibit isoform-specific phosphorylations by different kinases, sometimes classified as PKC sites or PKA sites, which may contribute somewhat to the existence of opposing and ambiguous effects described in literature (Solaro, 2008). For example, Wang *et al.* reported an increase in myofilament Ca^{2+} sensitivity by the PKC-βII phosphorylation of a specific site (Thr 144) on cardiac TnI in ventricular myocytes from mice (Wang *et al*., 2006). In the same line, but without identifying the isoform, PKC activity was connected to myofilament Ca^{2+}

sensitization and phosphorylation of TnI and cardiac myosin binding protein-C promoted by a positive inotropic effector (Cazorla *et al*., 2009). On the other hand, other PKC isozymes have been allocated to a negative cardiac inotropy, namely PKCα. (Liu *et al*., 2009). This PKC has been connected to Ca^{2+}-handling changes and negative inotropy, and its inhibition have demonstrated better outcomes in a mice model of heart failure (Liu *et al*., 2009).

Interestingly, specific regulation of myofilaments either by kinases or phosphatases may be relevant in some cardiovascular diseases if we take into account that some pathological conditions hold distinct protein expression/activity backgrounds. However, the functional effect of this site specific regulation on myofilament proteins is still ill-defined and additional work has to be done (Puceat and Vassort, 1996; Solaro, 2008).

Other important mechanism for myofilament Ca^{2+} sensitivity arise from the physiological relation between diastolic filling (preload) and cardiac output (heart rate x stroke volume), i.e. the Frank-Starling mechanism (Allen and Kentish, 1985; de Tombe *et al*., 2010). Thus, heart has itself an intrinsic mechanism that dynamically adjusts the active tension generated for a given diastolic blood volume. As the end-diastolic volume increases, the passive tension also increases (preload tension) and more tension is developed in ventricular myocytes. There is a clear relation between sarcomere length and muscle contractility that has, as its basis, the increase of myofilament Ca^{2+} sensitivity together with an increase of the number of successful cross-bridges number and also contractile force (Allen and Kentish, 1985). Despite the mechanism beneath this "myofilament length dependent activation" has been extensively studied, a clear theory that fits all experimental data is still lacking (de Tombe *et al*., 2010).

6. Adenosinergic triad: metabolism, receptors and function

6.1. Adenosine metabolism

ADO is an endogenous purine nucleoside implicated in many cellular key functions like nucleotide biosynthesis, amino acid metabolism and several energetically costly processes (Shryock and Belardinelli, 1997). Therefore, ADO is ubiquitously present in all cell types and, upon stressful stimuli (e.g. hypoxia, ischemia and adrenergic stimulation) its extracellular concentration quickly rises up (Sparks and Bardenheuer, 1986). In such situations, where oxygen supply is decreased and/or oxygen consumption is high, ADO released from metabolically compromised cells acts as a retaliatory metabolite decreasing energetic demand / supply ratio (Berne, 1963; Sparks and Bardenheuer, 1986). Metabolic impairment is not the only way to promote ADO release from cells other physiological and

pathological stimulus (e.g. inflammation, stretching) could also enhance ADO release levels (Headrick *et al*., 2011). Regardless, adenosinergic system is not restricted to retaliation, it also exhibits regulatory and more sustained adaptive responses, which are of great importance for the acute fine-tuning of many cellular processes under physiological conditions, but also for orchestrating structural and functional changes in the diseased cardiovascular system (Headrick *et al*., 2011).

In cardiac territory, cardiomyocytes, endothelial cells, and smooth muscle are the main sources of purines, but under oxygen deprivation purines derived from myocardial cells assumes particular importance (Shryock and Belardinelli, 1997). ADO metabolism is compartmentalized and it can be generated from both extracellular and intracellular compartments, the latter being responsible over 90% of the total ADO production in normoxia (Deussen, 2000). The extracellular ADO generation pathway comprises the enzymatic catabolism of adenine nucleotides (ATP, ADP and AMP) by nucleotide-converting ectoenzymes located on the surface membrane of many cells (Figure 4) (Yegutkin, 2008). Adenine nucleotides significantly rise in the extracellular milieu during low oxygen tension and high cardiac sympathetic drive (Vassort, 2001). Leakage of adenine nucleotides to the extracellular medium exposes them to the action ectonucleotidases action, which quickly metabolizes ATP and ADP into AMP. AMP is then irreversibly desphosphorylated to ADO by 5'-ectonucleotidase (CD73) (Deussen, 2000). Interestingly, before complete dephosphorylation takes place, extracellular nucleotides can exert a wide variety of signaling effects in cardiovascular regulation by acting on P2 receptors family that are further divided into ionotropic P2X1-7 and metabotropic $P2Y_{1,2,4,6,11,12,13,14}$ receptors (Figure 4) (Erlinge and Burnstock, 2008).

The main source of ADO is the intracellular pool of 5´-AMP, which undergoes dephosphorilation by cytosolic 5'-ectonucleotidase (Deussen, 2000; Headrick *et al*., 2011). Hydrolysis of s-adenosylhomocysteine is another intracellular source of ADO (Schrader *et al*., 1981). Stressful insults increase both extracellular and intracellular ADO generation pathways (Shryock and Belardinelli, 1997). In truth, energy status impairment dramatically increases about 61- to 73-fold ADO production rate as compared to basal conditions in the rat heart (Deussen, 2000). In such conditions, the amount of intracellular ADO is so high that ADO kinase, mainly responsible for its rephosphorylation, and ADO deaminase, which deaminates ADO to inosine, are saturated and are no longer able to stop the massive release of ADO and other nucleotides (Deussen, 2000). ADO and other nucleotides come to extracellular medium by facilitated transport through nucleotide transporters that span the cellular membrane. ADO and its nucleotides can also appear in the interstitial fluid by other mechanisms such as: cell damage; exocytosis; hemichannels and other ionic channels (Fredholm *et al*., 2011). Once in the extracellular medium, ADO

binds and stimulates its sensitive receptors (see below, Figure 4). After exerting its signaling effects, ADO is promptly removed from ADO receptors vicinity, thus localizing their effects to ADO releasing sites. This is accomplished by different mechanisms, in rough order of importance: cellular uptake through nucleoside transporters driven by ADO kinase and through enzymatic deamination by either intra- or extracellular ADO deaminase. If ADO removal does not take place (e.g. with dipyridamole), its extracellular concentration rises and, consequently, adenosinergic signaling increases (Shryock and Belardinelli, 1997; Deussen, 2000).

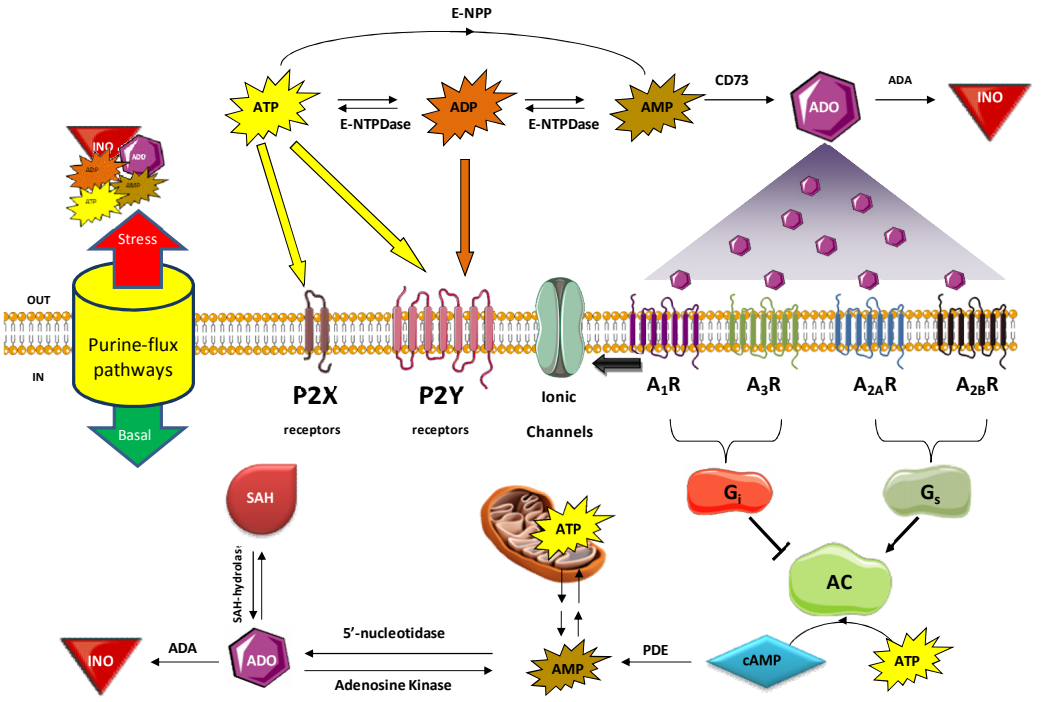

Figure 4. Metabolism and signaling properties of adenosine (ADO) and its nucleotides. Nucleotide-hydrolysing pathway comprises at least three ectoenzymes namely: ecto-nucleotide pyrophosphatase/phosphodiesterase (E-NPP), (E-NTPDase) and ecto-5'-nucleotidase (CD73). CD73 can be found in both extracellular and intracellular compartments. As extracellular nucleotides are sequentially inter-converted to ADO they act as ligands for P2 receptors. While ATP activate either ionotropic P2X or metabotropic P2Y receptors, ADP mainly activate P2Y receptors. Once ADP or ATP are dephosphorylated to AMP, it is hydrolyzed to adenosine by CD73. In turns, ADO activates four ADO-sensitive receptors with different binding affinities for this nucleoside. A_1R and A_3R are classical described as inhibitors of adenylyl cyclase (AC) whilst the remaining receptors ($A_{2A}R$ and $A_{2B}R$) stimulate its activity. Signaling pathways downstream of ADO receptors are not restricted to modulation of AC or other enzymes, they can also directly change the gating properties of some ionic channels. AC converts ATP to cAMP as long as the $G\alpha_s$ subunit is activated. Stimulatory effects of cAMP cease by phosphodiesterase (PDE)-mediated hydrolysis of its phosphodiester bonds leading to AMP formation. Inside cell, ADO is generated through of either S-adenosylhomocysteine (SAH) or AMP. Termination of adenosinergic signaling involves deamination ADO to inosine (INO) by ADO deaminase (ADA). Flux direction of adenine nucleosides and nucleotides are dependent of several factor, including cellular oxygen tension. Modified from (Yegutkin, 2008) and (Deussen, 2000).

6.2. Adenosine receptors and heart function

Intravenous administration of this nucleoside rapidly slows the sinus rhythm (negative chronotropism), decreases atrioventricular conduction (negative dromotropism), and contractile force (negative inotropism), dilates the coronary vessels and also has anti-arrhythmic effects (Drury and Szent-Gyorgyi, 1929). In the extracellular medium, ADO exerts protective effects through its binding to ADO-sensitive receptors, also known as P1 receptors. Up to date there are four different ADO receptor subtypes characterized, namely: A_1R, $A_{2A}R$, $A_{2B}R$, and A_3R (Figure 4) (Fredholm *et al*., 2011). ADO receptors are seven transmembrane-spanning proteins that belong to the large family of GPCR. Based on their preferential coupling to a trimeric G-protein subtype, ADO receptors are classical divided into stimulators ($A_{2A}R$ and $A_{2B}R$) and inhibitors (A_1R and A_3R) of adenylate cyclase activity (Figure 4). ADO receptors can be further divided into high affinity receptor, where A_1R and $A_{2A}R$ are included, whereas $A_{2B}R$ and A_3R receptors have low affinity for their endogenous ligand at least in rodents (Shryock and Belardinelli, 1997; Fredholm *et al*., 2011).

In the whole body, ADO produces a great diversity of effects, in agreement with the widely expression of ADO-sensitive receptors (Shryock and Belardinelli, 1997; Fredholm *et al*., 2011; Headrick *et al*., 2011). Coronary dilatation is definitively attributed to stimulatory ADO receptors (Berne, 1963), even though some controversy exists around the A_2 receptor(s) ($A_{2A}R$ and/or $A_{2B}R$) that mediate(s) coronary vessels dilatation (Shryock and Belardinelli, 1997; Headrick *et al*., 2011). The remaining effects above described by Drury and Szent-Gyorgyi were mostly mediated through A_1R activation. Thus endogenous ADO under stressful conditions, increases heart muscle feeding by increasing coronary flow while it reduces the overall energy demand by decreasing heart work (Berne, 1963; Shryock and Belardinelli, 1997; Headrick *et al*., 2011).

ADO's net signaling relies on its extracellular concentration, and also on the relative distribution, compartmentalization and expression pattern of ARs on the surface of individual cell types that constitutes a specific tissue in which they exist. Impairment of these signaling checkpoints may underlie the dysfunction observed in some pathological conditions (Headrick *et al*., 2011). The connection between ADO receptor and its signaling effectors is far from easy as so many proteins have been described as important regulators of adenosinergic signaling. These proteins include different G-proteins types, arrestins and other scaffold proteins (Verzijl and Ijzerman, 2011), which are organized and well-compartmentalized in membrane domains (Lasley, 2011). These signaling hotspots (membrane domains) have attracted much attention of the scientific community, not only in respect to ADO receptor signaling but to all GPCRs (Patel *et al*., 2008). Astonishingly, a

wide variety of experimental data has put forward the hypothesis that several pieces that gear the adenosinergic system (e.g. ADO receptors, nucleotidases, nucleoside transporters, signaling effectors) are confined within caveolae domains (Yang *et al*., 2009b; Lasley, 2011).

A_1R couples to $G\alpha_{i/o}$ proteins and when activated mediates K^+ efflux through the release of Gβγ (Kurachi *et al*., 1986) (see below) and decreases PKA activity via inhibition of AC (LaMonica *et al*., 1985), counteracting the responses yield from catecholamine binding to β_1-AR, also known as the anti-β-adrenergic effect (Dobson, 1983). Acting on presynaptic A_1R heteroreceptors from sympathetic cardiac nerve endings, ADO derived from sympathetic transmission refrain exocytotic catecholamine release, further contributing to anti-β-adrenergic effect (Lorbar *et al*., 2004). The anti-β-adrenergic effect seems to be more complex than a simple inhibitory action on AC activity. Recent reports have demonstrated a PKC-ε activation dependence on the anti-β-adrenergic effect upon A_1R stimulation (Fenton *et al*., 2009; Fenton *et al*., 2010). Therefore, A_1R may functionally couple to signaling pathways other than $G\alpha_{i/o}$ protein-mediated AC inhibition. Recent evidences clearly suggest that A_1R activation rapidly and selectively induces the translocation of epsilon and sigma PKC isoforms from cytosol to the caveolin-rich sarcolemma microdomains (Yang *et al*., 2009b). Previous findings demonstrated a functional coupling of A_1R to PKC-dependent process involving Gβγ subunits and PLC activation, accompanied by an increase of phospholipid turnover and, sometimes, Ca^{2+} mobilization (Gerwins and Fredholm, 1992; Dickenson and Hill, 1998; Cordeaux *et al*., 2000). However, this secondary pathway should only play a relevant role in tissues with higher A_1R density (Boyer *et al*., 1992; Biber *et al*., 1997). Thus, one should take care when interpreting these data since these atypical effects proposed for A_1R depends on the level of receptor expression and also on the type of agonist present (Ashkenazi *et al*., 1987; Biber *et al*., 1997; Cordeaux *et al*., 2000; Verzijl and Ijzerman, 2011).

$A_{2A}R$ signaling, as referred above, is primarily mediated via its coupling to $G\alpha_s$-protein (Shryock and Belardinelli, 1997), which is sensitive to cholera toxin treatment (Milligan and Kostenis, 2006). In the working myocardium there are some evidences that stimulation of this receptor elicit positive inotropic responses (Dobson and Fenton, 1997; Monahan *et al*., 2000; Tikh *et al*., 2006), although this has been challenged by others (Willems and Headrick, 2007; Chandrasekera *et al*., 2010). Given the stimulatory nature of this receptor on AC, which opposes A_1R action, $A_{2A}R$ may also control the anti-β-adrenergic action of A_1R (Tikh *et al*., 2006). The long cytoplasmic tail is also a characteristic of $A_{2A}R$, which makes it suitable for interaction with many other proteins that are summarized elsewhere (Verzijl and Ijzerman, 2011). The recent crystallographic data

of $A_{2A}R$ will certainly enlarge the number of proteins along with the number of ligands that interact with this receptor (Lebon *et al*., 2011).

$A_{2B}R$ is coupled to $G\alpha_s$-protein and stimulation of PLCβ activity has also been proposed for $A_{2B}R$, but its mechanism is still ill-defined, despite some evidence that points to be mediated via $G\alpha_{q/11}$ proteins (Linden *et al*., 1999). Furthermore, $A_{2B}R$ have direct positive inotropic properties in the working myocardium since its stimulation increases cardiac contractility (Chandrasekera *et al*., 2010).

Finally, the A_3R, apart from its conventional coupling to $G\alpha_{i/o}$-protein, couples to $G\alpha_{q/11}$ protein (Shryock and Belardinelli, 1997).

6.3. Adenosine and cardiac electrophysiology

For a long time, the scientific community has wondered about what it is behind ADO effects on cardiac territory. After numerous experiments, it is now recognized that cardiodepressor effects of ADO are mainly mediated through A_1R activation (Belardinelli *et al*., 1995). A_1R has both direct and indirect effects on supraventricular tissues and only indirect effects on ventricles of most mammals (Dobson, 1983; Belardinelli *et al*., 1995). Cardiac response to ADO exhibits a regional heterogeneity and species dependence, which possibly takes into account the differential expression pattern of this receptor or its effectors (e.g. GIRK/K_{IR}3 channels) throughout the heart of different species (Belardinelli *et al*., 1995). In fact, when compared with atrium, GIRK/K_{IR}3 channels are weakly expressed in the ventricular tissue from mammalian hearts (Krapivinsky *et al*., 1995; Dobrzynski *et al*., 2001). In general, the magnitude of cardiac electrophysiological response to ADO gradually vanishes from the SA node toward ventricles. In ventricles from several species (e.g. guinea pig, rabbit, bovine, human) it is thought that ADO exhibits only indirect effects, with exceptions for ferret and rat hearts (Belardinelli *et al*., 1995).

Activation of A_1R leads to K^+ efflux (I_{KAdo}) across the cell membrane (direct effects) thus reducing cellular electrical excitability (Belardinelli *et al*., 1988). This hyperpolarizing current resembles the one elicited by vagally released ACh. In fact, either ADO or ACh activate the same population of cardiac potassium channels (Kurachi *et al*., 1986), currently known as GIRK/K_{IR}3 channels (Krapivinsky *et al*., 1995). However, A_1R-mediated effects are not restricted to GIRK/K_{IR}3 channels opening, since in GIRK4/K_{IR}3.4-deficient mice (without $I_{KACh,Ado}$) a selective A_1R agonist was still able to elicit bradycardia (Wickman *et al*., 1998), in agreement with recent reports (Lyashkov *et al*., 2009). This insensitive bradycardic response to $I_{KACh,Ado}$ suppression (around 50% of the A_1R

response (Wickman *et al*., 1998)) is probably due to the inhibitory action of ADO on catecholamine-elicited effects, i.e. the anti-β-adrenergic effect (indirect effects) (Dobson, 1983). The anti-β-adrenergic effect of ADO is explained by the inhibitory nature of A_1R on AC (LaMonica *et al*., 1985). This enzyme is pivotal for the integration of signals that arise from $G\alpha_s$ protein-coupled receptors (e.g. β_1-AR) (Bers, 2002; Vinogradova *et al*., 2006; Lakatta *et al*., 2010). Interestingly, a recent study demonstrates that SA nodal cells have high basal levels of cAMP and PKA activity in resting conditions (Vinogradova *et al*., 2006). Therefore, in SA nodal cells, A_1R stimulation antagonizes catecholamine-stimulated ionic current (e.g. $I_{Ca,L}$ and I_f) even under basal conditions, and mediates K^+ efflux through GIRK/K_{IR}3 channels (Belardinelli *et al*., 1988).

The dual action of A_1R is still present in atrial myocardium (Belardinelli *et al*., 1995). ADO mediates negative inotropic responses in supraventricular tissues through its anti-β-adrenergic effect and activation of $I_{KACh,Ado}$ (LaMonica *et al*., 1985; Kurachi *et al*., 1986). When $G\alpha_s$ protein-coupled receptors of atrial cells are not being stimulated, the average cAMP content is very low (Vinogradova *et al*., 2006), hence inhibition of AC on atrial contraction is not meaningful (Belardinelli *et al*., 1995). In such conditions, ADO effects are almost mediated through engagement of direct mechanisms rather than its anti-β-adrenergic effect (Belardinelli *et al*., 1988). In addition, some authors have demonstrated direct and negative effects of ADO (via A_1R) and ACh (via M_2R) on non-stimulated $I_{Ca,L}$ in atrial cells (about 30% $I_{Ca,L}$ reduction) (Cerbai *et al*., 1988; Visentin *et al*., 1990). Conversely, other authors failed to observe any direct effect on these ionic currents after application of either ADO or ACh under basal conditions (Iijima *et al*., 1985; Wang and Belardinelli, 1994). Thus, the inhibition of basal $I_{Ca,L}$ is small and seems to require higher concentrations of agonist than those required to activate $I_{KADO,ACh}$ (Visentin *et al*., 1990; Wang and Belardinelli, 1994; Belardinelli *et al*., 1995). Since ADO accelerates membrane repolarisation (via I_{KAdo}), the reported reductions of the recorded $I_{Ca,L}$ after ADO/ACh exposure may result from a reduced time available for Ca^{2+} influx due to shorter APs (Iijima *et al*., 1985; Wang and Belardinelli, 1994; Ford and Broadley, 1999). Furthermore, hyperpolarizing K^+ current through GIRK/K_{IR}3 channels opening may also refrain electrogenic currents present in the rising phase of the AP, namely $I_{Ca,L}$ (Amin *et al*., 2010), and limit Ca^{2+} influx into cardiomyocytes, explaining the negative inotropy for ADO in non-catecholamine stimulated atrium. In an attempt to characterize the biphasic inotropic effect of ATP observed in diseased human atrium, Gergs and co-workers unexpectedly observed positive inotropic effects for higher ADO concentrations (above 5 μM) that were sensitive to A_1R blockade, even though A_1R agonist R-PIA produced only negative inotropic effects (Gergs *et al*., 2009). Likewise, selective A_1R stimulation elicited positive inotropy in atria from mice overexpressing A_1R, without affecting negative

chronotropy (Neumann *et al*., 1999). Therefore, impairment of A_1R function may underlie some of the paradoxical effects observed in the previous studies and emphasize its relevance in the development of cardiovascular diseases (Headrick *et al*., 2011). These inconsistencies certainly deserve further investigations.

The negative dromotropy of ADO is mostly derived by its action in the atrioventricular node, where it activates hyperpolarizing I_{KAdo}, thereby shortening the duration, rate and amplitude of APs (Belardinelli *et al*., 1995). The ADO effect in the atrioventricular node is particularly important to limit reentrant circuits responsible for arrhythmogenic episodes (DiMarco *et al*., 1983). Therefore, ADO and its derivates have cardiac properties that make it suitable for treatment of some type of supraventricular tachyarrhythmias (Blomstrom-Lundqvist *et al*., 2003; Ellenbogen *et al*., 2005).

Intravenous administration of ADO bolus (Adenocard®), together with the Ca_V1 (L-type) channels blocker verapamil, has been extensively used for many years in the clinical setting for acute conversion of paroxysmal supraventricular tachycardia (PSVT) into sinus rhythm (DiMarco *et al*., 1983; Riccardi *et al*., 2008). ADO, due to its short half-life, electrophysiological and atrial-selective properties, has also been used as a diagnostic of certain wide QRS complex tachyarrhythmias (O'Rourke *et al*., 1999) and assessment of accessory atrioventricular pathway ablation (Keim *et al*., 1992). Due to its anti-β-adrenergic effect, ADO can abrogate ventricular arrhythmias elicited by catecholamines (Lerman *et al*., 1986). However, administration of large ADO amounts into bloodstream has some side effects such as flushing, dyspnea, chest discomfort, and hypotension, but fortunately they are short-lived and generally not severe (Riccardi *et al*., 2008). In order to overcome these side effects, new stable and ADO receptor selective agonists have been developed and tested in clinical trials. For example, tecadenoson® (CVT-510) is a stable A_1R-selective agonist that already entered clinical trials to circumvent paroxysmal supraventricular tachycardia and atrial fibrillation, without any significant side effects reported (Ellenbogen *et al*., 2005). The powerful electrophysiological effects of ADO may sensitize supraventricular tissues for rhythmic disorders. Indeed, proarrhythmic episodes have been reported and connected to shorter atrial AP and refractoriness after ADO administration (Kabell *et al*., 1994) and, more recently, to A_1R/PLC/PKC pathway, followed by downstream sarcolemmal Ca^{2+} entry through transient receptor potential canonical (TRPC) channel 3 (Sabourin *et al*., 2012). Therefore, one should consider the likelihood of arrhythmias development promoted by higher ADO levels in the interstitial fluid of the myocardium, as observed during hypoxia or ischemia (Berne, 1963; Sparks and Bardenheuer, 1986)

II. Aims of research

Heart function matches body needs through numerous neurohormonal agents released from the myocardium itself, neurons, as well as other molecules secreted into bloodstream from distant cells. While catecholamines bind to β_1-AR to increase cardiac output, ACh released from vagal fibers activates M_2R to break cardiac activity. Nonetheless, cardiovascular homeostasis cannot be achieved solely through these two neurohormonal systems; other molecules provide the fine-tuning needed for a synchronous heart activity with instantaneous body demands. ADO is one of the best-known molecules involved in regulation and retaliation of the cardiovascular system (Headrick *et al*., 2011). Despite decades of research there is still much which remains unknown about the role of ADO on several physiological and pathophysiological processes. The physiological and clinical relevance of ADO led us to investigate signaling events initiated by purinergic receptors in supraventricular tissues. Previous findings from our lab conducted in spontaneously beating rat atria demonstrated that ADO, via A_1R activation, is an atrial-selective depressant that exhibits a higher sensitivity for chronotropy than for inotropy regulation (Oliveira-Monteiro *et al*., unpublished observations). In this context, the present study was undertaken to investigate the rationale for the A_1R-mediated chronoselectivity in the spontaneously beating rat atria. Since, A_1R is extensively linked to electrophysiological changes through modulation of sarcolemmal Ca^{2+} and K^+ oscillations, we aimed at evaluating whether A_1R chronoselectivity was somehow connected to the activity of subtype-selective cardiac ion channels and whether it was also coupled to intracellular enzymatic pathways. To this end, we took advantage of several techniques that are routinely used by our group, namely *in vitro* myographic recordings and laser scanning confocal microscopy to evaluate the function and distribution of A_1R, ionic channels and other downstream effectors. For comparison purposes, we also evaluated the activity and distribution of M_2 receptors in rat atria.

III. Materials and methods

1. Animals

The experiments were carried out on isolated spontaneously beating atria of Wistar rats (*Rattus norvegicus*; 250-300 g) of either sex (Charles River - CRIFFA, Barcelona, Spain; Vivarium ICBAS, Porto, Portugal). Rats were kept at a constant temperature (21º C) and a regular light (06.30-19.30h)-dark (19.30-06.30h) cycle, with food and water *ad libitum*. The animals were killed by decapitation followed by exsanguination (Rodent guillotine, Stoelting 51330). Animal handling and experiments followed the guidelines defined by the European Communities Council Directive (86/609/EEC).

2. Isolated perfused spontaneously beating rat atria

Isolated perfused beating atria were prepared using a previously described method (Ford and Broadley, 1999), with minor modifications. In brief, hearts were rapidly excised and placed in a physiological solution (Tyrode's solution) composed of (mM): NaCl 137; KCl 2.7; $CaCl_2$ 1.8; $MgCl_2$ 1; NaH_2PO_4 0.4; $NaHCO_3$ 11.9; glucose 11.2 and gassed with 95% O_2 + 5% CO_2 (at pH 7.4). Hearts were allowed to beat freely for a few seconds at room temperature, to empty its blood content. The paired rat atria were dissected out, cleaned of fatty tissues, and suspended in a 14-mL organ bath containing gassed Tyrode's solution at 37ºC. Each end of the preparation was tied and connected with thread to the organ bath wall and to an isometric force transducer (MLT050/D; AD Instruments, Colorado Springs, CO, USA). Changes in isometric tension were recorded continuously by use of a PowerLab data acquisition system (Chart 5, version 4.2; AD Instruments, Colorado Springs, CO, USA). The preparations were allowed to equilibrate for 30-40 min (in perfusion). During this time, tension was adjusted to a final tension of 9.8 mN. This procedure allows atria (with intact SA node) to progressively recover rhythmic spontaneous beatings.

3. Experimental design

After reaching a steady-state, the perfusion with Tyrode´s solution was stopped and the preparations were incubated with increasing concentrations of R-(-)-N^6-(2-phenylisopropyl)adenosine (R-PIA, 0.001-1 μM), a stable ADO A_1R agonist, or oxotremorine (0.01-3 μM), a muscarinic M_2 receptor agonist, either in the absence and in

the presence of 1,3-dipropyl-8-cyclopentylxanthine (DPCPX, 100 nM) or AF-DX 116 (10 μM), which respectively block A_1 and M_2 receptors. The A_{2A} receptor agonist, 2-p-(2-carboxyethyl)phenethylamino-5′-N-ethylcarboxamidoadenosine (CGS21680, 0.3 nM-1 μM) was also tested in some of the experiments. Agonists were added cumulatively to the bathing solution every 2 minutes.

To examine the role of K^+ and Ca^{2+} channel currents in the effects of ADO A_1 and muscarinic M_2 receptors activation, concentration-response curves to R-PIA (0.001-1 μM) and oxotremorine (0.01-3 μM) were established in the presence of the following inhibitors: 4-aminopyridine (4-AP, 10 μM), a nonspecific voltage-dependent K_v channel blocker, glibenclamide (10 μM), a selective blocker of ATP-sensitive $K_{ATP}/K_{IR}6$ channels, tertiapin Q (300 nM), a blocker of GIRK/$K_{IR}3$ channels with high affinity for K_{IR} 3.1/3.4 channels, apamin (30 nM), an inhibitor of small-conductance Ca^{2+}-activated K^+ ($K_{Ca}2$/SK) channels, verapamil (1 μM), a selective blocker of high voltage-activated Ca_v1 (L-type) channels, and mibefradil (3 μM), a low voltage-activated Ca_v3 (T-type) channel blocker. The influence of the PLCβ-PKC pathway on the effects of A_1R and M_2R stimulation was also evaluated in this study by using several modulators of this signal transduction pathway: U73122 (3 μM), a phospholipase C inhibitor, chelerythrine chloride (3 μM), a potent and cell-permeable inhibitor of several PKC isoforms, phorbol 12-myristate 13-acetate (PMA, 10 μM), a potent and broadly-activator of PKCs, AngII, an endogenous peptide agonist of angiontensin receptor, and UTP, as an P2Y receptor agonist (particularly $P2Y_{2,4}$). All the inhibitors were pre-incubated with the preparations for at least 15 min before R-PIA or oxotremorine application. The concentrations of the inhibitors in this study were within the range of channel selectivity described in the literature. To evaluate intrinsic effects of each drug on spontaneously beating rat atria under basal conditions, concentration-response curves were constructed for all drugs by adding them in a cumulative stepwise manner every 2 minutes.

4. Immunofluorescence staining and confocal microscopy studies

Rat hearts were excised (see above) and placed in oxygenated Tyrode's solution at 33–34°C. Following heart excision the right atrium containing the SA node region and surrounding atrial muscle was accurately isolated. Tissue fragments were stretched to all directions, pinned flat onto cork slices and embedded in Shandon cryomatrix (Thermo Scientific) before frozen in a liquid nitrogen-isopentane bath. Frozen sections with 8 μm of thickness were cut perpendicular to the *crista terminalis* of the right atrium (see Figure 5A). Once defrosted, tissue sections were fixed in phosphate buffered saline (PBS) containing 50% acetone and 2% paraformaldehyde. Following fixation, the preparations

were washed three times for 10 min each using 0.1 M PBS and incubated with a blocking buffer, consisting in fetal bovine serum 10%, bovine serum albumin 1%, Triton X-100 0.3% in PBS, for 2 h. After blocking and permeabilization, samples were incubated with selected primary antibodies (Table 1) diluted in incubation buffer (fetal bovine serum 5%, serum albumin 1%, Triton X-100 0.3% in PBS), overnight at 4ºC. For double immunostaining, antibodies were combined before application to tissue samples. Following the washout of primary antibodies with PBS (3 cycles of 10 min), tissue samples were incubated with species-specific secondary antibodies (Table 1) in the dark for two hours, at room temperature. Finally, VectaShield mounting medium, with 4´-6-diamidino-2-phenylindole (DAPI) to stain the nuclei, (H-1200; Vector Labs) was used to cover-slip the glass slides. Observations were performed and analyzed with a laser-scanning confocal microscope (Olympus Fluo View, FV1000, Tokyo, Japan).

Table 1. Antibodies used in immunohistochemistry studies and their technical specifications.

Antibody	Host	Code	Dilution	Supplier
Primary Antibodies				
A_1R	Rabbit	AB 1587P	1:100	Chemicon
$A_{2A}R$	Rabbit	A2aR21-A	1:75	Alpha Diagnostic
M_2R	Rabbit	AMR-002	1:200	Alomone
NF160	Mouse	ab7794	1:1000	Abcam
Cx43	Rabbit	ab11370	1:700	
GIRK1/K_{ir}3.1	Rabbit	ab61191	1:500	
$Ca_V\alpha_2\delta$-1	Mouse	ab2864	1:50	
K_{Ca}2.2/SK2	Goat	AP10032PU-N	1:200	
K_{Ca}2.3/SK3	Rabbit	ab83737	1:300	
Secondary Antibodies				
Alexa Fluor 488 anti-rabbit	Donkey	A-21206	1/1500	Molecular Probes
Alexa Fluor 568 anti-mouse	Donkey	A-10037	1/1500	
Alexa Fluor 568 anti-goat	Donkey	A-21082	1/1500	

The SA node region is found in close proximity to subepicardial sinus node artery (arrow in Figure 5B). SA node is characterized by a large number of neurofilament 160 (NF-160) positive neuronal fibres (Dobrzynski *et al*., 2005; Tellez *et al*., 2006; Allah *et al*., 2011), and small-size cardiomyocytes that are negative against connexin-43 (Cx43) staining, a gap junction protein ubiquitously expressed in the heart apart from in nodal tissue (van Kempen *et al*., 1991) (Figure 5C). Cells within SA node are surrounded by dense connective tissue; collagen fibres (light blue staining) can be differentiated from cardiomyocytes (red staining) with the Masson's trichrome staining (Figure 5B).

5. Masson's trichrome staining

Masson's trichrome staining was carried out in right atrial sections from rat heart. Briefly, right atrial appendage was dissected, excised and immersed in 4% formalin buffered solution, followed by routine tissue processing for paraffin embedding. Paraffin blocks were sectioned (≈ 10 μM sections) perpendicular to the *crista terminalis* of right atria wall, in a similar manner to that performed for immunfluorescence staining. Paraffin-embedded sections were dewaxed and rehydrated with xylene followed by a graded alcohol series [100%, 95% and 70% (v/v) mixtures of ethanol and water] to distilled water. Atrial sections were subsequently fixed in Bouin's solution for 1 hour at 60ºC and rinsed in tap water. Sections were first stained with Celestine blue (5 min) and Gill Hematoxylin 2 afterwards (4 min). Each staining step was followed by a 15-minute washout period in distilled water. Secondly, a mixture of 1% (v/v) acid fuchsin solution in 1% (v/v) ponceau de xylidine solution, both in 1% (v/v) acetic acid, was added to sections for 5 min to stain atrial muscle red. Sections were then washed in distilled water and placed in phosphomolybdic acid solution (1% [w/v] phosphomolybdic acid) for 15 minutes and later stained with 2.5 % (v/v) aniline blue solution (in 2.5 % [v/v] acetic acid) during 5 minutes till new wash with distilled water. After staining procedure, sections were dehydrated (stepwise increases of ethanol in water from 70-100% [v/v]), cleared (xylene for 2 minutes) and mounted in coverslip slides using D.P.X. mounting medium (Sigma). Masson's trichrome technique stains nuclei dark blue whilst muscle and connective tissue are stained red and blue, respectively. Stained sections were viewed and photographed using light microscopy (Olympus Fluo View, FV1000, Tokyo, Japan) and *Cell F* software (Olympus, Japan) was used to collect the images.

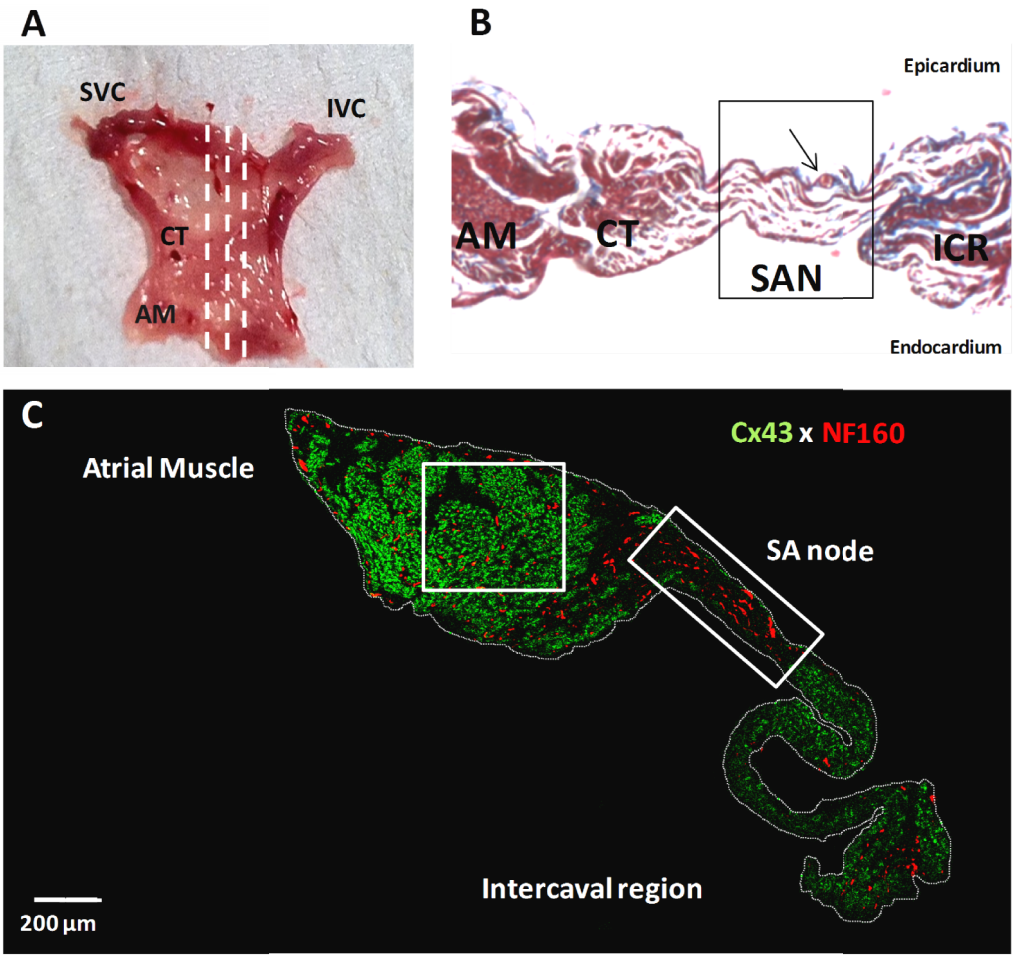

Figure 5. Anatomical and molecular identification of the rat SA node (A, B and C). A, Endocardial view of a typical rat atrial muscle-SA node preparation. Dashed lines indicate the orientation of cuts performed on the right atrial appendage for Masson's trichrome staining and immunofluorescence analysis. B, High-magnification (400x) images of Masson's trichrome staining of SA node (dashed box) and surrounding regions; AM, atrial muscle; CT, *crista terminalis*; ICR, intercaval region. Red staining, myocytes; blue staining, connective tissue. Black arrow indicates the SA node artery. C, Montage of confocal optical sections showing immunelabelling for connexin 43 protein (Cx43, green signal) and neurofilament 160 (NF160, red signal) throughout the right atrial appendage from the rat. Boxes depict representative areas of the right atrium muscle and SA node used for immunolocalization of receptors and ionic channels.

6. Solutions and chemicals

4-aminopyridine (4-AP), apamin, 2-p-(2-carboxyethyl)phenethylamino-5′-N-ethylcarboxamidoadenosine (CGS21680C), 1,3-dipropyl-8-cyclopentyl-xanthine (DPCPX), R-(-)-N^6-(2-phenylisopropyl)adenosine (R-PIA), uridine 5′-triphosphate trisodium salt hydrate (UTP); Angiotensin II human (AngII) were from Sigma-Aldrich (St. Louis, MO, USA). AF-DX 116, oxotremorine sesquifumarate, 2-Aminoethoxydiphenylborane (2-APB), phorbol 12-myristate 13-acetate (PMA), chelerythrine chloride, U73122, mibefradil dihydrochloride and verapamil hydrochloride were from Tocris Cookson Inc. (Bristol, UK); glibenclamide and tertiapin Q were from Ascent Scientific (Bristol, UK);

Dimethylsulphoxide (DMSO), serum albumin and Triton X-100 were from Merck (Darmstadt, Germany).

AF-DX 116, glibenclamide, PMA and 2-APB were made up in DMSO stock solution. DPCPX was made up in 99% DMSO / 1% NaOH 1 mmol L^{-1} (v/v). R-PIA, U73122, verapamil were made up in ethanol; these solutions were kept protected from the light to prevent photodecomposition. Other drugs were prepared in distilled water. All stock solutions were stored as frozen aliquots at -20ºC. Dilutions of these stock solutions were made daily and appropriate solvent controls were used. No statistically significant differences between control experiments, made in the absence or in the presence of the solvents at the maximal concentrations used (0.5% v/v), were observed. The pH of the superfusion solution did not change by the addition of the drugs in the maximum concentrations applied to the preparations.

7. Presentation of data and statistical analysis

The isometric contractions were recorded and analyzed before and after the addition of each drug at the desired concentration. Results were presented as percentages of variation compared to baseline, obtained before the administration of the evaluated drug. The data are expressed as mean ± SEM, with *n* indicating the number of animals used for a particular group of experiments. Spontaneous mechanical tension (inotropic effect) and contraction rate (chronotropic effect) were evaluated by analysis of variance, having been selected the most appropriate ANOVA test for each experimental protocol. IC_{50} (concentrations of drug producing 50% of the maximal inhibition) values were obtained by computer-assisted curve fitting of Hill function with variable slopes by use of the computer program GraphPad Prism (version 4.0, USA). Statistical analysis of data was carried out by using Student-Newman-Keuls test for paired data. A value of $P<0.05$ was considered to represent a significant difference.

IV. Results

1. Adenosine acting via A_1 receptors is a chronoselective atrial depressant as compared to the muscarinic M_2 receptor agonist, oxotremorine

Figure 6 shows that activation of ADO A_1 and muscarinic M_2 receptors, respectively with R-PIA (0.001-1 μM) and oxotremorine (0.01-3 μM), decreased in a concentration-dependent manner the rate (negative chronotropic effect) and the force (negative inotropic effect) of spontaneous contractions of the rat atria. However, the negative chronotropic effect of R-PIA (IC_{50}~0.03 μM, Figure 6B) was evidenced at much lower (~30 times) concentrations than the negative inotropic action (IC_{50}~1 μM, Figure 6B), whereas oxotremorine-induced depression of both the rate and the tension was observed in the same concentration range (IC_{50}~0.1-0.3 μM) (Figures 6D). Thus, R-PIA is a chronoselective depressant as compared to oxotremorine in spontaneously beating rat atria. In fact, low concentration of R-PIA produced a mild positive inotropic effect (100 nM, +32±10%, *P*<0.05 vs basal, *n*=48, Figure 6B), contrary to oxotremorine. Both agonistic effects were reversibly reverted during the washout period to basal chronotropic and inotropic states before drug application.

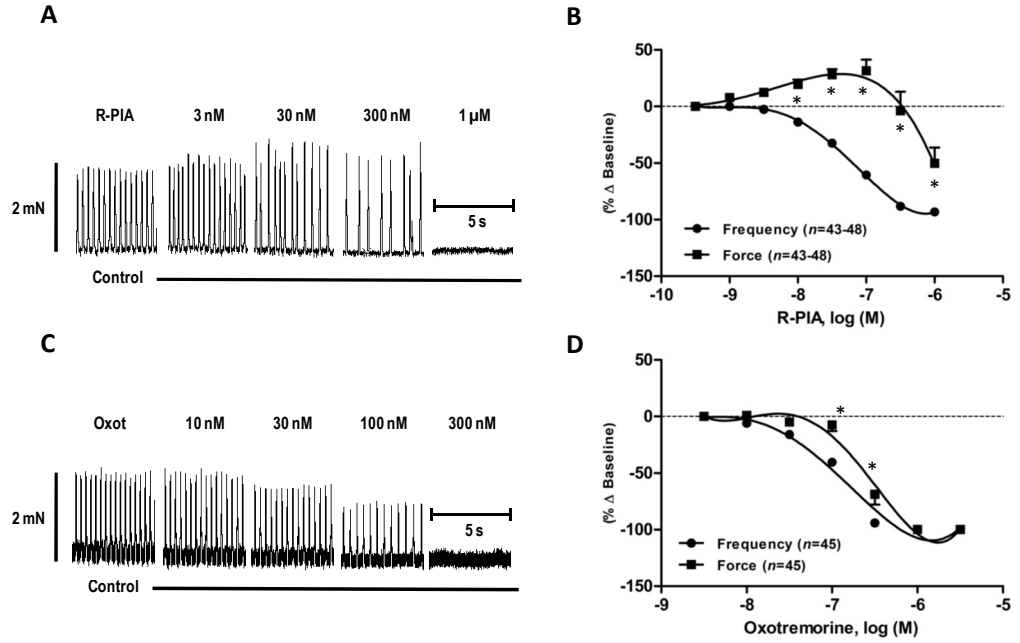

Figure 6. Adenosine is a chronoselective atrial depressant. In right panels (A and C) are depicted representative original recordings of isometric contractions of rat atrial muscle in response to increasing concentrations of R-PIA (0.001-1 μM) and oxotremorine (0.01-3 μM), respectively. R-PIA and oxotremorine were applied once every 2 min at increasing concentrations. In left panels are depicted concentration-response curves of R-PIA (B) and oxotremorine (D) on the spontaneously beating rat atria. The ordinates are percentage of variation of spontaneous contraction rate (chronotropic effect) and mechanical tension (inotropic effect) as compared to baseline values obtained before application of the corresponding agonist. The data are expressed as mean ± SEM from an *n* number of individual experiments. **P*<0.05 compared with the concentration-response curve for the chronotropic effect of the corresponding agonist.

Figures 7A and B show that selective blockade of ADO A_1 receptors with DPCPX (100 nM), significantly shifted to the right the concentration-response curves for R-PIA (0.001-1 μM) in the spontaneously beating rat atria. The blocking effect of DPCPX was dependent on the concentration (2.5, 10 and 100 nM, *n*=4-6, data not shown), thus indicating that the A_1R must be the dominant receptor involved in the negative chronotropic and inotropic actions of R-PIA. Increasing concentrations of DPCPX (2.5-100 nM) *per se* were devoid of effect (*P*>0.05 vs basal values, data not shown).

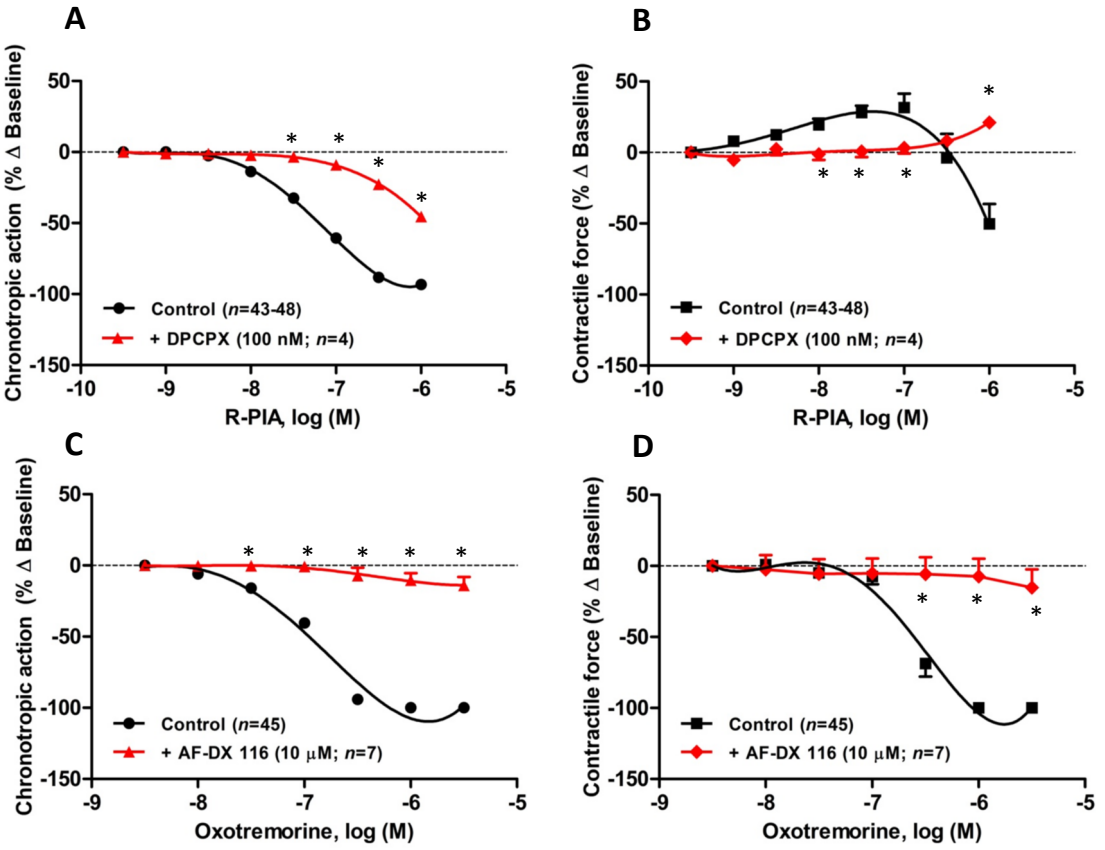

Figure 7. Inhibitory effects of R-PIA and oxotremorine on contractile and chronotropic responses are mediated through A_1R and M_2R activation, respectively. Concentration-response curves of R-PIA (A and B) and oxotremorine (C and D) on the spontaneously beating rat atria in the absence (Control) and in the presence of selective A_1 (DPCPX) and M_2 (AF-DX 116) receptor antagonists. Oxotremorine (0.01-3 μM) and R-PIA (0.001-1 μM) were applied once every 2 min at increasing concentrations; AF-DX 116 (10 μM) and DPCPX (100 nM) were added to the incubation fluid 15 minutes before application of R-PIA or oxotremorine. The ordinates are percentage of variation of spontaneous contraction rate (chronotropic effect, A and C) and mechanical tension (inotropic effect, B and D) as compared to baseline values obtained before application of the corresponding agonist. The data are expressed as mean ± SEM from an *n* number of individual experiments. **P*<0.05 compared with the effect of oxotremorine (C and D) or R-PIA (A and B) in the absence of receptor antagonists AF-DX 116 and DPCPX.

Likewise, data from Figures 7C and D show that depression of the rate and the tension of spontaneous atrial contractions caused by oxotremorine (0.01-3 μM) were both completely prevented by pre-incubation with the muscarinic M_2 receptor antagonist, AF-DX 116 (10 μM). AF-DX 116 at 10 μM did not produce any significant alterations on

evaluated parameters (*P*>0.05 vs basal values). Therefore, the effects of oxotremorine and R-PIA in the spontaneously beating rat atria are due to activation of M_2R and A_1R, respectively.

The chronoselective effect operated by R-PIA in the spontaneously beating rat atria could be simply explained by a differential expression of A_1R between the SA node and atrial muscle. Immunofluorescence confocal microscopy studies showed that A_1 and M_2 receptors are evenly expressed in SA node and atrial cardiomyocytes (Figure 8), thus indicating that differences in the regional distribution of receptors do not account for ADO chronoselectivity in the spontaneously beating rat atria. Of note that M_2R labeling pattern was quite different from that observed for A_1R. A_1R demonstrated both outer cell membrane and internal labeling, whereas M_2R labeling (Figure 8) was strongly present in the outer cell membrane. The differential labeling pattern between A_1 and M_2 receptor might mirror different cellular locations for these receptors.

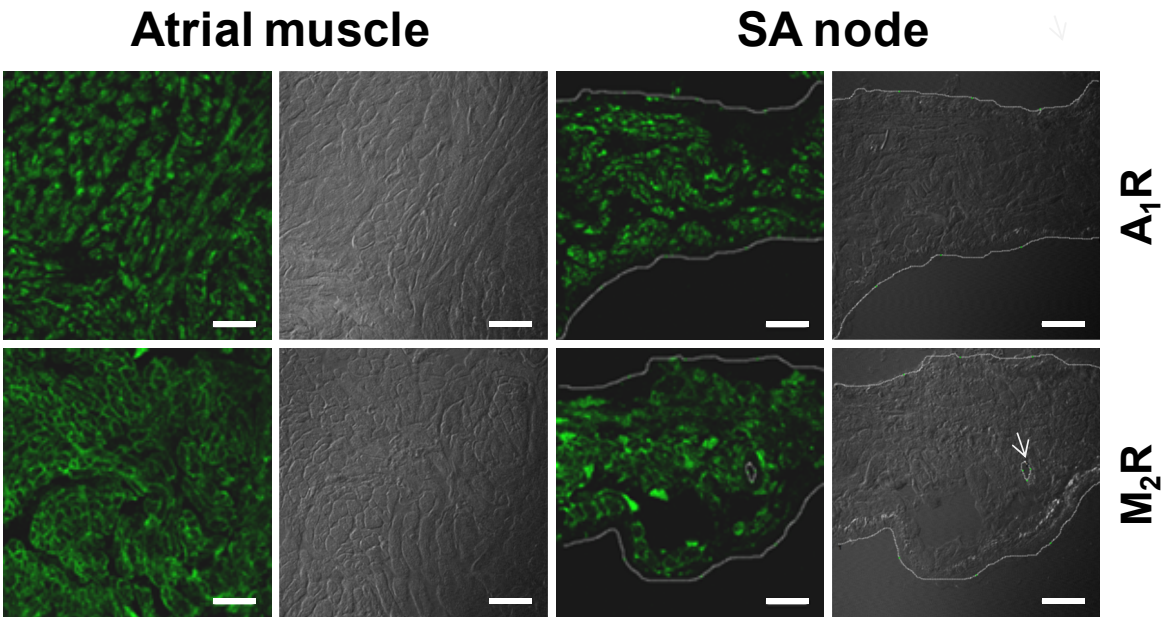

Figure 8. A_1R and M_2R are expressed in rat atria. Representative confocal micrographs of the rat SA node and neighboring atrial muscle showing immunofluorescence labeling of A_1 (upper panels) and M_2 (lower panels) receptors; the corresponding differential interference contrast (DIC) images are also shown for comparison. Similar results were obtained in 6 additional experiments. Horizontal bar=30 μm. The white arrow indicates the SA node artery.

2. Activation of A_{2A}Rs are not involved in adenosine chronoselectivity

Even though most cardiac effects of R-PIA had been extensively antagonized with DPCPX, we cannot dismiss the involvement of A_{2A}R. Therefore, to exclude a possible interplay of A_{2A}R on the ADO's chronoselective effect, we evaluated the functional effects of A_{2A}R stimulation by using its agonist CGS 21680 (0.003-1 μM) on force and rate of

contraction of spontaneously beating rat atria. The selective ADO A_{2A} receptor agonist, CGS21680, when applied in a similar concentration range (0.003-1 μM) as R-PIA (0.001-1 μM), tended to increase basal inotropy (maximal stimulation, ~5% at 300 nM) (Figure 9) but the effect did not reach statistical significance (P>0.05 vs basal values, n=59). These findings suggest that the A_{2A} receptor has limited importance in the response to ADO in the denervated rat atria.

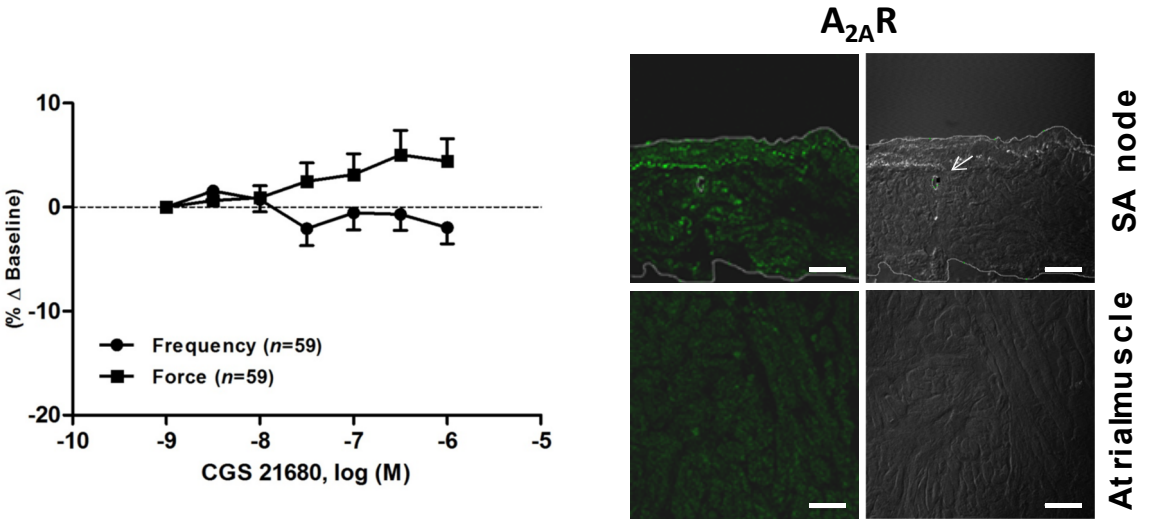

Figure 9. A_{2A}R activation does not play a significant role on atrial inotropy and chronotropy. In the left side is shown the concentration-response curves of CGS 21680 (0.003-1 μM) in spontaneously beating rat atria. CGS 21680 was applied once every 2 min at increasing concentrations. The ordinates are percentage of variation of spontaneous contraction rate (chronotropic effect) and mechanical tension (inotropic effect) as compared to baseline values obtained before application of CGS 21680. The data are expressed as mean ± SEM from an *n* number of individual experiments. In the right panels are representative confocal micrographs of the rat SA node (upper panels) and neighboring atrial muscle (lower panels) showing immunofluorescence labeling of A_{2A}R; the corresponding differential interference contrast (DIC) images are also shown for comparison. Similar results were obtained in 2 additional experiments. Horizontal bar=30 μm. The white arrow indicates the SA node artery.

To support functional results about the meaningless effects of A_{2A}R activation in rat atria, we used immunofluorescence confocal microscopy to examine the location and relative expression of this receptor. Images taken from SA node area and atrial muscle sections immunolabeled for A_{2A}R showed that this receptor is expressed in supraventricular tissues of rat, but its overall immunoreactivity was very weak, which suggest a low expression of A_{2A}R in the rat atria (Figure 9).

3. G protein-coupled inwardly rectifying K^+ (GIRK/K_{IR}3.1/3.4) channels operate atrial depression caused by A_1R and M_2R activation

It is well known from the literature that ADO and ACh share a common signal transduction pathway that reduces chronotropy and inotropy through direct opening of

GIRK/K_{IR}3.1/3.4 channels (Kurachi *et al*., 1986; Krapivinsky *et al*., 1995; Han and Bolter, 2011). Consistent with a direct action on GIRK/K_{IR}3 channels, the inhibitory effect of R-PIA and oxotremorine on spontaneous atrial contractions were totally prevented by tertiapin-Q (300 nM), a selective GIRK/K_{IR}3 channel blocker peptide, seen as a rightward displacement of the concentration-response curve and reduction of the maximum response for R-PIA and oxotremorine (Figure 10). Tertiapin Q did not affect spontaneous atrial contractions when applied once every 2 min at increasing concentrations from 30 nM to 1 µM (data not shown).

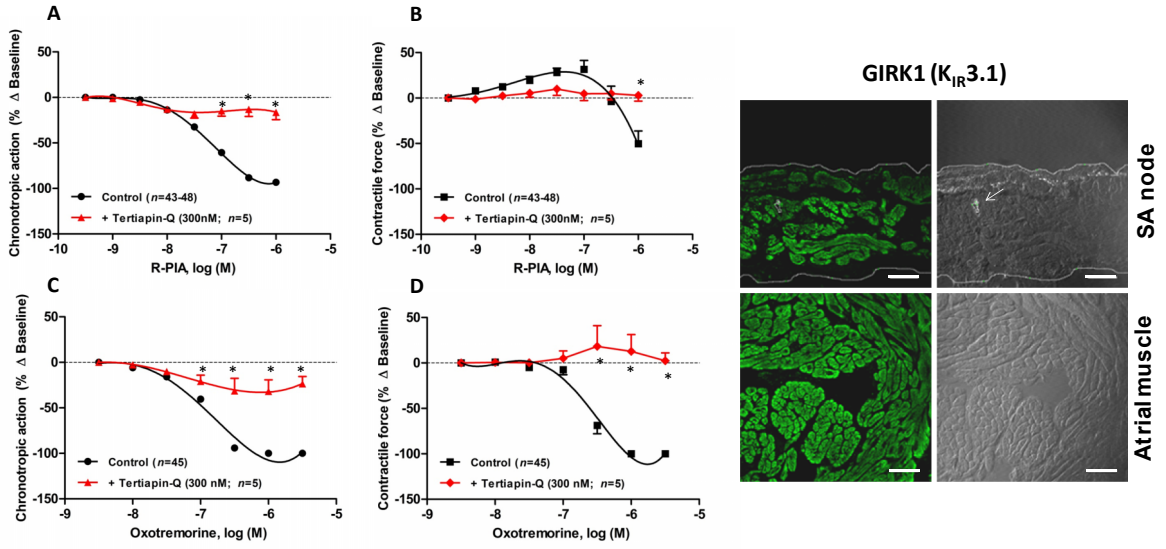

Figure 10. Atrial GIRK/K_{IR}3 channels mediate cholinergic and adenosinergic cardiodepression. Concentration-response curves of R-PIA (A, B) and oxotremorine (C, D) in the absence (Control) or in the presence of tertiapin-Q (300 nM). R-PIA (0.001-1 µM) and oxotremorine (0.01-3 µM) were applied once every 2 min at increasing concentrations; Tertiapin Q (300 nM), a potassium GIRK/K_{IR}3 channel blocker, was added to the incubation fluid 15 minutes before application of R-PIA or oxotremorine. The ordinates are percentage of variation of spontaneous contraction rate (chronotropic effect, A and C) and mechanical tension (inotropic effect, B and D) as compared to baseline values obtained before application of the corresponding agonist. Vertical lines indicate ± SEM for the indicated number (*n*) of individual experiments. **P*<0.05 compared with the effect of both agonists in the absence of potassium GIRK/K_{IR}3 channel blocker. In the right side of this figure is present representative confocal micrographs of the rat SA node (upper panels) and neighboring atrial muscle (lower panels) showing immunofluorescence labeling of GIRK1/K_{IR}3.1 channel subunit; the corresponding differential interference contrast (DIC) images are also shown for comparison. Similar results were obtained in 6 additional experiments. Horizontal bar=30 µm. The white arrow indicates the SA node artery.

In addition, GIRK/K_{IR}3 channels expression was examined because of its relevance as an effector of the atrial depression elicited by A_1R and M_2R. According to the functional studies, immunolabeling of GIRK1/K_{ir}3.1 subunits confirmed GIRK/K_{IR}3 channel expression throughout the right atria including the SA node. It can be seen from confocal micrographs that GIRK1/K_{ir}3.1 subunits were highly and equally expressed in both SA node and right atrial muscle cells (Figure 10). Similarly to that observed for A_1R

immunolocalization (Figure 8), $K_{ir}3.1$ labeling was present in the outer cell membrane and it was also present inside myocytes.

4. A_1R-mediated chronoselectivity is prevented by blocking Ca_V1 (L-type) channels and $K_{Ca}2$/SK currents with verapamil and apamin, respectively

Immunolocalization studies showed that differences in the distribution of A_1R between SA node and atrial cardiomyocytes do not afford a rationale for ADO chronoselectivity. In view of this, the underlying mechanism(s) responsible for ADO chronoselectivity is possibly downstream the receptor level.

Giving the pivotal role of Ca_v1 (L-type) channels on E-C coupling and spontaneous generation of pacemaker AP (Bers, 2002; Lakatta *et al*., 2010), we aimed at exploring the rationale for ADO chronoselectivity testing the effect of the nucleoside in the presence of Ca_v1 (L-type) channels blockers in the rat spontaneously beating atria. On its own, blockade of Ca_v1 (L-type) channels with the phenylalkylamine, verapamil (0.01-10 μM) (Catterall, 2011), decreased the rate and the strength of contractions of the rat spontaneously beating atria in a concentration dependent manner (data not shown). Verapamil, applied in a concentration (1 μM) that reduced atrial chronotropy roughly by 25%, sensitized atria to the negative inotropic action of R-PIA (0.001-1 μM) without much affecting the action of the A_1 receptor agonist on the rate of atrial contractions. The negative inotropic effect of R-PIA changed from an IC_{50} value of about 1 μM in control conditions to 0.1 μM in the presence of Ca_V1 (L-type) channels blocker. The negative chronotropic and inotropic actions of R-PIA were both evident in the same range of concentrations (IC_{50}~0.03-0.1 μM) in the presence of verapamil, thus leading to a loss of the atrial chronoselectivity of ADO A_1 receptors (Figure 11). Conversely, blockade of Ca_V1 (L-type) channels with 1 μM verapamil failed to modify oxotremorine (0.01-3 μM)-induced depression in the rat spontaneously beating atria (Figure 12). These findings contrast with those obtained with the ADO A_1 receptor agonist (Figure 11), suggesting that the negative chronotropic and inotropic actions of oxotremorine are independent on Ca^{2+} influx through Ca_V1 (L-type) channels, relying most probably on the control of K^+ currents via GIRK/$K_{IR}3$ sensitive to tertiapin Q.

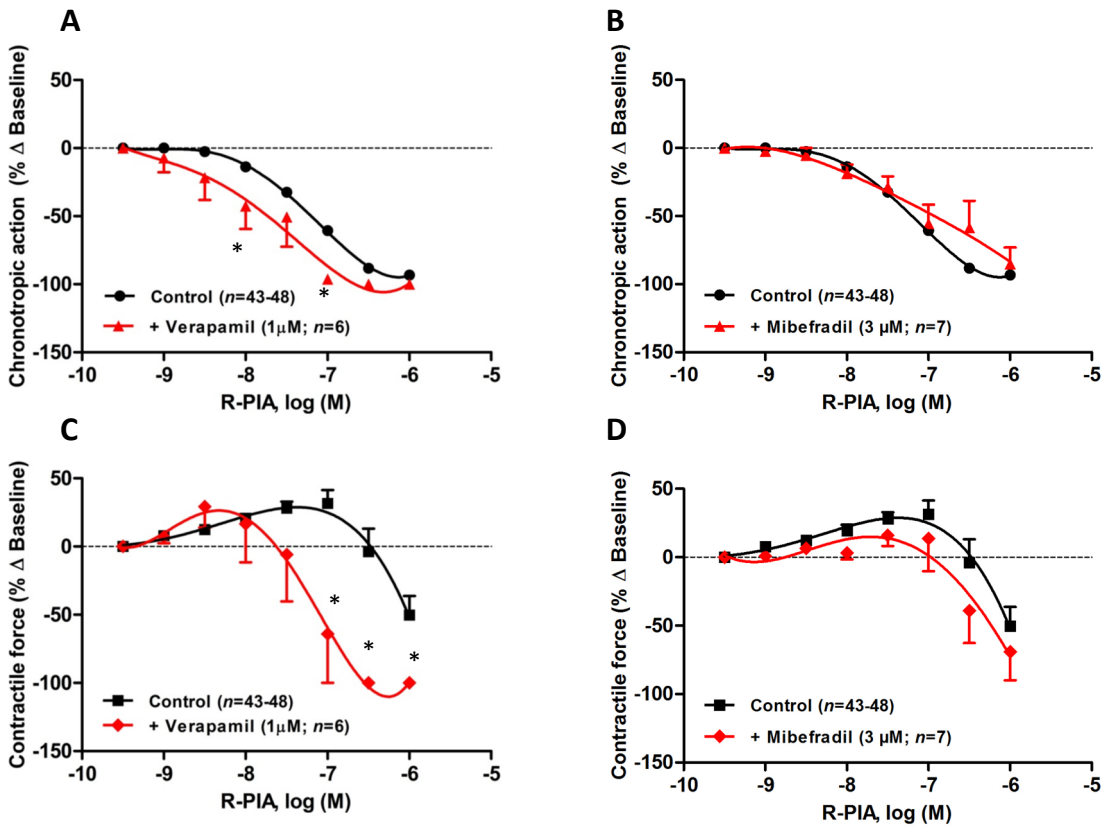

Figure 11. A_1R-mediated negative inotropy was potentiated by the L-type calcium channels blockade. Concentration-response curves of R-PIA on the spontaneously beating rat atria in the absence (Control) and in the presence of voltage-sensitive calcium channels inhibitors: verapamil (1 μM, A and C) and mibefradil (3 μM, B and D). R-PIA (0.001-1 μM) was applied once every 2 min at increasing concentrations; voltage-sensitive calcium channels blockers, verapamil (1 μM) and mibefradil (3 μM), were added to the incubation fluid 15 minutes before application of R-PIA. The ordinates are percentage of variation of spontaneous contraction rate (chronotropic effect, A and B) and mechanical tension (inotropic effect, C and D) as compared to baseline values obtained before application of R-PIA. The data are expressed as mean ± SEM from an *n* number of individual experiments. **P*<0.05 compared with the effect of R-PIA in the absence of voltage-sensitive calcium channels inhibitors.

Blockade of low voltage-activated Ca_V3 (T-type) channels with mibefradil (0.1-10 μM) concentration-dependently reduced atrial chronotropy to a maximum of 30% (*n*=7), without affecting the force of spontaneous atrial contractions (data not shown). Mibefradil (3 μM) failed to modify the effects of both R-PIA (0.001-1 μM) and oxotremorine (0.01-3 μM) in the rat spontaneously beating atria (Figures 11 and 12).

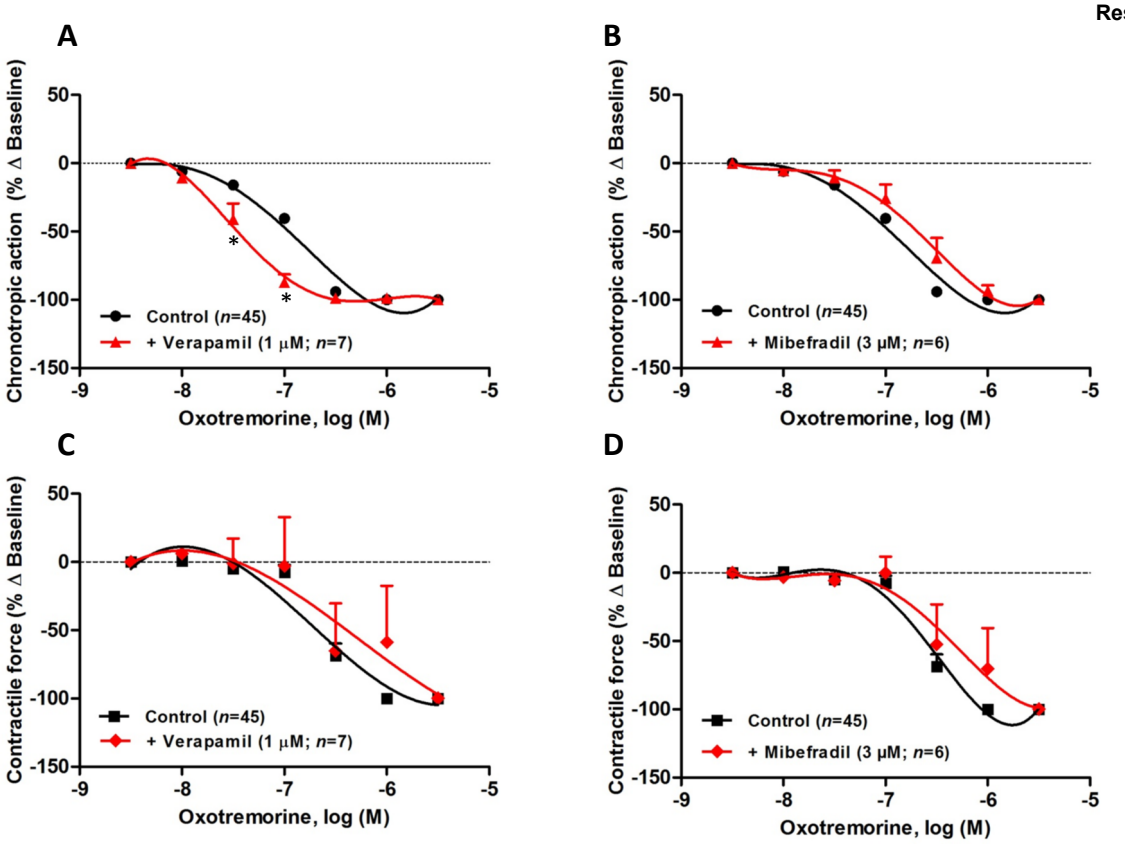

Figure 12. M_2R-mediated negative inotropy is insensitive to voltage-sensitive calcium channels blockade. Concentration-response curves of oxotremorine on the spontaneously beating rat atria in the absence (Control) and in the presence of voltage-sensitive calcium channels inhibitors: verapamil (1 μM, A and C) and mibefradil (3 μM, B and D). Oxotremorine (0.01-1 μM) was applied once every 2 min at increasing concentrations; voltage-sensitive calcium channels blockers, verapamil (1 μM) and mibefradil (3 μM), were added to the incubation fluid 15 minutes before application of R-PIA. The ordinates are percentage of variation of spontaneous contraction rate (chronotropic effect, A and B) and mechanical tension (inotropic effect, C and D) as compared to baseline values obtained before application of oxotremorine. The data are expressed as mean ± SEM from an *n* number of individual experiments. **P*<0.05 compared with the effect of oxotremorine in the absence of voltage-sensitive calcium channels inhibitors.

Next, it was evaluated whether K^+ channels other than GIRK/K_{IR}3 channels were involved in A_1R- and M_2R-mediated atrial depression. Like that observed in the guinea-pig atria (De Biasi *et al*., 1989), blockade of voltage-gated K_v and ATP-sensitive K_{ATP}/K_{IR}6 channels respectively with 4-aminopyridine (4-AP, 10 μM) and glibenclamide (10 μM) had no significant (*P*>0.05) effects on the negative chronotropic and inotropic actions of R-PIA and oxotremorine (Figure 13). Similar results were obtained when the concentration of 4-AP was increased from 10 to 100 μM (*n*=6, data not shown).

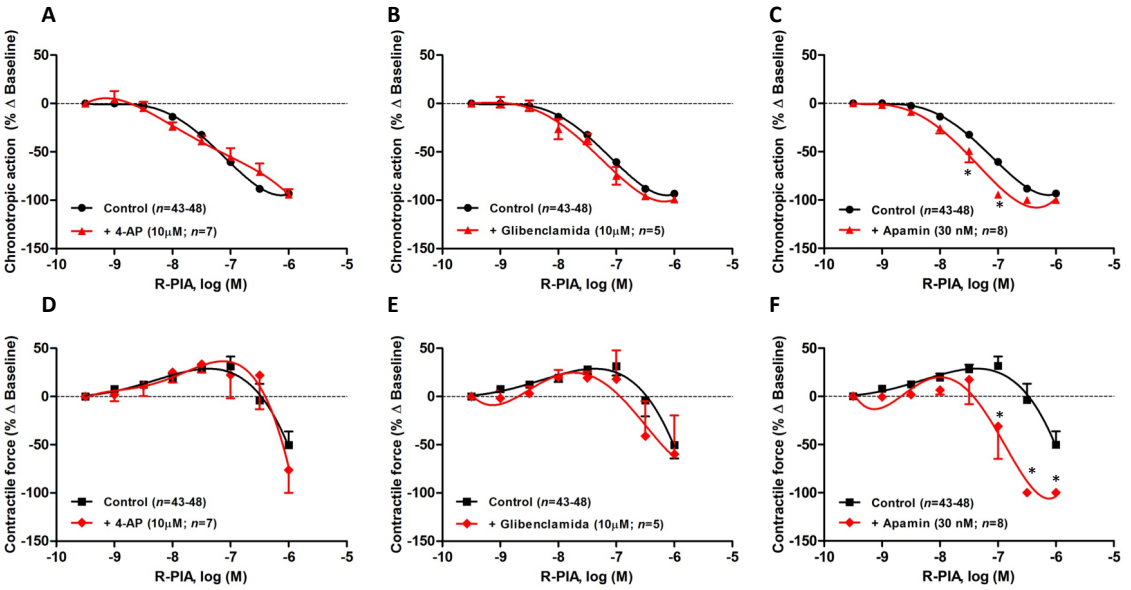

Figure 13. A_1R is modulated by small conductance calcium-activated potassium channels operation. Concentration-response curves of R-PIA on the spontaneously beating rat atria in the absence (Control) and in the presence of potassium channels blockers: 4-AP (10 μM, A and D), glibenclamide (10 μM, B and E), and apamin (30 nM, C and F). R-PIA (0.001-1 μM) was applied once every 2 min at increasing concentrations; potassium channel blockers 4-AP (10 μM), glibenclamide (10 μM) and apamin (30 nM), were added to the incubation fluid 15 minutes before application of R-PIA. The ordinates are percentage of variation of spontaneous contraction rate (chronotropic effect, A, B and C) and mechanical tension (inotropic effect, D, E and F) as compared to baseline values obtained before application of R-PIA. The data are expressed as mean ± SEM from an *n* number of individual experiments. **P*<0.05 compared with the effect of R-PIA in the absence of potassium channel blockers.

Contrariwise, blockade of Ca^{2+}-activated $K_{Ca}2$/SK channels with apamin (30 nM) shifted to the left (*P*<0.05) the concentration-response of R-PIA (0.001-1 μM) regarding the negative inotropic component of the A_1R action (Figure 13F), without much affecting the action of the nucleoside on the rate of atrial contractions (Figure 13C). That is, pre-treatment with apamin (30 nM) sensitized atria to the negative inotropic effect of R-PIA in a way that the negative chronotropic and inotropic actions of the A_1 receptor agonist became evident in the same range of concentrations (IC_{50}~0.03-0.1 μM) (see above). These findings suggest that the bradicardic and the negative inotropic actions of ADO may be dissociated in terms of the intracellular mechanisms being involved. Apamin (30 nM) failed to affect the depressant effects of oxotremorine (0.01-3 μM) in the rat spontaneously beating atria under similar experimental conditions (Figure 14).

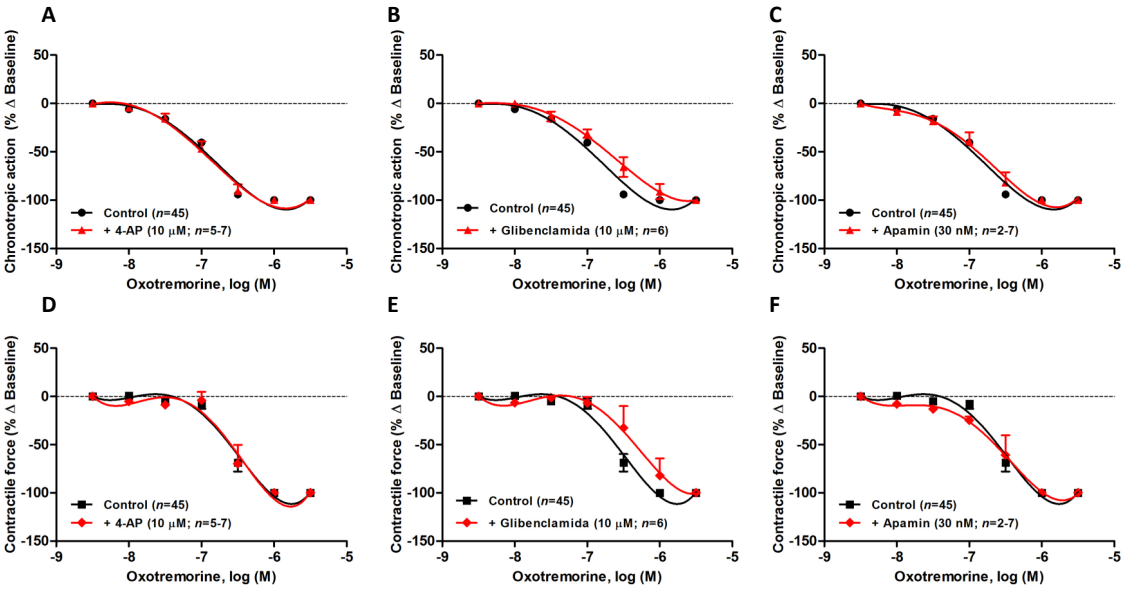

Figure 14. M_2R-mediated negative inotropy is insensitive to small conductance calcium-activated potassium channels blockade. Concentration-response curves of oxotremorine on the spontaneously beating rat atria in the absence (Control) and in the presence of potassium channels blockers: 4-AP (10 μM, A and D), glibenclamide (10 μM, B and E), and apamin (30 nM, C and F). Oxotremorine (0.01-1 μM) was applied once every 2 min at increasing concentrations; potassium channel blockers 4-AP (10 μM), glibenclamide (10 μM) and apamin (30 nM), were added to the incubation fluid 15 minutes before application of oxotremorine. The ordinates are percentage of variation of spontaneous contraction rate (chronotropic effect, A, B and C) and mechanical tension (inotropic effect, D, E and F) as compared to baseline values obtained before application of oxotremorine. The data are expressed as mean ± SEM from an *n* number of individual experiments. **P*<0.05 compared with the effect of oxotremorine in the absence of potassium channel blockers.

5. $K_{Ca}2$/SK and Ca_V1 (L-type) channels are expressed both in SA node and atrial cardiomyocytes

Considering that blockade of $K_{Ca}2$/SK and Ca_V1 (L-type) channels, respectively with apamin and verapamil, predisposes atria to the negative inotropic action of ADO, we tested whether these channels were expressed in the rat atria by immunofluorescence confocal microscopy.

Ca_V1 (L-type) channels, like other high-voltage operated Ca^{2+} channels, are heteromeric proteins formed by the pore-forming α-subunit together with β, α2/δ and γ accessory subunits (Catterall, 2011). In the heart the phenylalkylamine-sensitive ionic current ($I_{Ca,L}$) is mainly attributable to ionic channels containing α_{1C} ($Ca_V1.2$) and α_{1D} ($Ca_V1.3$) subunits (Best and Kamp, 2012). In this study we used a commercial available antibody against the extracellular $\alpha_2\delta$-1 subunit to localize Ca_V1 (L-type) channels in the rat atria. Although $\alpha_2\delta$ subunits are present in all high-voltage-gated Ca^{2+} channels including L-, P/Q-, N- and R-types, cardiac expression of high-voltage operated calcium channels other than the Ca_V1 (L-type) channels subtype is negligible (Catterall, 2011).

Figure 15 shows that both SA node and atrial cardiomyocytes evenly exhibit immunoreactivity against the extracellular $\alpha_2\delta$-1 subunit of Ca_V1 (L-type) channels.

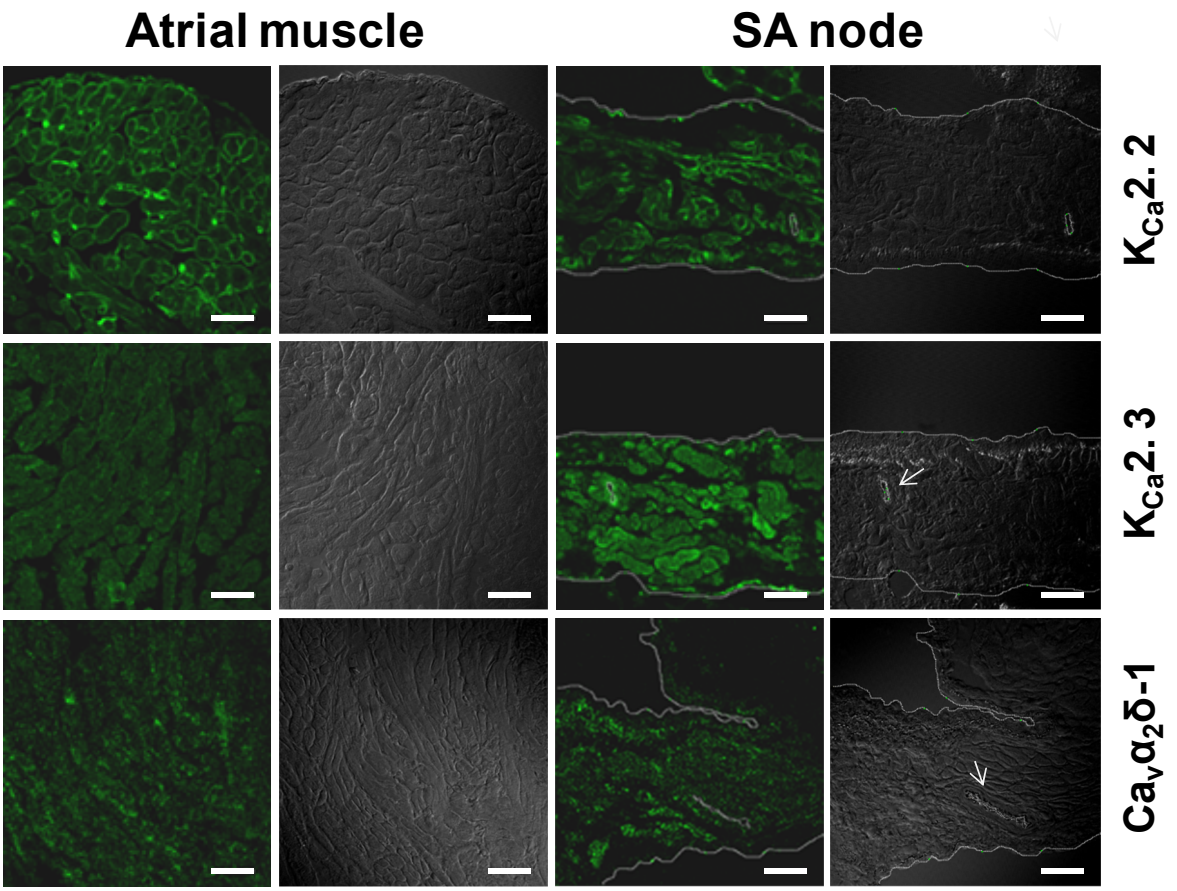

Figure 15. The molecular players of A_1R-mediated chronoselectivity, $K_{Ca}2$/SK and Ca_V1 (L-type) channels, are expressed throughout the rat atria. Representative confocal micrographs of rat right atria and SA node sections showing immunofluorescence labeling for $K_{Ca}2.2$ (SK2), $K_{Ca}2.3$ (SK3) and $Ca_V\alpha_2\delta$-1 channel subunits (first and third columns); the corresponding differential interference contrast (DIC) images are also shown for comparison (second and fourth columns). Similar results were obtained in 5 additional experiments. Horizontal bar=30 μm. White arrows indicate SA node artery.

The concentration of apamin used in this study (30 nM) effectively blocks $K_{Ca}2.2$/ SK2 and $K_{Ca}2.3$/SK3 channels (Ishii *et al*., 1997), which are probably the subtypes most expressed in mammalian atria (Chandler *et al*., 2009; Yanni *et al*., 2011). Figure 15 shows that both SA node and atrial cardiomyocytes exhibit immunoreactivity against $K_{Ca}2.2$ and $K_{Ca}2.3$. Differences might exist in the distribution of apamin-sensitive $K_{Ca}2.2$ and $K_{Ca}2.3$ channels, being the latter more abundant in the SA node as compared with atrial cardiomyocytes, while the opposite seems to occur regarding $K_{Ca}2.2$.

6. Chronoselectivity of A_1R is dependent on PLC/PKC coupling

Several pieces of evidence showed that A_1R activation may stimulate PIP_2 hydrolysis linking this receptor to the PLCβ/PKC second messenger system (Kohl *et al*., 1990; Gerwins and Fredholm, 1992; Dickenson and Hill, 1998; Cordeaux *et al*., 2000; Lester and Hofmann, 2000; Parsons *et al*., 2000; Fenton *et al*., 2010). As outlined in the introduction, modulation of the PKC activity might change contractile parameters, which led us to investigate PKC and upstream targets of this kinase on ADO-induced atrial depression. For comparison purposes, we also tested the involvement of the PLCβ/PKC pathway on muscarinic M_2R responses.

Inhibition of PLC with U73122 (3 μM) sensitized atria to A_1R contractile depression. The magnitude of the leftward shift of the concentration-response curve of R-PIA (0.001-1 μM) was more obvious regarding the negative inotropic effect (Figure 16B) as compared to the negative chronotropic action of the nucleoside (Figure 16A). The negative inotropic effect of R-PIA changed from an IC_{50} value of ~1 μM in control conditions to 0.1 μM (*n*=7) in the presence of the PLC inhibitor, U73122 (3 μM). Under these circumstances, the negative chronotropic and inotropic actions of R-PIA were both evident in the same range of concentrations (IC_{50}~0.03-0.1 μM) indicating that inhibition of PLC leads to a loss of the atrial chronoselectivity of A_1R. Contrariwise, blockade PLC with U73122 (3 μM) failed to modify oxotremorine (0.01-3 μM)-induced depression in the rat spontaneously beating atria (Figures 16C and D). On its own, U73122 (3 μM) was devoid of chronotropic (-4±4%, *P*>0.05, *n*=13) and inotropic (-3±4%, *P*>0.05, *n*=13) effects of the spontaneously beating rat atria (data not shown).

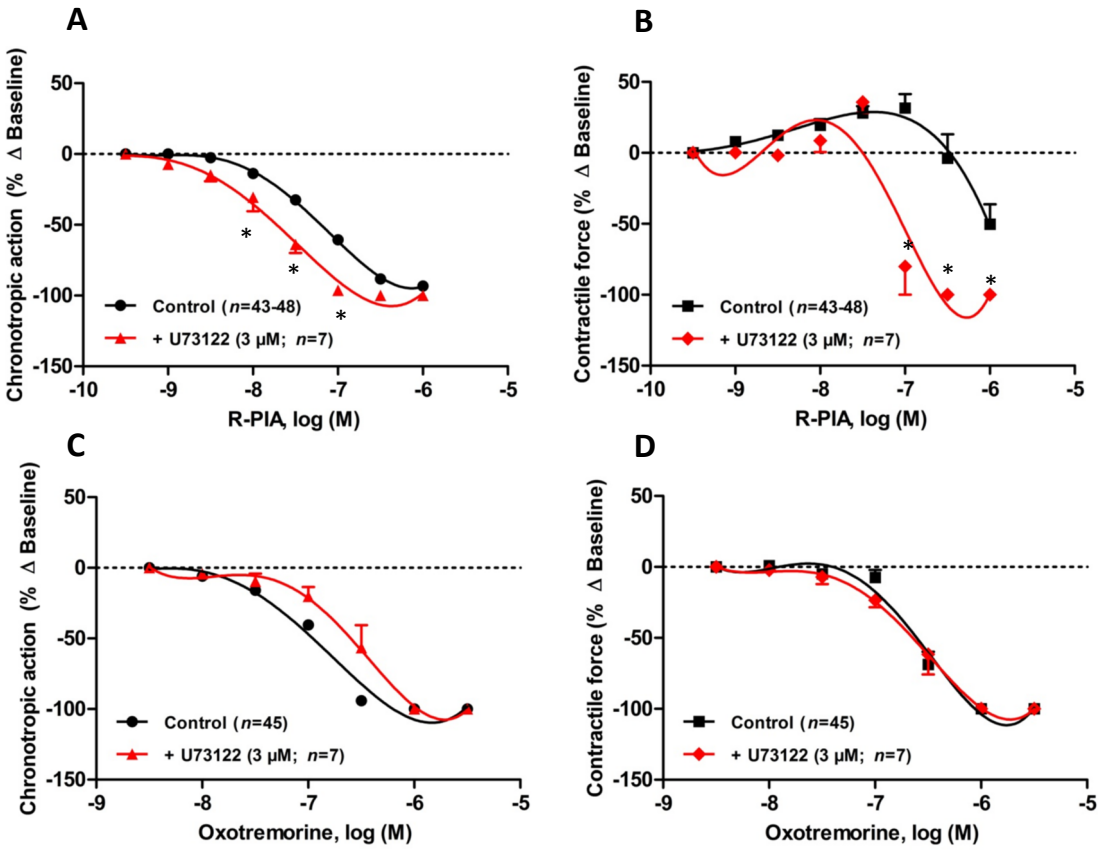

Figure 16. Inhibition of PLC with U73122 (3 μM) sensitized atria to A_1R contractile depression. Concentration-response curves of R-PIA (A and B) and oxotremorine (C and D) in the absence (Control) or in the presence of the PLC inhibitor, U73122 (3 μM). R-PIA (0.001-1 μM) (A and B) and oxotremorine (0.01-3 μM) (C and D) were applied once every 2 min at increasing concentrations. U73122 was added to the incubation fluid 15 minutes before application of agonists. The ordinates are percentage of variation of spontaneous contraction rate (chronotropic effect, A and C) and mechanical tension (inotropic effect, B and D) as compared to baseline values obtained before application of R-PIA or oxotremorine. The data are expressed as mean ± SEM from an *n* number of individual experiments. **P*<0.05 compared with the effect of agonists in the absence of phospholipase C inhibitor.

Diffusible IP_3 and DAG are generated from PIP_2 hydrolysis catalyzed by PLC. IP_3 is responsible for cytosolic Ca^{2+} recruitment from SR (Berridge, 1993), thus enhancing E-C coupling and spontaneous AP firing in the heart (Lipp *et al*., 2000; Bers, 2002). Taking this into account, we aimed at investigating whether A_1R coupling to PLC (see above) would generate enough IP_3 to levels required to counteract adenosine negative inotropic action. To test this hypothesis, we sought it would be helpful to block the IP_3R with 2-aminoethoxydiphenylborane (2-APB) prior to R-PIA (0.001-1 μM) application. Unfortunately 2-APB, used in a concentration (30 μM) within the range of that needed to inhibit IP_3-induced SR Ca^{2+} recruitment (Maruyama *et al*., 1997), abolished atrial spontaneous activity (*n*=5) (Figure 17). Under these circumstances, the strong inhibitory effect of 2-APB (30 μM) on atrial activity persisted for a long period of time, even after washing the drug from the bath. Before atrial arrest, 2-APB (30 μM) caused significant

mechanical instability characterized by aberrant contractions (Figure 17), as observed by other authors (Wolkowicz *et al*., 2007). Given the strong inhibitory effect of 2-APB (30 μM) on atrial spontaneous activity, no further studies were performed with this compound.

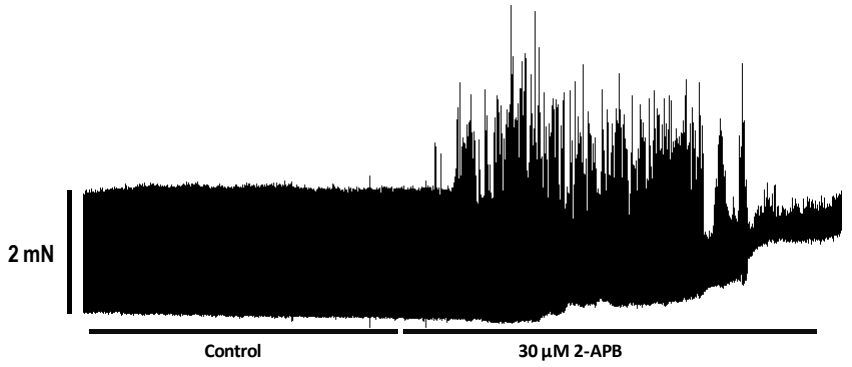

Figure 17. 2-APB abolishes spontaneous atrial activity and induces severe mechanical instability. Representative original recordings of isometric contraction force of rat atrial muscle. 2-APB at 30 μM was applied to organ bath after an equilibrium period. Similar results were obtained for 5 experiments.

As mentioned above, beside IP_3 formation, PIP_2 hydrolysis also generates DAG which in turn activates several DAG-sensitive PKC isozymes. The concentration-response curve of the negative inotropic response to R-PIA (0.001-1 μM) was significantly (P<0.05) shifted to the left by chelerythrine (3 μM), a potent cell-permeable and broad-spectrum PKC inhibitor (Figure 18B). Like that observed with the PLC inhibitor, U73122 (3 μM), negative chronotropic and inotropic actions of R-PIA were both seen in the same concentration range (IC_{50}~0.03-0.1 μM), thus indicating that inhibition of the PLC/PKC pathway leads to a loss of A_1R-mediated atrial chronoselectivity by sensitizing atria to the negative inotropic action of the nucleoside (Figure 16B and 18B). PKC blockade with chelerythrine (3 μM) did not modify oxotremorine (0.01-3 μM)-induced depression in the rat spontaneously beating atria (Figures 18C and D). Cumulative application of chelerythrine (0.03-3 μM) *per se* did not have a major impact (P>0.05 vs basal values) on atrial chronotropy and inotropy (data not shown).

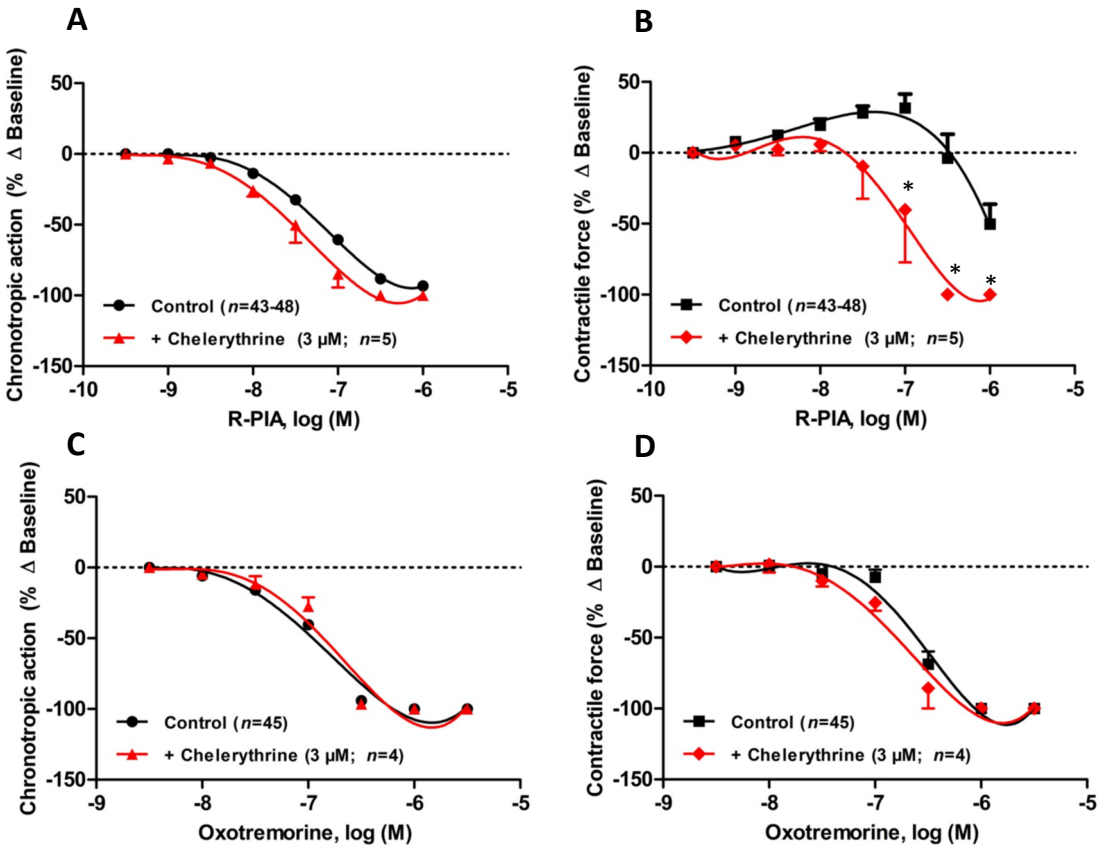

Figure 18. Protein kinase C (PKC) is modulated by A_1R. Concentration-response curves of R-PIA (A and B) and oxotremorine (C and D) in the absence (Control) or in the presence of the PKC inhibitor, chelerythrine (3 μM). R-PIA (0.001-1 μM) (A and B) and oxotremorine (0.01-3 μM) (C and D) were applied once every 2 min at increasing concentrations. Chelerythrine was added to the incubation fluid 15 minutes before application of agonists. The ordinates are percentage of variation of spontaneous contraction rate (chronotropic effect, A and C) and mechanical tension (inotropic effect, B and D) as compared to baseline values obtained before application of R-PIA or oxotremorine. The data are expressed as mean ± SEM from an *n* number of individual experiments. **P*<0.05 compared with the effect of agonists in the absence of PKC inhibitor.

PKC activity has been associated to myofilament Ca^{2+} sensitization and phosphorylation of TnI and cardiac myosin binding protein-C promote a positive inotropic effect (Cazorla *et al*., 2009). This mechanism may add another possible explanation for the preferential chronoselective action of ADO in the rat spontaneously beating atria. Enrolment of the PLCβ/PKC signaling cascade pathway triggered by A_1R activation partially counteracts the negative inotropic effect of the nucleoside that one would expect by simply hyperpolarizing atrial cardiomyocytes and, thereby, decreasing intracellular Ca^{2+} accumulation. Unraveling these complexities requires further experimental work. Unexpectedly, non-specific activation of PKC with the phorbol 12-myristate 13-acetate, PMA (0.03-10 μM) (Puceat and Vassort, 1996), concentration-dependently increased sinus rate reaching a maximum at 10 μM (+11±3%, *P*<0.05; *n*=11), yet no effect was observed in the strength of contractions of the spontaneously beating rat atria (*P*>0.05;

n=11, data not shown). Pre-incubation of the preparations with PMA (10 μM, for 15 minutes) did not significantly (*P*>0.05) change R-PIA (0.001-1 μM) and oxotremorine (0.01-3 μM) atrial depression (Figure 19).

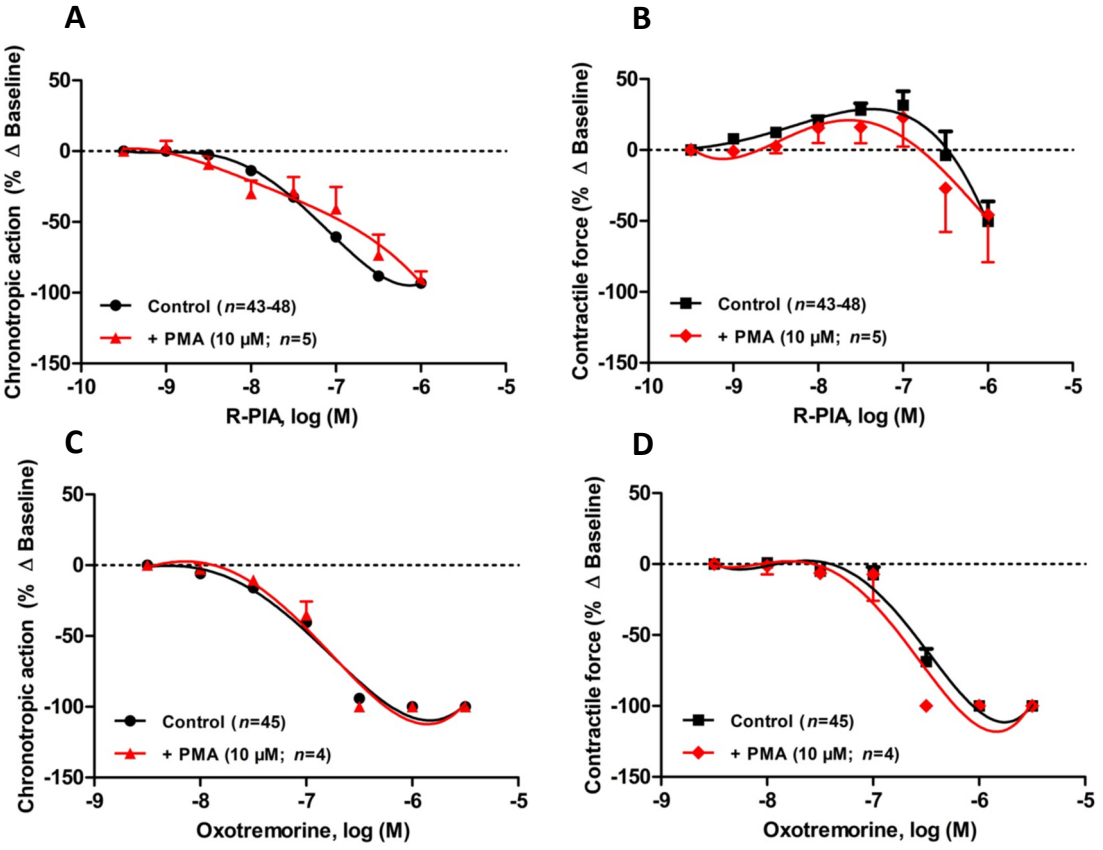

Figure 19. PKC activation failed to modify the effects of A_1R and M_2R. Concentration-response curves of R-PIA (A and B) and oxotremorine (C and D) in the absence (Control) or in the presence of the PKC activator, PMA (10 μM). R-PIA (0.001-1 μM) (A and B) and oxotremorine (0.01-3 μM) (C and D) were applied once every 2 min at increasing concentrations. PMA was added to the incubation fluid 15 minutes before application of agonists. The ordinates are percentage of variation of spontaneous contraction rate (chronotropic effect, A and C) and mechanical tension (inotropic effect, B and D) as compared to baseline values obtained before application of R-PIA or oxotremorine. The data are expressed as mean ± SEM from an *n* number of individual experiments. **P*<0.05 compared with the effect of agonists in the absence of PKC activator.

In spite of these unexpected results, we cannot rule out the participation of PKC in A_1R-mediated atrial depression, since PMA acts as a non-selective activator of PKC leading to enzyme desensitization. Furthermore, growing evidence points towards specific activation and translocation of some PKC isozymes secondary to A_1R activation (Lester and Hofmann, 2000; Yang *et al*., 2009b). In order to avoid non-selective activation of PKC by PMA, we performed experiments with two G-protein-coupled neurohormonal agents known to couple positively to the PLC/PKC pathway via the $G\alpha_q$ subunit (Puceat and Vassort, 1996). This was carried out by using angiotensin II (AngII), as an AT_1 receptor agonist considering its ability to engage specifically the activation of novel PKCs isoforms

(PKC-ε and PKC-δ) (Kilts *et al*., 2005), and UTP, as an activator of cardiac $P2Y_2$ and $P2Y_4$ receptors coupled to $G\alpha_q$ subunits.

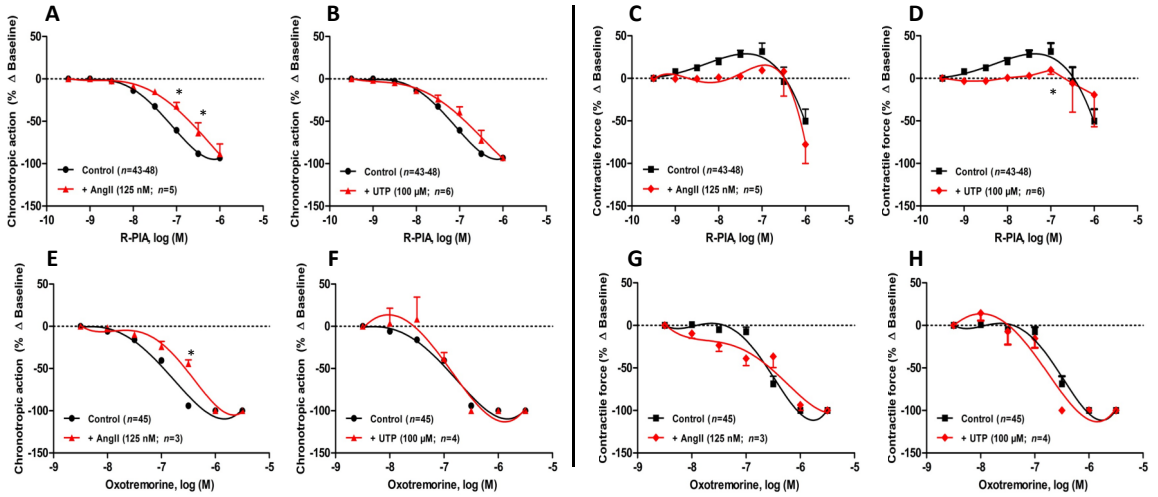

Figure 20. $G\alpha_q$ protein-coupled receptors (AT_1 and $P2Y_{2,4}$ receptors) did not interfere with signaling properties of both A_1R and M_2R. Left panels (A, B, E and F) are plotted concentration-related chronotropic for R-PIA (A and B) and for oxotremorine (E and F) in the absence (Control) or in the presence of AngII (A and E) or UTP (B and F). Right panels (C, D, G and H) are plotted concentration-related inotropic for R-PIA (C and D) and for oxotremorine (G and H) in the absence (Control) or in the presence of AngII (C and G) or UTP (D and H). R-PIA (0.001-1 μM) and oxotremorine (0.01-3 μM) were applied once every 2 min at increasing concentrations; AT_1 and $P2Y_{2,4}$ agonists, Ang II (125 nM) and UTP (100 μM), respectively, were added to the incubation fluid 15 minutes before application of R-PIA or oxotremorine. The ordinates are percentage of variation of spontaneous contraction rate (chronotropic effect, left panels) and mechanical tension (inotropic effect, right panels) as compared to baseline values obtained before application of R-PIA or oxotremorine. The data are expressed as mean ± SEM from an *n* number of individual experiments.*P<0.05 is considered statistically different compared with the corresponding control curve for each agonist.

As expected, AngII (125 nM) developed statistically significant positive inotropic (+8±3%, P<0.05; n=8) and chronotropic (+10±3%, P<0.05; n=8) responses (data not shown) (Li *et al*., 1996). On the other hand, UTP (100 μM) did not significantly change the sinoatrial rate (P>0.05), although it mildly increase the atrial inotropy (+17±4%, P<0.001; n=14) (data not shown). Pre-incubation with AngII (125 nM) or UTP (100 μM) did not significantly modify the effects of R-PIA (0.001-1 μM) and oxotremorine (0.01-3 μM) in the rat spontaneously beating atria (Figure 20).

IV. Discussion

In the present work we evaluated the effects of two well-know neurohormonal agents ADO and ACh on the spontaneously beating rat atria. ADO and ACh analogues exerted pronounced negative chronotropic and inotropic effects (Figure 6) respectively through A_1AR and M_2R (De Biasi *et al*., 1989; Kohl *et al*., 1990; Ford and Broadley, 1999). Interestingly, the negative chronotropic effect of A_1R activation was evidenced at much lower concentrations (~30 fold) than the negative inotropic effect. The ADO chronoselective effect was a singular hallmark of A_1R, since the M_2R agonist oxotremorine was equipotent upon reducing chronotropy and inotropy (Figure 6). So, we first investigated whether A_1R chronoselectivity could be an outcome of a higher expression of this receptor in the SA node than in the atrial muscle. We observed that A_1R and M_2R are abundantly expressed in rat atria, as previously described (Krejci and Tucek, 2002; Myslivecek *et al*., 2008; Chandler *et al*., 2009) (Figure 8). Immunolocalization experiments did not reveal any noticeable difference regarding the A_1R staining across the entire right atria, as it was observed for the M_2R (Chandler *et al*., 2009; Yanni *et al*., 2011). These observations suggest that the chronoselectivity induced by A_1R stimulation is not supported by a differential expression of this receptor within the atrial tissue in particular the SA node, strengthening the hypothesis that other mechanisms must be involved.

Additionally, we further speculated on whether ADO chronoselectivity could hold an A_{2A}R-mediated component. The selective A_{2A}R agonist, CGS 21680, revealed a negligible positive inotropy at higher concentrations (Chandrasekera *et al*., 2010). Although, A_{2A}R was found to be expressed in mammalian atria (Hove-Madsen *et al*., 2006), we found low levels of immunofluorescence representation of this receptor at the rat atria as compared to the A_1R (Figure 9). While the role of A_{2A}R in cardiac inotropism is still a matter of debate, some authors argue that A_{2A}R activation can increase the sensitivity of the contractile apparatus (Hove-Madsen *et al*., 2006), thereby enhancing myocardial contraction (Dobson and Fenton, 1997; Monahan *et al*., 2000; Tikh *et al*., 2006). Conversely, other authors failed to detect positive inotropic effects after A_{2A}R stimulation (Willems and Headrick, 2007; Gergs *et al*., 2009; Chandrasekera *et al*., 2010). These contradictory data support the hypothesis that A_{2A}R only plays a role in the modulation of the β-adrenergic action rather than a direct effect on cardiac inotropism (Tikh *et al*., 2006; Fenton *et al*., 2009; Chandrasekera *et al*., 2010).

It is well-known that A_1R and M_2R stimulate outward K^+ currents ($I_{KAdo,ACh}$) through Gβγ subunits activation of G protein-coupled inwardly rectifying (tertiapin Q-sensitive) GIRK/K_{IR}3.1/3.4 channels (Kurachi *et al*., 1986; Logothetis *et al*., 1987; Krapivinsky *et al*., 1995; Han and Bolter, 2011). This action reduces the electrogenic current carried by ion

channel/exchangers involved in the diastolic depolarization (phase 4) and speeds up the AP repolarization phase. The overall effect of this GIRK/K_{IR}3 current is a decreased excitability of the SA nodal cells, *i.e.* negative chronotropy. Faster AP repolarization (phase 3) also reduces the time available for Ca^{2+} influx during phase 2 of the AP, thereby putatively reducing atrial inotropism (Kurachi *et al*., 1986; Wang and Belardinelli, 1994; Belardinelli *et al*., 1995; Lyashkov *et al*., 2009). Taking into account that all experiments described herein were carried out in the absence of electrical pacing or adrenergic stimulation, the effects operated by A_1R and M_2R activation are likely to be mediated directly by GIRK/K_{IR}3 opening, as proven by the attenuation of the cardiodepressant effects of A_1R and M_2R agonist upon inhibition of these channels with tertiapin-Q. It is worth noting that GIRK1/K_{IR}3.1channel subunits are expressed throughout the rat atria, in both the SA node and the atrial cardiomyocytes, as detected by immunofluorescence confocal laser microscopy in this study (Figure 10), which confirmed other authors' findings (Dobrzynski *et al*., 2001; Chandler *et al*., 2009; Yanni *et al*., 2011).

We further investigated the role of other ionic channels on A_1R- and M_2R-elicited responses, in order to explore if they were functionally coupled to A_1R, but not to M_2R, which could justify the preferential A_1R-mediated chronoselective atrial depressant effect. Among the channel blockers tested in this study, namely verapamil (a Ca_V1 (L-type) channel blocker), mibefradil (a low voltage-activated Ca_V3 (T-type) channel blocker), 4-aminopyridine (a non-specific voltage-dependent K_v channel blocker), glibenclamide (a selective ATP-sensitive $K_{ATP}/K_{IR}6$ channel blocker) and apamin (a $K_{Ca}2$/SK channel blocker), only verapamil and apamin selectively affected the contractile responses elicited by A_1R activation, which put forward the putative enrollment of Ca_V1 (L-type) and SK/$K_{Ca}2$ channels on ADO chronoselectivity. Our results are in general agreement with previous isometric contraction studies performed in the guinea-pig atria, where 4-AP (0.3-3 mM) failed to modify chronotropic and inotropic effects elicited by increasing concentrations of R-PIA (De Biasi *et al*., 1989). Conversely, other authors reported the ability of 4-AP to counteract the negative chronotropic and inotropic effects of M_2 and A_1 receptor agonists in atrial preparations (Urquhart and Broadley, 1991; Ford and Broadley, 1999). Due to the high concentrations of 4-AP used in the latter studies, which were 1000 times higher than that used in this report (10 μM), a question remains unanswered about the K_v channel selectivity of the 4-AP blocking effect under those circumstances. Regarding glibenclamide-sensitive K^+ channels, some authors connected its opening to protective effects of ADO under conditions of low oxygen tension (e.g. ischemia, hypoxia) (Kirsch *et al*., 1990). However, under well-oxygenated conditions, high levels of ATP tonically inhibits ATP-sensitive $K_{ATP}/K_{IR}6$ channel opening, explaining the lack of effect of glibenclamide in antagonizing the responses to M_2 and A_1 receptor agonists in the rat

atria, in good agreement with previous studies (Keith and Flack, 1907; Urquhart *et al*., 1993; Ford and Broadley, 1999). Beyond these K^+ currents, Ca^{2+} current carried by Ca_V3 (T-type) channel is excluded from adenosinergic as well as cholinergic regulation of atrial function (Cerbai *et al*., 1988).

The leftward displacement of the concentration-response curve regarding the inotropic effect of R-PIA upon blocking Ca_V1 (L-type) channels (with verapamil) has two reasonable interpretations: 1) A_1R stimulation inhibits Ca_V1 (L-type) channels that is further potentiated by Ca_V1 (L-type) channels blockade, or 2) under basal conditions, A_1R stimulation decreases to a lesser extent the net Ca^{2+} entry into atrial myocytes when compared to M_2R, attenuating the cardiodepressor effect promoted by opening of GIRK/$K_{IR}3$ channels.

The first explanation is somehow controversial; there are no clear evidences that $G\alpha_i$-coupled receptors, such as A_1R and M_2R, decrease directly the Ca_V1 (L-type) channels, although some authors detected a small inhibitory actions of adenosinergic and cholinergic agonists on this currents (Cerbai *et al*., 1988; De Biasi *et al*., 1989; Visentin *et al*., 1990). Recent experimental data also proposed an inhibition of $I_{Ca,L}$ currents in the course of releasing Gβγ subunits from activated $G\alpha_i$/o-coupled receptors (O-Uchi *et al*., 2008). Conversely, in guinea pig atrial myocytes, ADO did not show any significant changes on $I_{Ca,L}$, in the presence of its activator BAY K 8644 (Wang and Belardinelli, 1994).Ca_V1 (L-type) channels inhibition operated by A_1R and M_2R activation may, most probably, be an indirect effect, considering that GIRK/$K_{IR}3$ opening shortens AP duration and reduces the time available for the influx of Ca^{2+} (Iijima *et al*., 1985; Wang and Belardinelli, 1994; Belardinelli *et al*., 1995; Ford and Broadley, 1999).

The second hypothesis fits our data if we take into consideration a presumable interaction between A_1R and apamin-sensitive SK/$K_{Ca}2$ channels (Figure 13). SK/$K_{Ca}2$ channels behave like truly intracellular Ca^{2+} sensors by changing their K^+ conductance and membrane resting potential. At least three types of ion channels may participate in this mechanism, namely SK1/$K_{Ca}2.1$, SK2/$K_{Ca}2.2$ and SK3/$K_{Ca}2.3$. These channels exhibit weak-voltage dependence, differences in Ca^{2+}-dependent activation and variable sensitivity to apamin (Ishii *et al*., 1997; Xu *et al*., 2003; Tuteja *et al*., 2005). Interestingly, the concentration-response curve for the negative inotropic effect of R-PIA was significantly modified upon blockade of SK/$K_{Ca}2$ channels with apamin, without affecting the effect of oxotremorine. This renders a functional crosstalk between A_1R and SK/$K_{Ca}2$ channels on inotropy, highly probable. This experimental result therefore challenges previous assumption that A_1R function is insensitive to SK/$K_{Ca}2$ channels blockade in the guinea-pig atria (De Biasi *et al*., 1989). Sensitization of rat atria to the negative inotropic effect of the A_1R agonist in the presence of the SK/$K_{Ca}2$ channel blocker affords a

functional role for these channels on E-C coupling mechanisms. Blockade of SK/K_{Ca}2 channels may cause a delay in the repolarization phase of atrial APs (Xu *et al*., 2003; Tuteja *et al*., 2005), despite of Nagy and co-workers have failed to detect any electrophysiological change upon apamin exposure (Nagy *et al*., 2009). In our hands, blockade of SK/K_{Ca}2 channels caused *per se* a slight increase in the strength of contraction, which might be related to an increase in the available time for Ca^{2+} influx via Ca_V1 (L-type) channels due to AP prolongation. Interestingly, Ca_V1 (L-type) channels are sought to be functionally coupled to SK2/K_{Ca}2.2 channels, sharing the same cytoskeletal protein α-actinin2 (Lu *et al*., 2007). Even more interestingly, these authors showed that this multiprotein complex formed by SK2/K_{Ca}2.2, Ca_V1 (L-type) channel and α-actinin2 is located in cardiac t-tubules, where the functional units of the cardiac E-C coupling are located, reinforcing the importance of a hypothetical regulation of Ca_V1 (L-type) channels gating by SK/K_{Ca}2 channels operation, with important outcomes on inotropy regulation (Bers, 2002; Catterall, 2011). Thus, a possible explanation for ADO chronoselectivity is that A_1R partially inhibits SK/K_{Ca}2 channel, decreasing the voltage- and time-dependent inactivation of Ca_V1 (L-type) channels during AP repolarization phase, leading to a lesser net decrease of Ca^{2+} influx into atrial myocytes during A_1R (vs M_2R) stimulation (Xu *et al*., 2003; Tuteja *et al*., 2005).

Despite being an attractive hypothesis, at this moment there is no clear evidence that supports inhibition SK/K_{Ca}2 channels by A_1R activation. Keeping in mind this hypothetical scenario, it would be expected a higher activity of inward currents, like $I_{Ca,L}$, during pharmacological inhibition of SK/K_{Ca}2 channels and, thus, a rightward displacement of the inotropic concentration-response curve for R-PIA. Of note is that our experimental procedure to evaluate inotropy is based on variations of the contractile tension that might reflect Ca^{2+} influx from Ca_V1 (L-type) channels (Bers, 2002). Therefore, the leftward displacement of the inotropic concentration-curve for R-PIA with either SK/K_{Ca}2 or Ca_V1 (L-type) channels blockade might be interpreted as a relative increase of GIRK/K_{IR}3-mediated K^+ efflux and cell hyperpolarization *per* GPCR activated, thus affecting the relative potency of the A_1R agonist. As mentioned above, a greater contribution of GIRK/K_{IR}3-mediated K^+ efflux will shorten much more the atrial APs, thereby reducing even more the Ca^{2+} influx through Ca_V1 (L-type) channels (Iijima *et al*., 1985; Wang and Belardinelli, 1994; Belardinelli *et al*., 1995). We believe that SK/K_{Ca}2 channels should only have a modulator role on A_1R-mediated responses, since apamin *per se* did not have a meaningful effect on inotropy. Interestingly, a recent report has demonstrated an interaction between A_1R and SK/K_{Ca}2 channels in retinal ganglion cells, which was dependent on IP_3-induced Ca^{2+} release from internal stores, even though it has been concluded that SK/K_{Ca}2 channel opens in response to A_1R activation (Clark *et al*.,

2009). Despite SK/K_{Ca}2 channels expression in the SA node (Figure 15), their blockade did neither affected spontaneous AP firing rate under basal conditions nor the chronotropic concentration-response curves for R-PIA and oxotremorine (Figures 13 and 14), which might suggest a non-functional role on chronotropy regulation, at least in healthy and adult heart mammals. As presented in Figure 15, both SK2/K_{Ca}2.2 and SK3/K_{Ca}2.3 are both present throughout the right atria, despite their dissimilar labeling pattern. The SK2/K_{Ca}2.2 channels are mainly present around the myocytes, even though some authors have showed a t-tubule location (Lu *et al*., 2007). SK3/K_{Ca}2.3 showed an internal labeling pattern and lower immunoreactivity in atrial myocytes as observed by others (Tuteja *et al*., 2005). However, myocytes of the SA nodal showed a high level of staining using anti-SK3/K_{Ca}2.3 antibody when compared to surrounding tissue, compatible with the differential abundance of SK3/K_{Ca}2.3 transcripts within the rat atria (Yanni *et al*., 2011). It is worth of notice that the abundance of SK1/K_{Ca}2.1 and SK3/K_{Ca}2.3 channels, but not SK2/K_{Ca}2.2 channel, was greatly increased in the SA node during heart failure (Yanni *et al*., 2011). The physiological importance of these regional differences for SK/K_{Ca}2 channels has yet to be determined.

Immunofluorescence micrographs (Figure 15) confirmed the presence of verapamil and apamin-sensitive channels and support the pharmacological data elicited by these two blockers. Immunofluorescence analysis exhibited weaker immunoreactivity intensity for the extracellular $\alpha_2\delta$-1 subunit of the Ca_V1 (L-type) channels. In studies performed in the right atrium of either human or rat heart, the accessory $\alpha_2\delta$-1 subunit was found equally expressed between SA node and atrial muscle (Chandler *et al*., 2009; Yanni *et al*., 2011). From the analysis of these two studies we can argue that accessory subunit of Ca_V1 (L-type) channel is relatively high expressed in mammal's right atrium and there is no clear relation with the expression of each Ca_V1 (L-type) channels pore-forming α subunit (α_{1C} and α_{1D}). Ca_V1 (L-type) α_{1C} subunit ($Ca_V1.2$) is much more expressed in atrial muscle than in SA node of adult mammals, while the Ca_V1 (L-type) channels α_{1D} ($Ca_V1.3$) subunit has an opposite expression pattern (Tellez *et al*., 2006; Chandler *et al*., 2009; Allah *et al*., 2011). Here, despite the unexpected low immunoreactivity for Ca_V1 (L-type) channels $\alpha_2\delta$ subunits, the absence of its differential expression between SA node and atrial muscle matches with reported experimental data regarding $\alpha_2\delta$-1 subunit expression. At the best of our knowledge, this is the first study designed to analyze the Ca_V1 (L-type) $\alpha_2\delta$-1 subunit expression in the mammalian heart by confocal microscopy.

Other putative explanation for ADO chronoselectivity was brought to light from recent studies on the molecular signaling dynamics and compartmentalization of the receptors and channels in sarcolemma microdomais, like caveolae. Here, we showed that A_1R-mediated responses are somehow linked to the PLCβ-PKC pathway, in opposition to

M_2R responses (Figure 16 and 18). A_1R and M_2R are both $G\alpha_i$-coupled receptors and their activation leads to dissociation of the Gβγ dimer. Since free Gβγ subunits may stimulate PLCβ (Boyer *et al*., 1992), one might predict that the M_2R-mediated effects would be also sensitive to inhibition of PLCβ by U73122, as it happened with the negative inotropic response elicited by A_1R activation (Figure 16). Therefore, following A_1R activation we should expect increases in PLCβ end products, such as IP_3 and diacylglycerol (Nishizuka, 1992). Overwhelming experimental data demonstrated that A_1R agonists increase the levels of both IP_3 and DAG in a large variety of cell types (Kohl *et al*., 1990; Gerwins and Fredholm, 1992; Dickenson and Hill, 1998; Cordeaux *et al*., 2000; Lester and Hofmann, 2000; Parsons *et al*., 2000; Fenton *et al*., 2010). Although we did not measure IP_3 and DAG levels, data obtained with the PLC inhibitor applied prior to stepwise addition of R-PIA significantly sensitized atria to the negative inotropic effect of A_1R and removed ADO chronoselectivity. But how does PLCβ attenuate the inotropic depressor effect of A_1R? To answer this question we need to go back and look carefully to the concentration-responses curves of R-PIA in the absence and presence of tertiapin-Q (Figure 10). When GIRK/K_{IR}3 channels were blocked, spontaneous atrial beatings did not stop neither atrial contractile tension was reduced during stimulation of both cholinergic and ADO receptors. Thus, regarding GIRK/K_{IR}3 channels one may argue that they might play an important role on E-C coupling from supraventricular tissues during cholinergic and adenosinergic stimuli, and their opening mediates a negative inotropic response (Iijima *et al*., 1985; Wang and Belardinelli, 1994; Belardinelli *et al*., 1995; Ford and Broadley, 1999). The relation between GIRK/K_{IR}3 channels and PLCβ activity come up from the well-accepted PIP_2 role on GIRK/K_{IR}3 channel gating (Whorton and MacKinnon, 2011).

ADO and ACh stimulate GIRK/K_{IR}3 channels opening but with different magnitudes and kinetics (Kurachi *et al*., 1986; Cho, 2010; Littwitz *et al*., 2011). In atrial myocytes both the onset kinetics and the total GIRK/K_{IR}3 current activated by supramaximal concentrations of ADO (> 10 μM) ($I_{K,ADO}$) are slower and of a lesser magnitude than those obtained with ACh (> 10 μM) ($I_{K,ACh}$) (Cho, 2010). Besides that, $I_{K,ADO}$ is more sensitive to $G\alpha_q$-coupled receptor modulation (e.g. α_1-adrenoceptors) than $I_{K,ACh}$ (Cho, 2010; Cui *et al*., 2010). As claimed in these authors' studies, PIP_2 signaling microdomain and caveolar receptor compartmentalization might be the basis for the differential receptor-mediated activation and regulation of GIRK/K_{IR}3 channels. PIP_2 is needed for GIRK/K_{IR}3 channels opening and its catabolism inhibits the hyperpolarizing K^+ current (Kobrinsky *et al*., 2000). Interestingly, using neomycin as a measure of PIP_2 affinity, M_2R-activated GIRK/K_{IR}3 current showed higher affinity for PIP_2 than the ones elicited by A_1R activation (Cho, 2010). Comparatively $I_{K,ACh}$ is a stronger current with a lesser sensitivity to PIP_2 perturbation than $I_{K,ADO}$, at least in mouse atrial myocytes (Cho, 2010; Cui *et al*., 2010). If

we take into consideration that the A_1R-activated GIRK/$K_{IR}3$ current is weaker, along with the putative A_1R-mediated PIP_2 hydrolysis, it may be reasonable to assume that the lesser A_1R-mediated contractile depression compared to M_2R activation might be a consequence of the limited negative inotropy when GIRK/$K_{IR}3$ couples do A_1R activation. Consistent with this theory, inhibition of PLCβ with U73122 protected PIP_2 from A_1R -mediated hydrolysis and enhanced GIRK/$K_{IR}3$ channels activity, which in turns potentiates the negative inotropy (Figure 16). In this context there seems to be a spatiotemporal regulation of PIP_2 signaling within caveolae that connects receptor function to ionic channel currents. A_1R stimulation might, therefore, have a less impact on negative inotropy probably because this receptor recruits signaling machinery to caveolae where GIRK/$K_{IR}3$ channels are located, stimulating GIRK/$K_{IR}3$ channel activation followed by its inactivation, whereas M_2R lack this effect. Lesser K^+ conductance carried by GIRK/$K_{IR}3$ channel conductance mirrors smaller voltage- and time-dependent inactivation of Ca_V1 (L-type) channels located in the t-tubules that, in a final step, yields a lesser reduction of net Ca^{2+} influx into atrial myocytes as compared to M_2R. It is worth mentioning the lower chronotropic sensitivity to PLC inhibition (Figure 16A and C), demonstrating that the control of spontaneous generation of pacemaker AP is not so sensitive to GIRK/$K_{IR}3$ channel modulation as atrial myocytes, and might involve other key mechanisms in adenosinergic and cholinergic depression (Wickman *et al*., 1998; Vinogradova *et al*., 2006; Lyashkov *et al*., 2009).

Nevertheless, the previous theory proposed for ADO chronoselectivity may not rely solely on the reorganization of signaling proteins and lipids within caveolae. We need to go beyond sarcolemma microdomains and look to downstream targets of PLCβ. There is growing evidence for an increase of DAG and IP_3 from PIP_2 hydrolysis following A_1R stimulation (Kohl *et al*., 1990; Gerwins and Fredholm, 1992; Dickenson and Hill, 1998; Cordeaux *et al*., 2000; Lester and Hofmann, 2000; Parsons *et al*., 2000; Fenton *et al*., 2010). For example, after specific A_1R activation, a meaningful increase of inositol phosphates and DAG levels has been observed in cultured chick embryo ventricular myocytes, which was attenuated by the PLC inhibitor U73122 (10 μM) (Parsons *et al*., 2000). Other studies also detected a Gβγ-dependent increase of IP_3 levels following A_1R stimulation in mouse heart myocytes (Fenton *et al*., 2010). Even though it was not expected an outstanding modulation of PLCβ by A_1R, as observed with stimulation of other $G\alpha_q$-coupled receptors (e.g. odd-numbered muscarinic receptors, AT_1 receptors), because Gβγ subunits are less potent activators of PLC compared with G protein α_q subunits (Boyer *et al*., 1992; Biber *et al*., 1997). Positive chronotropic and inotropic effects are connected to $G_{\alpha q}$ proteins-coupled receptor stimulation (He *et al*., 2000; Lipp *et al*., 2000; Bers, 2002; O-Uchi *et al*., 2008; Ju *et al*., 2011).

Multiple analysis of IP_3 receptors revealed higher expression and function of subtype II in atrial myocytes than in ventricular ones (about 6-fold) together with a subsarcolemmal location near junctional RyRs (Lipp *et al*., 2000). IP_3 formation induces Ca^{2+} release from internal stores (Berridge, 1993). Thus, in supraventricular tissues IP_3 enables stimulating effects on atrial E-C coupling (Lipp *et al*., 2000; Bers, 2002). With respect to our results, the contractile depression observed with PLC inhibition during A_1R stimulation (Figure 16) might also be interpreted as a blunted PLC-mediated positive stimulus. Positive inotropic responses following A_1R stimulation were also observed in other reports (Neumann *et al*., 1999; Gergs *et al*., 2009). The present results implies a direct cross-talk between A_1R and PLCβ (Fenton *et al*., 2010), which may increase IP_3-induced Ca^{2+} release from intracellular stores (Berridge, 1993) attenuating the negative inotropy mediated through GIRK/K_{IR}3-mediated K^+ efflux.

The supposed connection between ADO chronoselectivity and the A_1R-induced IP_3 increase could not be addressed in our experimental model because 2-APB (30 μM), an IP_3 receptor blocker (Maruyama *et al*., 1997), blocked the spontaneous atrial contractions (Figure 17). This result means that there is a basal and critical activity for IP_3 receptors on the spontaneous generation of AP at the SA node. In fact, several reports argue in favor of a relevant function of IP_3R on cardiac pacemaker activity (Ju *et al*., 2011). However, we cannot exclude the lack of pharmacological selectivity by 2-APB on other critical pacemaker components. The proposed mechanism for 2-APB was the inhibition of SERCA pump, leading to a progressive depletion of Ca^{2+} stores followed by an E-C coupling impairment (Peppiatt *et al*., 2003).

Moving towards downstream targets of the PLCβ generated products, we explored the role of PKC on both A_1R- and M_2R-mediated responses. Inhibition of PKC with chelerythrine significantly potentiated the negative inotropy mediated by A_1R activation with no appreciable effects on the negative chronotropy (Figures 18A and B). Surprisingly, PKC inhibition did not affect both chronotropy and inotropy effects of M_2R stimulation (Figures 18C and D), unveiling another signal transduction disparity between the A_1R and M_2R signaling. The role of PKC in A_1R-mediated responses is not surprisingly since PLCβ is an effector of the ADO signaling pathway, providing stimuli input for PKC activation through DAG formation and IP_3-dependent Ca^{2+} release (Parsons *et al*., 2000; Fenton *et al*., 2010). Indeed, there are numerous reports supporting the existence of PKC and A_1R crosstalk in a wide variety of responses like in adrenoprotection (Lester and Hofmann, 2000; Fenton *et al*., 2009; Fenton *et al*., 2010). According to our results, there is a clear tendency for PKC counteracting the A_1R-mediated contractile depression. Therefore, it would be expected a positive inotropic effect upon atria exposure to increasing concentration of the PKC activator, PMA. Unexpectedly, the concentration-response curve

of PMA, as well as the direct application of PMA (10 μM) for 15 min, did not show any considerable effect on atrial contraction force and only a minor positive chronotropy was observed (data not shown). Moreover, PMA was not able to modify both inotropic and chronotropic curves for A_1R as well as for M_2R stimulation (Figure 19).

PKC has a broad-spectrum of substrates that comprises ionic channels, myofilaments, and even kinases (Puceat and Vassort, 1996; Kamp and Hell, 2000; Solaro, 2008; Yang *et al*., 2009a), but there is no consensus in the scientific community about the functional effects of PKC on heart function. While some authors ascribe positive inotropic effects for PKC others allocate negative or no effects (Capogrossi *et al*., 1990; MacLeod and Harding, 1991; Karmazyn and Haist, 1993). Even more intriguing about PKC is the fact that a wide variety of positive inotropic mechanisms are usually dependent on PKC function (He *et al*., 2000; Kilts *et al*., 2005; O-Uchi *et al*., 2008; Cazorla *et al*., 2009; Oestreich *et al*., 2009). An explanation for these controversies around PKC could rely on broadly activation of several PKC isozymes due to lack of selective drugs, in contrast to neurohormonal agonists; animal species and their development stage; time, type, concentration and even in the mode of PKC-targeted drugs administration (Karmazyn and Haist, 1993; Puceat and Vassort, 1996; He *et al*., 2000).

Rather than a non-selective activation of PKC isozymes, A_1R signaling has been connected to selective activation of PKC-ε and PKC-δ isozymes, which are the major Ca^{2+}-independent and the most abundant PKC isoforms found in adult rat cardiomyocytes (Yang *et al*., 2009b). However, while the selective activation, translocation and anchoring of PKC isozymes to specific subcellular locations is undoubtedly important for ADO signaling, it remains to be elucidated how this is accomplished and what are the functional effects on heart's function. Concerning cardiac contractile function, some reports describe PKC-ε as a negative effector of A_1R-mediated cardiodepression (Lester and Hofmann, 2000; Fenton *et al*., 2009; Fenton *et al*., 2010). Conversely, other studies regarding functional effects of PKC-ε have challenged the above mentioned PKC-ε-mediated negative effect (Kang and Walker, 2005; Kilts *et al*., 2005; O-Uchi *et al*., 2008). Myocytes overexpressing either PKC-ε or PKC-δ react to PKC activator phorbol 12,13-dibutyrate (PDBu) developing a short negative followed by a sustained positive inotropic response, i.e. biphasic response, while control myocytes only developed negative responses. Interestingly, pharmacological maneuvers selectively targeted to Ca^{2+}-dependent PKC isoforms inhibition (Gö 6976, 1 μM) only removed negative inotropic responses elicited by phorbol esters, which suggests an involvement of conventional (e.g. α, β) and novel PKCs (e.g. ε, δ) on the negative and positive inotropic responses, respectively (Kang and Walker, 2005), in good agreement with recent reports (Kilts *et al*., 2005; O-Uchi *et al*., 2008; Liu *et al*., 2009). Thus, PKC isoforms are likely to have different or even opposing

effects on heart muscle contractility; hence, the non-selective PKC activation (Yang *et al*., 2009b) may explain the absence of effect observed with PMA (Figure 19). It is worth noting that PMA is a broad spectrum activator of PKC and that property could mask the involvement of some PKC isoforms on A_1R-mediated effects. To overcome the lack of specificity by PMA in PKC activation, we employ UTP and AngII as neurohormonal agents known for their action on $G\alpha_q$-coupled receptors (Puceat and Vassort, 1996; Kilts *et al*., 2005). Unfortunately, previous activation of the downstream $G\alpha_q$-coupled receptors pathways either with AngII or UTP failed to change the typical atrial effects produced by A_1 and M_2 agonists (Figure 20). However, we should not rule the hypothetical connection between A_1R and PKC, since the experimental approach used in this work might not be suitable to unveil this crosstalk. Our results point to an interplay of PKC with the A_1R (Figure 18), but further investigations are needed to clearly understand what is behind the chronoselective effect.

At this moment, limited conclusions are available regarding the effects of PKC isozyme(s) in the regulation of contractile force (Puceat and Vassort, 1996). For those who support a negative contractile response, a decrease in myofilament Ca^{2+} sensitivity and cross-bridge cycling, is a likely explanation (Lester and Hofmann, 2000; Solaro, 2008; Fenton *et al*., 2009), while for the others modulation of Ca^{2+}-handling proteins (e.g. phospholamban, Ca_V1 (L-type) channels, RyR) and myofilament Ca^{2+} sensitization are on the basis of positive inotropic responses (He *et al*., 2000; Kang and Walker, 2005; Wang *et al*., 2006; Cazorla *et al*., 2009; Oestreich *et al*., 2009).

V. Conclusion

In conclusion, we demonstrated that atrial chronoselectivity observed for ADO A_1R-mediated responses is not supported by a higher expression of A_1R in the SA node as compared to the atrial muscle. The matchless chronoselectivity for A_1R, observed in the spontaneously beating rat atria, may yield from the molecular enrolment of A_1R with $SK/K_{Ca}2$ and Ca_V1 (L-type) channels, a PLC and downstream effectors as well.

At the mechanistic level, we showed that contractile depression triggered by A_1R and M_2R activation are mostly restricted to K^+ efflux through $GIRK/K_{IR}3$ channels opening, especially when atria are not under sympathetic influence. Given the pivotal role of PIP_2 on $GIRK/K_{IR}3$ channel gating (Kobrinsky *et al*., 2000; Whorton and MacKinnon, 2011), any perturbation in the steady-state PIP_2 levels may lastly interfere with $GIRK/K_{IR}3$-regulated atrial contraction. In fact, our study provides strong evidences that the membrane-restricted PIP_2 signaling could be modulated by A_1R. Both A_1R and M_2R activate $GIRK/K_{IR}3$ channel, in a Gβγ- dependent manner. However, since K^+ current carried by $GIRK/K_{IR}3$ channels upon A_1R stimulation is much more sensitive to PIP_2 perturbation, the proposed A_1R-mediated stimulation of PLCβ activity may decrease PIP_2 levels within sarcolemmal microdomais where $GIRK/K_{IR}3$ channels are located, then promoting $GIRK/K_{IR}3$ channel deactivation along with a less $GIRK/K_{IR}3$-mediated contractile depression, at least in comparison to M_2R (Figure 21). The interplay of A_1R with PLCβ may also trigger SR Ca^{2+} release through generation of IP_3 (Berridge, 1993) that should attenuate negative inotropy, but this remains a speculative assumption since our experimental approach does not prove it.

Beside $GIRK/K_{IR}3$ channels, our functional experiments go in line with a restrained $SK/K_{Ca}2$ channel operation during A_1R stimulation that greatly affects the atrial inotropic status. Inhibition of repolarizing K^+ currents during AP repolarization phase, like K^+ currents carried by $GIRK/K_{IR}3$ and $SK/K_{Ca}2$ channels should in a final step interfere with Ca^{2+} dynamics that drive E-C coupling in atrial myocytes. These channels can be regarded as gatekeepers of cellular excitability readily to be recruited during stressful conditions. If these repolarizing K^+ currents shorten AP, thereby obviating time course for Ca^{2+} influx (Iijima *et al*., 1985; Capogrossi *et al*., 1990; Wang and Belardinelli, 1994; Belardinelli *et al*., 1995), it is reasonable to assume that the contrary is true for the proposed inhibition of these currents upon A_1R activation. Thus, negative inotropism of A_1R holds a compensatory contractile mechanism comprised by K^+ channels inhibition and, consequently, longer times for Ca^{2+} entry into atrial myocytes. Unlike atrial muscle cells, SA nodal cells seem to be tougher to modulation of $SK/K_{Ca}2$ gating and PLCβ/PKC axis. Hence, in SA nodal cells the depressor balance supplied by these signaling proteins

might not be relevant for A_1R chronotropic regulation, explaining why A_1R act as chronoselective atrial depressant effector (Figure 16 and 18). Of note, our research also demonstrated that PKC function impairment sensitizes atria for contractile depression during graded increase of adenosinergic stimuli. It is hard to establish a solid and coherent connection among A_1R, PKC and chronoselectivity because, at the best of our knowledge, no one has provided evidences strong enough to rule out the doubtfulness around the role of PKC isozymes on regulation of myofilament properties and other components of the EC-coupling mechanism, like Ca_V1 (L-type) channels.

Finally, these data also reinforces the dissimilarity between the signaling of A_1R and M_2R on heart function regulation, also supported by the fact that ACh did not modify atrial cardiodepression, as observed with A_1R agonists (data not shown). Looking at atrial regulation as an integrative process of several neural and non-neural mechanisms, activation of cardiac M_2R is under hierarchical control of ACh releasing mechanisms from the vagus nerve terminals while ADO releasing mechanisms are naturally less controlled. In other words, the subordinate neurotransmitter of the parasympathetic nervous system offer a strong control of cardiac output by changing with similar potency heart rate and inotropy (stroke volume depends on atrial inotropy). Conversely, retaliatory ADO is brought to the extracellular medium by neural and non-neural mechanisms during stressful conditions and therefore, not so tightly regulated as ACh release. If ADO shared the same pattern of cardiodepression as ACh, large amounts of this nucleoside released during low oxygen tension (Sparks and Bardenheuer, 1986; Deussen, 2000) would be much more life-threatening than it really is. Thus, and according to the results of the current study, it could be suggested that the safety margin of these two cardiodepressor agents is provided by meticulous neural mechanisms (for ACh) and by the chronoselective property of the A_1R itself (for ADO).

From a clinical point of view, the selective heart rate-reducing induced by ADO may be advantageous to protect hearts from deleterious effects of tachycardias and metabolic compromised states (e.g. hypoxia, ischemia, higher sympathetic tonus), in particular in those hearts with ventricular myocardial dysfunction (e.g. heart failure) where excessive atrial cardiodepression could be life-threatening. The overall effect of ADO outflow to the extracellular medium during metabolic challenge, or intravenous bolus administration of these nucleoside/derivates, is reoxygenation of the myocardium since energy expenditure is reduced by a decrease of heart rate and oxygen consumption (via A_1R) and rise of myocardial oxygen-supply by coronary dilation (via A_2R) (Shryock and Belardinelli, 1997; Headrick *et al*., 2011). The cytoprotector and antidysrhythmic profile of this endogenous nucleoside and its derivates (e.g. tecadenoson) are not accomplished at the expense of a greater negative inotropic action as compared to other cardiodepressant

molecules (e.g. ACh), which reinforces their therapeutic value and safety in arrhythmias reversion, in particular those originated in supraventricular tissues.

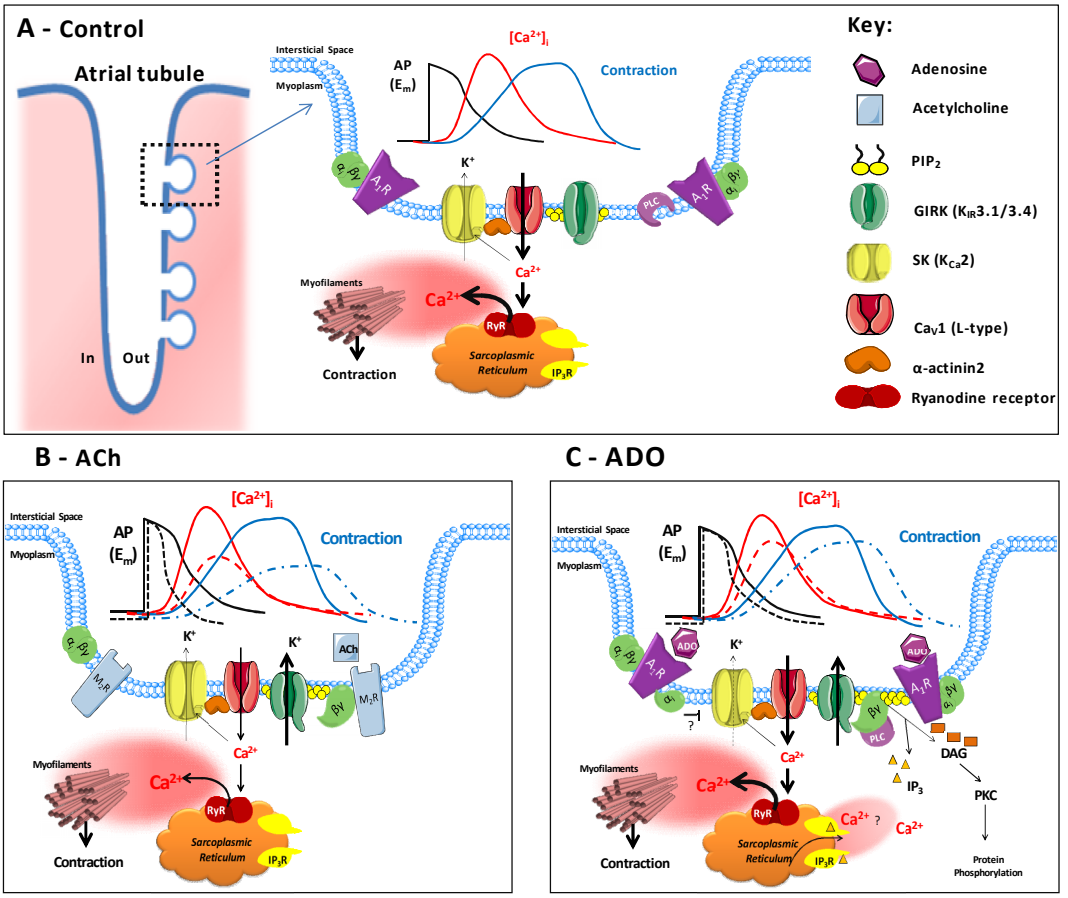

Figure 21. General mechanistic scheme for the chronoselectivity of ADO. In upper panel (A) is depicted a tubular system of an atrial myocyte and some of the molecular elements involved in its E-C coupling under basal conditions. Voltage-dependent activation of $Ca_V1(L)$ allows Ca^{2+} entry ($I_{Ca,L}$) into myoplasm that triggers RyR and leads to massive Ca^{2+} release from SR. $[Ca^{2+}]_i$ transient initiates a rapid contraction of atrial myocytes. Control of Ca^{2+} current carried by $Ca_V1(L)$ can occur through a variety of mechanism, including SK/$K_{Ca}2$ channels activation that reacts against calcium influx. In lower panels are represented two situations: atrial myocytes exposed to ACh (B) and ADO (C). The potent negative inotropic effect of ACh is based on activation of M_2R and subsequent K^+ efflux through GIRK/$K_{IR}3$ channel opening. Since this hyperpolarizing K^+ current shortens the repolarization phase of the AP, M_2R decrease the time available for calcium influx ($I_{Ca,L}$) leading to a reduction in atrial muscle contraction (B). Similar to M_2R, A_1R also elicits a negative inotropy through Gβγ-mediated GIRK/$K_{IR}3$ channel opening. However, A_1R stimulates the activity of phospholipase C (PLC) that, in turn, stimulate breakdown of GIRK/$K_{IR}3$ channel activator PIP_2. Therefore, following stimulation of GIRK carried currents A_1R inhibits GIRK/$K_{IR}3$ channels by depleting PIP_2 in the sarcolemma. Impairment of GIRK/$K_{IR}3$ channel function by A_1R activation yields a lesser reduction of Ca^{2+} influx during E-C coupling, which is further potentiated by SK/$K_{Ca}2$ channel inhibition. Positive inotropic mechanisms may also occur during A_1R stimulation such as IP_3-induced SR Ca^{2+} release (via PIP_2 breakdown) and further balance of the negative inotropic effect of GIRK/$K_{IR}3$ channel. Besides IP_3, PIP_2 hydrolysis also generate PKC-activator messenger, diacylglicerol (DAG). In summary, when compared to M_2R, A_1R exhibits an attenuated GIRK/$K_{IR}3$-mediated contractile suppression that involves inhibition of SK/$K_{Ca}2$ channel and activation of PLC, explaining why A_1R acts as chronoselective atrial depressant effector. Solid lines represent AP, $[Ca^{2+}]_I$ and contraction profile under basal conditions, whereas dashed lines represent the same parameters when either cholinergic or adenosinergic agonist are present.

VI. References

Allah EA, Tellez JO, Yanni J, Nelson T, Monfredi O, Boyett MR, Dobrzynski H. 2011. Changes in the expression of ion channels, connexins and Ca2+-handling proteins in the sino-atrial node during postnatal development. Exp Physiol 96:426-438.

Allen DG, Kentish JC. 1985. The cellular basis of the length-tension relation in cardiac muscle. J Mol Cell Cardiol 17:821-840.

Amin AS, Tan HL, Wilde AA. 2010. Cardiac ion channels in health and disease. Heart Rhythm 7:117-126.

Anderson RH, Ho SY. 1998. The architecture of the sinus node, the atrioventricular conduction axis, and the internodal atrial myocardium. J Cardiovasc Electrophysiol 9:1233-1248.

Ashkenazi A, Winslow JW, Peralta EG, Peterson GL, Schimerlik MI, Capon DJ, Ramachandran J. 1987. An M2 muscarinic receptor subtype coupled to both adenylyl cyclase and phosphoinositide turnover. Science 238:672-675.

Balbi T, Ghimenton C, Pasquinelli G, Foroni L, Grillini M, Pierini G. 2011. Advancement in the examination of the human cardiac sinus node: an unexpected architecture and a novel cell type could interest the forensic science. Am J Forensic Med Pathol 32:112-118.

Belardinelli L, Giles WR, West A. 1988. Ionic mechanisms of adenosine actions in pacemaker cells from rabbit heart. J Physiol 405:615-633.

Belardinelli L, Shryock JC, Song Y, Wang D, Srinivas M. 1995. Ionic basis of the electrophysiological actions of adenosine on cardiomyocytes. FASEB J 9:359-365.

Berne RM. 1963. Cardiac nucleotides in hypoxia: possible role in regulation of coronary blood flow. Am J Physiol 204:317-322.

Berridge MJ. 1993. Inositol trisphosphate and calcium signalling. Nature 361:315-325.

Bers DM. 2002. Cardiac excitation-contraction coupling. Nature 415:198-205.

Best JM, Kamp TJ. 2012. Different subcellular populations of L-type Ca2+ channels exhibit unique regulation and functional roles in cardiomyocytes. J Mol Cell Cardiol 52:376-387.

Biber K, Klotz KN, Berger M, Gebicke-Harter PJ, van Calker D. 1997. Adenosine A1 receptor-mediated activation of phospholipase C in cultured astrocytes depends on the level of receptor expression. J Neurosci 17:4956-4964.

Blomstrom-Lundqvist C, Scheinman MM, Aliot EM, Alpert JS, Calkins H, Camm AJ, Campbell WB, Haines DE, Kuck KH, Lerman BB, Miller DD, Shaeffer CW, Stevenson WG, Tomaselli GF, Antman EM, Smith SC, Jr., Faxon DP, Fuster V, Gibbons RJ, Gregoratos G, Hiratzka LF, Hunt SA, Jacobs AK, Russell RO, Jr., Priori SG, Blanc JJ, Budaj A, Burgos EF, Cowie M, Deckers JW, Garcia MA, Klein WW, Lekakis J, Lindahl B, Mazzotta G, Morais JC, Oto A, Smiseth O, Trappe HJ. 2003. ACC/AHA/ESC guidelines for the management of patients with supraventricular arrhythmias--executive summary. a report of the American college of cardiology/American heart association task force on practice guidelines and the European society of cardiology committee for practice guidelines (writing committee to develop guidelines for the management of patients with supraventricular arrhythmias) developed in collaboration with NASPE-Heart Rhythm Society. J Am Coll Cardiol 42:1493-1531.

Bogdanov KY, Vinogradova TM, Lakatta EG. 2001. Sinoatrial nodal cell ryanodine receptor and Na(+)-Ca(2+) exchanger: molecular partners in pacemaker regulation. Circ Res 88:1254-1258.

Bootman MD, Smyrnias I, Thul R, Coombes S, Roderick HL. 2011. Atrial cardiomyocyte calcium signalling. Biochim Biophys Acta 1813:922-934.

Boyer JL, Waldo GL, Harden TK. 1992. Beta gamma-subunit activation of G-protein-regulated phospholipase C. J Biol Chem 267:25451-25456.

Boyett MR, Honjo H, Kodama I. 2000. The sinoatrial node, a heterogeneous pacemaker structure. Cardiovasc Res 47:658-687.

Capogrossi MC, Kaku T, Filburn CR, Pelto DJ, Hansford RG, Spurgeon HA, Lakatta EG. 1990. Phorbol ester and dioctanoylglycerol stimulate membrane association of protein kinase C and have a negative inotropic effect mediated by changes in cytosolic Ca2+ in adult rat cardiac myocytes. Circ Res 66:1143-1155.

Catterall WA. 2011. Voltage-gated calcium channels. Cold Spring Harb Perspect Biol 3:a003947.

Cazorla O, Lucas A, Poirier F, Lacampagne A, Lezoualc'h F. 2009. The cAMP binding protein Epac regulates cardiac myofilament function. Proc Natl Acad Sci U S A 106:14144-14149.

Cerbai E, Klockner U, Isenberg G. 1988. Ca-antagonistic effects of adenosine in guinea pig atrial cells. Am J Physiol 255:H872-878.

Chandler NJ, Greener ID, Tellez JO, Inada S, Musa H, Molenaar P, Difrancesco D, Baruscotti M, Longhi R, Anderson RH, Billeter R, Sharma V, Sigg DC, Boyett MR, Dobrzynski H. 2009. Molecular architecture of the human sinus node: insights into the function of the cardiac pacemaker. Circulation 119:1562-1575.

Chandrasekera PC, McIntosh VJ, Cao FX, Lasley RD. 2010. Differential effects of adenosine A2a and A2b receptors on cardiac contractility. Am J Physiol Heart Circ Physiol 299:H2082-2089.

Cheng H, Lederer WJ. 2008. Calcium sparks. Physiol Rev 88:1491-1545.

Cho H. 2010. Regulation of Adenosine-activated GIRK Channels by Gq-coupled Receptors in Mouse Atrial Myocytes. Korean J Physiol Pharmacol 14:145-150.

Clark BD, Kurth-Nelson ZL, Newman EA. 2009. Adenosine-evoked hyperpolarization of retinal ganglion cells is mediated by G-protein-coupled inwardly rectifying K+ and small conductance Ca2+-activated K+ channel activation. J Neurosci 29:11237-11245.

Cordeaux Y, Briddon SJ, Megson AE, McDonnell J, Dickenson JM, Hill SJ. 2000. Influence of receptor number on functional responses elicited by agonists acting at the human adenosine A(1) receptor: evidence for signaling pathway-dependent changes in agonist potency and relative intrinsic activity. Mol Pharmacol 58:1075-1084.

Cui S, Ho WK, Kim ST, Cho H. 2010. Agonist-induced localization of Gq-coupled receptors and G protein-gated inwardly rectifying K+ (GIRK) channels to caveolae determines receptor specificity of phosphatidylinositol 4,5-bisphosphate signaling. J Biol Chem 285:41732-41739.

De Biasi M, Froldi G, Ragazzi E, Pandolfo L, Caparrotta L, Fassina G. 1989. Potassium channel blockers differentially affect carbachol and (-)-N6-phenylisopropyladenosine on guinea-pig atria. Br J Pharmacol 97:866-872.

de Tombe PP. 2003. Cardiac myofilaments: mechanics and regulation. J Biomech 36:721-730.

de Tombe PP, Mateja RD, Tachampa K, Ait Mou Y, Farman GP, Irving TC. 2010. Myofilament length dependent activation. J Mol Cell Cardiol 48:851-858.

Deussen A. 2000. Metabolic flux rates of adenosine in the heart. Naunyn Schmiedebergs Arch Pharmacol 362:351-363.

Dickenson JM, Hill SJ. 1998. Involvement of G-protein betagamma subunits in coupling the adenosine A1 receptor to phospholipase C in transfected CHO cells. Eur J Pharmacol 355:85-93.

DiFrancesco D, Tortora P. 1991. Direct activation of cardiac pacemaker channels by intracellular cyclic AMP. Nature 351:145-147.

DiMarco JP, Sellers TD, Berne RM, West GA, Belardinelli L. 1983. Adenosine: electrophysiologic effects and therapeutic use for terminating paroxysmal supraventricular tachycardia. Circulation 68:1254-1263.

Dobrzynski H, Li J, Tellez J, Greener ID, Nikolski VP, Wright SE, Parson SH, Jones SA, Lancaster MK, Yamamoto M, Honjo H, Takagishi Y, Kodama I, Efimov IR, Billeter R, Boyett MR. 2005. Computer three-dimensional reconstruction of the sinoatrial node. Circulation 111:846-854.

Dobrzynski H, Marples DD, Musa H, Yamanushi TT, Henderson Z, Takagishi Y, Honjo H, Kodama I, Boyett MR. 2001. Distribution of the muscarinic K+ channel proteins Kir3.1 and Kir3.4 in the ventricle, atrium, and sinoatrial node of heart. J Histochem Cytochem 49:1221-1234.

Dobson JG, Jr. 1983. Mechanism of adenosine inhibition of catecholamine-induced responses in heart. Circ Res 52:151-160.

Dobson JG, Jr., Fenton RA. 1997. Adenosine A2 receptor function in rat ventricular myocytes. Cardiovasc Res 34:337-347.

Drury AN, Szent-Gyorgyi A. 1929. The physiological activity of adenine compounds with especial reference to their action upon the mammalian heart. J Physiol 68:213-237.

Ellenbogen KA, O'Neill G, Prystowsky EN, Camm JA, Meng L, Lieu HD, Jerling M, Shreeniwas R, Belardinelli L, Wolff AA. 2005. Trial to evaluate the management of paroxysmal supraventricular tachycardia during an electrophysiology study with tecadenoson. Circulation 111:3202-3208.

Erlinge D, Burnstock G. 2008. P2 receptors in cardiovascular regulation and disease. Purinergic Signal 4:1-20.

Fabiato A. 1983. Calcium-induced release of calcium from the cardiac sarcoplasmic reticulum. Am J Physiol 245:C1-14.

Fenton RA, Komatsu S, Ikebe M, Shea LG, Dobson JG, Jr. 2009. Adenoprotection of the heart involves phospholipase C-induced activation and translocation of PKC-epsilon to RACK2 in adult rat and mouse. Am J Physiol Heart Circ Physiol 297:H718-725.

Fenton RA, Shea LG, Doddi C, Dobson JG, Jr. 2010. Myocardial adenosine A(1)-receptor-mediated adenoprotection involves phospholipase C, PKC-epsilon, and p38 MAPK, but not HSP27. Am J Physiol Heart Circ Physiol 298:H1671-1678.

Ford WR, Broadley KJ. 1999. Effects of K(+)-channel blockers on A1-adenosine receptor-mediated negative inotropy and chronotropy of guinea-pig isolated left and right atria. Fundam Clin Pharmacol 13:320-329.

Fredholm BB, AP IJ, Jacobson KA, Linden J, Muller CE. 2011. International Union of Basic and Clinical Pharmacology. LXXXI. Nomenclature and classification of adenosine receptors--an update. Pharmacol Rev 63:1-34.

Gergs U, Boknik P, Schmitz W, Simm A, Silber RE, Neumann J. 2009. A positive inotropic effect of adenosine in cardiac preparations of right atria from diseased human hearts. Naunyn Schmiedebergs Arch Pharmacol 379:533-540.

Gerwins P, Fredholm BB. 1992. ATP and its metabolite adenosine act synergistically to mobilize intracellular calcium via the formation of inositol 1,4,5-trisphosphate in a smooth muscle cell line. J Biol Chem 267:16081-16087.

Han SY, Bolter CP. 2011. The muscarinic-activated potassium channel always participates in vagal slowing of the guinea-pig sinoatrial pacemaker. Auton Neurosci 164:96-100.

He JQ, Pi Y, Walker JW, Kamp TJ. 2000. Endothelin-1 and photoreleased diacylglycerol increase L-type Ca2+ current by activation of protein kinase C in rat ventricular myocytes. J Physiol 524 Pt 3:807-820.

Headrick JP, Peart JN, Reichelt ME, Haseler LJ. 2011. Adenosine and its receptors in the heart: regulation, retaliation and adaptation. Biochim Biophys Acta 1808:1413-1428.

Hove-Madsen L, Prat-Vidal C, Llach A, Ciruela F, Casado V, Lluis C, Bayes-Genis A, Cinca J, Franco R. 2006. Adenosine A2A receptors are expressed in human atrial myocytes and modulate spontaneous sarcoplasmic reticulum calcium release. Cardiovasc Res 72:292-302.

Huser J, Blatter LA, Lipsius SL. 2000. Intracellular Ca2+ release contributes to automaticity in cat atrial pacemaker cells. J Physiol 524 Pt 2:415-422.

Iijima T, Irisawa H, Kameyama M. 1985. Membrane currents and their modification by acetylcholine in isolated single atrial cells of the guinea-pig. J Physiol 359:485-501.

Ishii TM, Maylie J, Adelman JP. 1997. Determinants of apamin and d-tubocurarine block in SK potassium channels. J Biol Chem 272:23195-23200.

James TN, Sherf L, Fine G, Morales AR. 1966. Comparative ultrastructure of the sinus node in man and dog. Circulation 34:139-163.

Ju YK, Liu J, Lee BH, Lai D, Woodcock EA, Lei M, Cannell MB, Allen DG. 2011. Distribution and functional role of inositol 1,4,5-trisphosphate receptors in mouse sinoatrial node. Circ Res 109:848-857.

Kabell G, Buchanan LV, Gibson JK, Belardinelli L. 1994. Effects of adenosine on atrial refractoriness and arrhythmias. Cardiovasc Res 28:1385-1389.

Kamp TJ, Hell JW. 2000. Regulation of cardiac L-type calcium channels by protein kinase A and protein kinase C. Circ Res 87:1095-1102.

Kang M, Walker JW. 2005. Protein kinase C delta and epsilon mediate positive inotropy in adult ventricular myocytes. J Mol Cell Cardiol 38:753-764.

Karmazyn M, Haist JV. 1993. Calcium dependent positive inotropic effects of low phorbol ester concentrations in isolated rat hearts. Cardiovasc Res 27:390-395.

Keim S, Curtis AB, Belardinelli L, Epstein ML, Staples ED, Lerman BB. 1992. Adenosine-induced atrioventricular block: a rapid and reliable method to assess surgical and radiofrequency catheter ablation of accessory atrioventricular pathways. J Am Coll Cardiol 19:1005-1012.

Keith A, Flack M. 1907. The Form and Nature of the Muscular Connections between the Primary Divisions of the Vertebrate Heart. J Anat Physiol 41:172-189.

Kilts JD, Grocott HP, Kwatra MM. 2005. G alpha(q)-coupled receptors in human atrium function through protein kinase C epsilon and delta. J Mol Cell Cardiol 38:267-276.

Kirsch GE, Codina J, Birnbaumer L, Brown AM. 1990. Coupling of ATP-sensitive K+ channels to A1 receptors by G proteins in rat ventricular myocytes. Am J Physiol 259:H820-826.

Kobrinsky E, Mirshahi T, Zhang H, Jin T, Logothetis DE. 2000. Receptor-mediated hydrolysis of plasma membrane messenger PIP2 leads to K+-current desensitization. Nat Cell Biol 2:507-514.

Kohl C, Linck B, Schmitz W, Scholz H, Scholz J, Toth M. 1990. Effects of carbachol and (-)-N6-phenylisopropyladenosine on myocardial inositol phosphate content and force of contraction. Br J Pharmacol 101:829-834.

Krapivinsky G, Gordon EA, Wickman K, Velimirovic B, Krapivinsky L, Clapham DE. 1995. The G-protein-gated atrial K+ channel IKACh is a heteromultimer of two inwardly rectifying K(+)-channel proteins. Nature 374:135-141.

Krejci A, Tucek S. 2002. Quantitation of mRNAs for M(1) to M(5) subtypes of muscarinic receptors in rat heart and brain cortex. Mol Pharmacol 61:1267-1272.

Kurachi Y, Nakajima T, Sugimoto T. 1986. On the mechanism of activation of muscarinic K+ channels by adenosine in isolated atrial cells: involvement of GTP-binding proteins. Pflugers Arch 407:264-274.

Kurachi Y, Terzic A, Cohen M, Sperelakis N. 2000. Heart Physiology and Pathophysiology, 4th ed: Academic Press.

Lakatta EG, Maltsev VA, Vinogradova TM. 2010. A coupled SYSTEM of intracellular Ca2+ clocks and surface membrane voltage clocks controls the timekeeping mechanism of the heart's pacemaker. Circ Res 106:659-673.

LaMonica DA, Frohloff N, Dobson JG, Jr. 1985. Adenosine inhibition of catecholamine-stimulated cardiac membrane adenylate cyclase. Am J Physiol 248:H737-744.

Lasley RD. 2011. Adenosine receptors and membrane microdomains. Biochim Biophys Acta 1808:1284-1289.

Lebon G, Warne T, Edwards PC, Bennett K, Langmead CJ, Leslie AG, Tate CG. 2011. Agonist-bound adenosine A2A receptor structures reveal common features of GPCR activation. Nature 474:521-525.

Lerman BB, Belardinelli L, West GA, Berne RM, DiMarco JP. 1986. Adenosine-sensitive ventricular tachycardia: evidence suggesting cyclic AMP-mediated triggered activity. Circulation 74:270-280.

Lester JW, Hofmann PA. 2000. Role for PKC in the adenosine-induced decrease in shortening velocity of rat ventricular myocytes. Am J Physiol Heart Circ Physiol 279:H2685-2693.

Li Q, Zhang J, Pfaffendorf M, van Zwieten PA. 1996. Direct positive chronotropic effects of angiotensin II and angiotensin III in pithed rats and in rat isolated atria. Br J Pharmacol 118:1653-1658.

Linden J, Thai T, Figler H, Jin X, Robeva AS. 1999. Characterization of human A(2B) adenosine receptors: radioligand binding, western blotting, and coupling to G(q) in human embryonic kidney 293 cells and HMC-1 mast cells. Mol Pharmacol 56:705-713.

Lipp P, Laine M, Tovey SC, Burrell KM, Berridge MJ, Li W, Bootman MD. 2000. Functional InsP3 receptors that may modulate excitation-contraction coupling in the heart. Curr Biol 10:939-942.

Littwitz C, Timpert M, Bender K, Pott L, Kienitz MC. 2011. Autocrine signaling via A(1) adenosine receptors causes downregulation of M(2) receptors in adult rat atrial myocytes in vitro. Pflugers Arch 461:165-176.

Liu Q, Chen X, Macdonnell SM, Kranias EG, Lorenz JN, Leitges M, Houser SR, Molkentin JD. 2009. Protein kinase C{alpha}, but not PKC{beta} or PKC{gamma}, regulates contractility and heart failure susceptibility: implications for ruboxistaurin as a novel therapeutic approach. Circ Res 105:194-200.

Logothetis DE, Kurachi Y, Galper J, Neer EJ, Clapham DE. 1987. The beta gamma subunits of GTP-binding proteins activate the muscarinic K+ channel in heart. Nature 325:321-326.

Lorbar M, Chung ES, Nabi A, Skalova K, Fenton RA, Dobson JG, Jr., Meyer TE. 2004. Receptors subtypes involved in adenosine-mediated modulation of norepinephrine release from cardiac nerve terminals. Can J Physiol Pharmacol 82:1026-1031.

Lu L, Zhang Q, Timofeyev V, Zhang Z, Young JN, Shin HS, Knowlton AA, Chiamvimonvat N. 2007. Molecular coupling of a Ca2+-activated K+ channel to L-type Ca2+ channels via alpha-actinin2. Circ Res 100:112-120.

Lukyanenko V, Gyorke I, Gyorke S. 1996. Regulation of calcium release by calcium inside the sarcoplasmic reticulum in ventricular myocytes. Pflugers Arch 432:1047-1054.

Lyashkov AE, Vinogradova TM, Zahanich I, Li Y, Younes A, Nuss HB, Spurgeon HA, Maltsev VA, Lakatta EG. 2009. Cholinergic receptor signaling modulates spontaneous firing of sinoatrial nodal cells via integrated effects on PKA-dependent Ca(2+) cycling and I(KACh). Am J Physiol Heart Circ Physiol 297:H949-959.

Mackenzie L, Roderick HL, Berridge MJ, Conway SJ, Bootman MD. 2004. The spatial pattern of atrial cardiomyocyte calcium signalling modulates contraction. J Cell Sci 117:6327-6337.

MacLeod KT, Harding SE. 1991. Effects of phorbol ester on contraction, intracellular pH and intracellular Ca2+ in isolated mammalian ventricular myocytes. J Physiol 444:481-498.

Maruyama T, Kanaji T, Nakade S, Kanno T, Mikoshiba K. 1997. 2APB, 2-aminoethoxydiphenyl borate, a membrane-penetrable modulator of Ins(1,4,5)P3-induced Ca2+ release. J Biochem 122:498-505.

Melo SR, Mandarim-de-Lacerda CA, Souza RR, Prates N. 2001. The sinoatrial node of rats (rattus norvegicus): histologic study Arq. Ciênc. Saúde Unipar 5:215-220.

Milligan G, Kostenis E. 2006. Heterotrimeric G-proteins: a short history. Br J Pharmacol 147 Suppl 1:S46-55.

Monahan TS, Sawmiller DR, Fenton RA, Dobson JG, Jr. 2000. Adenosine A(2a)-receptor activation increases contractility in isolated perfused hearts. Am J Physiol Heart Circ Physiol 279:H1472-1481.

Monfredi O, Dobrzynski H, Mondal T, Boyett MR, Morris GM. 2010. The anatomy and physiology of the sinoatrial node--a contemporary review. Pacing Clin Electrophysiol 33:1392-1406.

Myslivecek J, Klein M, Novakova M, Ricny J. 2008. The detection of the non-M2 muscarinic receptor subtype in the rat heart atria and ventricles. Naunyn Schmiedebergs Arch Pharmacol 378:103-116.

Nagy N, Szuts V, Horvath Z, Seprenyi G, Farkas AS, Acsai K, Prorok J, Bitay M, Kun A, Pataricza J, Papp JG, Nanasi PP, Varro A, Toth A. 2009. Does small-conductance calcium-activated potassium channel contribute to cardiac repolarization? J Mol Cell Cardiol 47:656-663.

Neumann J, Vahlensieck U, Boknik P, Linck B, Luss H, Muller FU, Matherne GP, Schmitz W. 1999. Functional studies in atrium overexpressing A1-adenosine receptors. Br J Pharmacol 128:1623-1629.

Nishizuka Y. 1992. Intracellular signaling by hydrolysis of phospholipids and activation of protein kinase C. Science 258:607-614.

O'Rourke DJ, Palac RT, Schindler JT, Keim SG. 1999. The clinical utility of adenosine in difficult to diagnose tachyarrhythmias. Clin Cardiol 22:633-636.

O-Uchi J, Sasaki H, Morimoto S, Kusakari Y, Shinji H, Obata T, Hongo K, Komukai K, Kurihara S. 2008. Interaction of alpha1-adrenoceptor subtypes with different G proteins induces opposite effects on cardiac L-type Ca2+ channel. Circ Res 102:1378-1388.

Oestreich EA, Malik S, Goonasekera SA, Blaxall BC, Kelley GG, Dirksen RT, Smrcka AV. 2009. Epac and phospholipase Cepsilon regulate Ca2+ release in the heart by activation of protein kinase Cepsilon and calcium-calmodulin kinase II. J Biol Chem 284:1514-1522.

Oosthoek PW, Viragh S, Mayen AE, van Kempen MJ, Lamers WH, Moorman AF. 1993. Immunohistochemical delineation of the conduction system. I: The sinoatrial node. Circ Res 73:473-481.

Park DS, Fishman GI. 2011. The cardiac conduction system. Circulation 123:904-915.

Parsons M, Young L, Lee JE, Jacobson KA, Liang BT. 2000. Distinct cardioprotective effects of adenosine mediated by differential coupling of receptor subtypes to phospholipases C and D. FASEB J 14:1423-1431.

Patel HH, Murray F, Insel PA. 2008. G-protein-coupled receptor-signaling components in membrane raft and caveolae microdomains. Handb Exp Pharmacol:167-184.

Peppiatt CM, Collins TJ, Mackenzie L, Conway SJ, Holmes AB, Bootman MD, Berridge MJ, Seo JT, Roderick HL. 2003. 2-Aminoethoxydiphenyl borate (2-APB) antagonises inositol 1,4,5-trisphosphate-induced calcium release, inhibits calcium pumps and has a use-dependent and slowly reversible action on store-operated calcium entry channels. Cell Calcium 34:97-108.

Pitt GS, Zuhlke RD, Hudmon A, Schulman H, Reuter H, Tsien RW. 2001. Molecular basis of calmodulin tethering and Ca2+-dependent inactivation of L-type Ca2+ channels. J Biol Chem 276:30794-30802.

Puceat M, Vassort G. 1996. Signalling by protein kinase C isoforms in the heart. Mol Cell Biochem 157:65-72.

Riccardi A, Arboscello E, Ghinatti M, Minuto P, Lerza R. 2008. Adenosine in the treatment of supraventricular tachycardia: 5 years of experience (2002-2006). Am J Emerg Med 26:879-882.

Sabourin J, Antigny F, Robin E, Frieden M, Raddatz E. 2012. Activation of Transient Receptor Potential Canonical 3 (TRPC3)-mediated Ca2+ Entry by A1 Adenosine Receptor in Cardiomyocytes Disturbs Atrioventricular Conduction. J Biol Chem 287:26688-26701.

Samet P. 1973. Hemodynamic sequelae of cardiac arrhythmias. Circulation 47:399-407.

Sanders L, Rakovic S, Lowe M, Mattick PA, Terrar DA. 2006. Fundamental importance of Na+-Ca2+ exchange for the pacemaking mechanism in guinea-pig sino-atrial node. J Physiol 571:639-649.

Schrader J, Schutz W, Bardenheuer H. 1981. Role of S-adenosylhomocysteine hydrolase in adenosine metabolism in mammalian heart. Biochem J 196:65-70.

Shryock JC, Belardinelli L. 1997. Adenosine and adenosine receptors in the cardiovascular system: biochemistry, physiology, and pharmacology. Am J Cardiol 79:2-10.

Sipido KR, Maes M, Van de Werf F. 1997. Low efficiency of Ca2+ entry through the Na(+)-Ca2+ exchanger as trigger for Ca2+ release from the sarcoplasmic reticulum. A comparison between L-type Ca2+ current and reverse-mode Na(+)-Ca2+ exchange. Circ Res 81:1034-1044.

Solaro RJ. 2008. Multiplex kinase signaling modifies cardiac function at the level of sarcomeric proteins. J Biol Chem 283:26829-26833.

Sparks HV, Jr., Bardenheuer H. 1986. Regulation of adenosine formation by the heart. Circ Res 58:193-201.

Sun XH, Protasi F, Takahashi M, Takeshima H, Ferguson DG, Franzini-Armstrong C. 1995. Molecular architecture of membranes involved in excitation-contraction coupling of cardiac muscle. J Cell Biol 129:659-671.

Tellez JO, Dobrzynski H, Greener ID, Graham GM, Laing E, Honjo H, Hubbard SJ, Boyett MR, Billeter R. 2006. Differential expression of ion channel transcripts in atrial muscle and sinoatrial node in rabbit. Circ Res 99:1384-1393.

Tikh EI, Fenton RA, Dobson JG, Jr. 2006. Contractile effects of adenosine A1 and A2A receptors in isolated murine hearts. Am J Physiol Heart Circ Physiol 290:H348-356.

Tuteja D, Xu D, Timofeyev V, Lu L, Sharma D, Zhang Z, Xu Y, Nie L, Vazquez AE, Young JN, Glatter KA, Chiamvimonvat N. 2005. Differential expression of small-conductance Ca2+-activated K+ channels SK1, SK2, and SK3 in mouse atrial and ventricular myocytes. Am J Physiol Heart Circ Physiol 289:H2714-2723.

Urquhart RA, Broadley KJ. 1991. Blockade by 4-aminopyridine of the muscarinic-receptor-mediated responses of guinea-pig atria and trachea. J Pharm Pharmacol 43:417-420.

Urquhart RA, Ford WR, Broadley KJ. 1993. Potassium channel blockade of atrial negative inotropic responses to P1-purinoceptor and muscarinic receptor agonists and to cromakalim. J Cardiovasc Pharmacol 21:279-288.

van Kempen MJ, Fromaget C, Gros D, Moorman AF, Lamers WH. 1991. Spatial distribution of connexin43, the major cardiac gap junction protein, in the developing and adult rat heart. Circ Res 68:1638-1651.

Vassort G. 2001. Adenosine 5'-triphosphate: a P2-purinergic agonist in the myocardium. Physiol Rev 81:767-806.

Verzijl D, Ijzerman AP. 2011. Functional selectivity of adenosine receptor ligands. Purinergic Signal 7:171-192.

Vinogradova TM, Lyashkov AE, Zhu W, Ruknudin AM, Sirenko S, Yang D, Deo S, Barlow M, Johnson S, Caffrey JL, Zhou YY, Xiao RP, Cheng H, Stern MD, Maltsev VA, Lakatta EG. 2006. High basal protein kinase A-dependent phosphorylation drives rhythmic internal Ca2+ store oscillations and spontaneous beating of cardiac pacemaker cells. Circ Res 98:505-514.

Vinogradova TM, Zhou YY, Maltsev V, Lyashkov A, Stern M, Lakatta EG. 2004. Rhythmic ryanodine receptor Ca2+ releases during diastolic depolarization of sinoatrial pacemaker cells do not require membrane depolarization. Circ Res 94:802-809.

Visentin S, Wu SN, Belardinelli L. 1990. Adenosine-induced changes in atrial action potential: contribution of Ca and K currents. Am J Physiol 258:H1070-1078.

Wang D, Belardinelli L. 1994. Mechanism of the negative inotropic effect of adenosine in guinea pig atrial myocytes. Am J Physiol 267:H2420-2429.

Wang H, Grant JE, Doede CM, Sadayappan S, Robbins J, Walker JW. 2006. PKC-betaII sensitizes cardiac myofilaments to Ca2+ by phosphorylating troponin I on threonine-144. J Mol Cell Cardiol 41:823-833.

Whorton MR, MacKinnon R. 2011. Crystal structure of the mammalian GIRK2 K+ channel and gating regulation by G proteins, PIP2, and sodium. Cell 147:199-208.

Wickman K, Nemec J, Gendler SJ, Clapham DE. 1998. Abnormal heart rate regulation in GIRK4 knockout mice. Neuron 20:103-114.

Willems L, Headrick JP. 2007. Contractile effects of adenosine, coronary flow and perfusion pressure in murine myocardium. Pflugers Arch 453:433-441.

Wolkowicz PE, Wu HC, Urthaler F, Ku DD. 2007. 2-APB induces instability in rat left atrial mechanical activity. J Cardiovasc Pharmacol 49:325-335.

Xu Y, Tuteja D, Zhang Z, Xu D, Zhang Y, Rodriguez J, Nie L, Tuxson HR, Young JN, Glatter KA, Vazquez AE, Yamoah EN, Chiamvimonvat N. 2003. Molecular identification and functional roles of a Ca(2+)-activated K+ channel in human and mouse hearts. J Biol Chem 278:49085-49094.

Yang L, Doshi D, Morrow J, Katchman A, Chen X, Marx SO. 2009a. Protein kinase C isoforms differentially phosphorylate Ca(v)1.2 alpha(1c). Biochemistry 48:6674-6683.

Yang Z, Sun W, Hu K. 2009b. Adenosine A(1) receptors selectively target protein kinase C isoforms to the caveolin-rich plasma membrane in cardiac myocytes. Biochim Biophys Acta 1793:1868-1875.

Yaniv Y, Spurgeon HA, Lyashkov AE, Yang D, Ziman BD, Maltsev VA, Lakatta EG. 2012. Crosstalk between mitochondrial and sarcoplasmic reticulum Ca2+ cycling modulates cardiac pacemaker cell automaticity. PLoS One 7:e37582.

Yanni J, Tellez JO, Maczewski M, Mackiewicz U, Beresewicz A, Billeter R, Dobrzynski H, Boyett MR. 2011. Changes in ion channel gene expression underlying heart failure-induced sinoatrial node dysfunction. Circ Heart Fail 4:496-508.

Yegutkin GG. 2008. Nucleotide- and nucleoside-converting ectoenzymes: Important modulators of purinergic signalling cascade. Biochim Biophys Acta 1783:673-694.